8976-0008-RU-000

AN ANALYSIS OF MOON-TO-EARTH TRAJECTORIES

P. A. Penzo

30 October 1961

SPACE TECHNOLOGY LABORATORIES, INC.
P.O. Box 95001, Los Angeles 45, California

8976-0008-RU-000
30 October 1961

AN ANALYSIS OF MOON-TO-EARTH TRAJECTORIES

P. A. Penzo

Prepared for

JET PROPULSION LABORATORY
California Institute of Technology
Contract No. 950045

Approved E. H. Tompkins
E. H. Tompkins
Associate Manager
Systems Analysis Department

SPACE TECHNOLOGY LABORATORIES, INC.
P. O. Box 95001
Los Angeles 45, California

CONTENTS

ACKNOWLEDGEMENTS

The author wishes to thank the programmers I. Kliger, C. C. Tonies and G. Hanson for their extensive effort in developing the logic and programming and checking out the Analytic Lunar Return Program. He is grateful to Mrs. L. J. Martin who generated and plotted the majority of the data presented here and who carried out the investigations discussed in Section III. Finally, he is indebted to E. H. Tompkins for checking and editing the report to its final form.

GENERAL NOTATION

x_j, u_j $(j = 1, 2, 3)$ = coordinates of position and velocity with respect to the earth (equatorial).

y_j, v_j $(j = 1, 2, 3)$ = coordinates of position and velocity with respect to the moon (equatorial).

"primes" attached to position and velocity denote selenographic coordinates

"bars" above position and velocity symbols denote vectors

α, δ = right ascension and eclination

λ, μ = selenographic longitude and latitude

η = angles measured in the trajectory plane; single subscript - from perifocus

θ = angles measured in the equatorial plane

a, e, i, Ω = normal conic elements (equatorial)

H, J = angular momentum in earth phase; moon phase

β = flight path angle measured from the vertical

A = azimuth angle

L = geographic longitude

"bars" above quantities other than position and velocity coordinates denote those with respect to the moon

D_ℓ, D_i = Julian Date of launch; impact

t = time measured from day of launch (O^h GMT)

t' = time measured from day of impact (O^h GMT)

T = time measured from perifocus (single subscript), time measured between two points (double subscript)

GENERAL NOTATION (Continued)

Subscripts:

o	=	launch point
b	=	burnout point
s	=	point of exit from MSA
i	=	point of impact (touchdown)
r	=	point of re-entry
m	=	quantities referring to the moon

I. INTRODUCTION

The present United States space program for manned lunar exploration has made it necessary to conduct thorough investigations of all trajectory and guidance aspects of lunar operations. Generally, such operations may be divided into three classes:

(1) earth-to-moon trajectories in which a spacecraft is transferred from earth to the lunar surface or an orbit about the moon,

(2) lunar return, or moon-to-earth trajectories where the spacecraft is launched from the surface of the moon or from a lunar orbit and returns to a designated landing site on earth, with prescribed re-entry conditions, and

(3) circumlunar trajectories in which the spacecraft is launched from earth, passes within a specified distance of the moon, and returns to earth with or without an added impulse in the vicinity of the moon.

This report is concerned with the second class of lunar trajectories. Its specific purpose is to provide an insight into the parametric relationships and geometric constraints existing among all of the principal trajectory variables. The procedure which was used to explore these relationships was to first develop an analytic model and an associated computer program which accurately describe three-dimensional moon-to-earth trajectories, and then to employ this computer program to make an extensive study of the trajectory properties.

The report has been divided into four sections which are essentially independent and these may be read in an order other than as presented here, if desired. The remainder of Section I discusses the nature and application of the analytic model. Section II gives a complete description of the "Analytic Lunar Return Program" which was used to generate information for the trajectory study. This material has been included since the model and computer program have other important uses besides the parametric study, and the discussion of the program logic itself displays many features of moon-to-earth trajectories. Section III deals with the program accuracy when compared to an n-body integration program, and describes a method by which this accuracy was greatly improved. The final section examines many of the

characteristics of moon-to-earth trajectories including required lunar launch conditions, geometric constraints among variables (such as allowable launch dates and re-entry locations), launch-to-re-entry error coefficients, and midcourse correction coefficients. Much of this information is presented graphically and may be used by the reader to analyse particular lunar return flights.

A. THE TRAJECTORY MODEL

The analytic model upon which this study is based was first presented by V. A. Egorov in 1956 [1].* In this model, all motion in cislunar space, i. e., motion in the gravitational field of the earth-moon system, is considered to be the result of two independent inverse-square force fields, that due to the earth and that due to the moon. Thus the perturbations of the sun and the planets are ignored. Further, Egorov divides earth-moon space into two regions such that only the moon's gravitational field is effective in one region and only the earth's gravitational field is effective in the remaining region. The dividing surface is defined as the locus of points at which the ratio between the force with which the earth perturbs the motion of a third body and the force of attraction of the moon is equal to the ratio between the perturbing force of the moon and the force of attraction of the earth. For the earth-moon system, this surface is approximately a sphere whose center is coincident with the center of the moon. The radius of this sphere is given by

$$r_s = 0.87 r_m \left(\frac{m}{M}\right)^{2/5} \cong 31,000 \text{ nautical miles}$$

where r_m = distance of the moon from the earth, and m/M = ratio of the mass of the moon to the mass of the earth.

Henceforth, this sphere will be referred to as the moon's sphere of action, or the MSA.

*Bracketed numbers refer to the list of references.

Due to the eccentricity of the lunar orbit, which is about 0.06, the distance of the moon from the earth will vary by about 10 percent during a lunar month. To be precise, the above value of r_s should change by this amount; however, the effects of the original simplifying assumptions will outweigh those due to variations in r_s.

Since each of the two regions defined above contains only the force field of its respective body, which is assumed to be an inverse square force field, all motion in the model will consist of conic sections. For the particular class of trajectories delt with in this report, the motion will initiate in the vicinity of the moon, or within the MSA, and terminate near the earth. This will require that the trajectory pass through the surface bounding the MSA. During the period in which the vehicle is within the MSA the moon has rotated through an angle about the earth. This is equivalent to the earth rotating about the moon through the same angle where the MSA is assumed fixed in inertial space. Also, since the same lunar face remains pointed to the earth, except for librations, the moon will seem to revolve about its axis through the same angle within the sphere of action. For typical moon-to-earth trajectories this angle will be about 6 degrees. To an outside observer, the conic within the MSA will be non-rotating. This effect is shown in Figure 1.

Once the vehicle has arrived at the surface of the MSA, it is necessary to transform its position and velocity to an earth-centered inertial coordinate system. This can be easily accomplished if the position and velocity of the moon are known at the time the vehicle passes through the surface. Specifically the earth referenced coordinates are given by,

$$x = \bar{y} + \bar{x}_m$$

$$u = \bar{v} + \bar{u}_m$$

where $(\bar{y}, \bar{v})$ are the vehicle's position and velocity referenced to the moon and $(\bar{x}_m, \bar{u}_m)$ are the moon's position and velocity referenced to the earth. All of these variables are, of course, three dimensional vectors. As shown in Figure 1, to an outside observer there will be no discontinuity in position

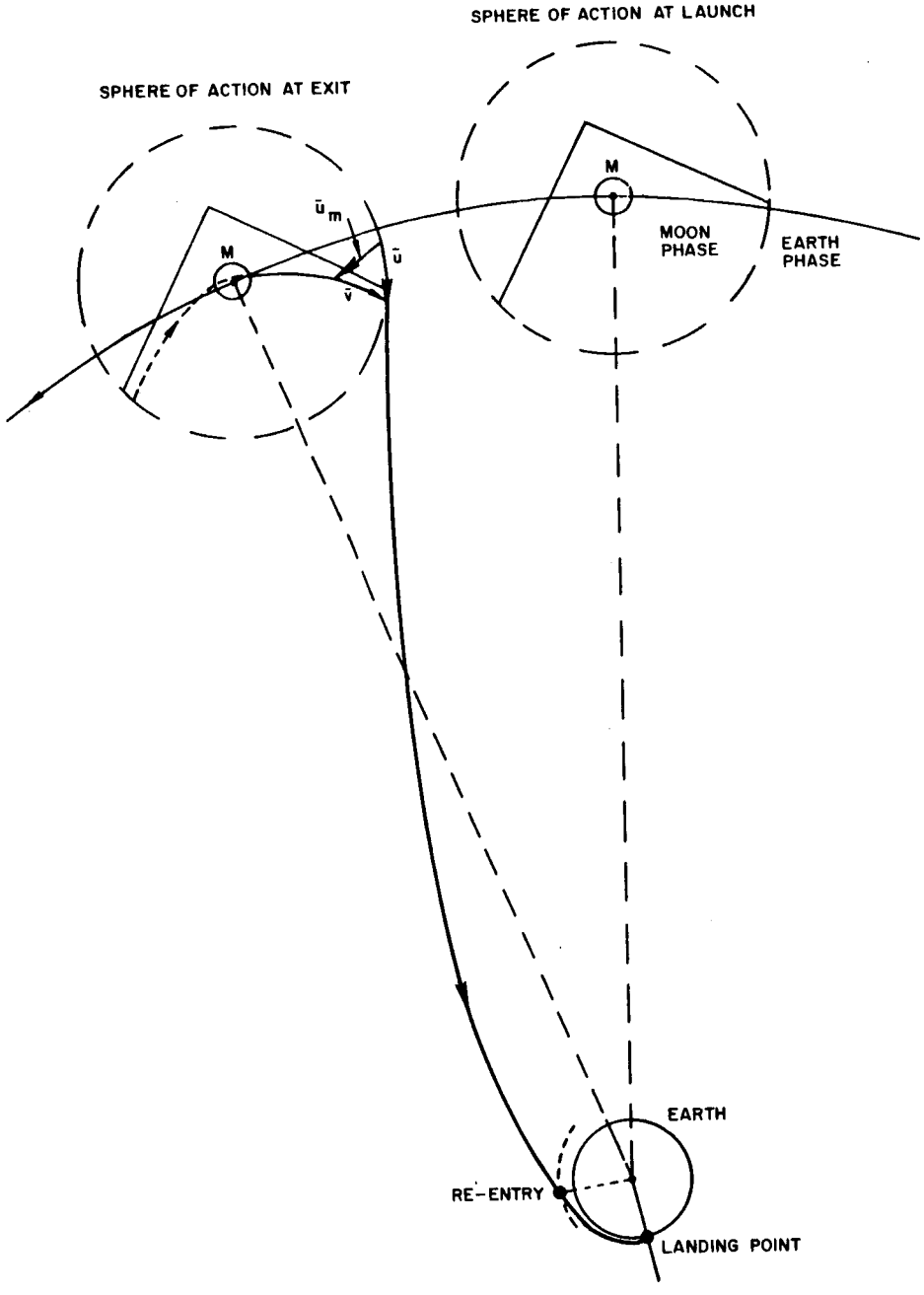

Figure 1. Schematic of Moon-to-Earth Flight.

but there is an apparent discontinuity in the velocity since we have drawn both moon-frame inertial and earth-frame inertial phases of the trajectory in the same picture.

The following additional assumptions will be made for the analysis presented in this report:

(1) In both moon and earth phases, only that section of the conic which lies on one side of the major axis will be considered.

(2) No powered flight maneuver is inserted in the nominal trajectory between lunar burnout and re-entry into the earth's atmosphere.

B. APPLICATIONS OF THE ANALYTIC PROGRAM

The analytic computing program based on the model described is useful in three areas:

(1) The analytic formulation allows a very high computational speed in comparison with an integrating program. It then becomes possible to perform very elaborate parametric studies which only the speed of an analytic program will allow with reasonable machine time. To facilitate such studies, search loops have been provided in the analytic program to solve the "split-end-point" problem where some useful independent variables are specified at initiation and others at termination of the trajectory, and the remaining conditions are sought.

(2) The program supplies quite accurate approximate lunar burnout conditions for use with an n-body integration program and linear iteration routines to determine "exact" trajectories. To aid in this possibility, the ephemeris tapes used in the n-body program are also used in the analytic program.

(3) The program may be made a part of other analytic programs requiring highest speed, such as a Monte Carlo guidance analysis program [2]. The Sensitivity Coefficient Routine of the program takes lunar burnout conditions, introduces incremental changes in each variable, and determines resulting perturbations at the earth. In a similar manner the routine computes effects on terminal conditions of midcourse corrections. By varying the size of the burnout or midcourse perturbations nonlinear effects may be examined. This ability to simulate accurately nonlinear behavior together with high computational speed makes practical a Monte Carlo simulation of midcourse guidance freed of the necessity for the usual linearity assumptions.

II. THE ANALYTIC PROGRAM

A. INDEPENDENT PARAMETERS

The motion of a body in any three dimensional gravitational field is limited to seven degrees of freedom. This is exclusive of the motion about its center of gravity, which does not concern us here. The motion of the body, i. e., center of gravity, is specified, for example, by its position and velocity (6 quantities) and the time at which it has these values. In the case of lunar trajectories, specifying these quantities will tell us very little if anything about the general nature of the motion, and certainly will not tell us what future values will be unless an integration, or approximate calculation of the trajectory is made. Therefore, as mentioned in Section I, it is much more convenient to specify an equivalent set of quantities, some at the start of the trajectory and some at the end, and to solve the split-end-point problem in the program. There are two limitations on this process: First, the number of independent (input) variables must not exceed the degrees of freedom of the trajectory motion. Second, within the chosen set of independent variables there may exist a set of restricting relationships or constraints which exclude certain numerical combinations among the variables. (Such restrictions do occur among the parameters chosen for the program and are discussed in Section IV). To aid in this process, the ephemeris tapes used in the n-body program are also used in the analytic program.

The following parameters have been chosen as input quantities in the program (see Figure 2):

(1) the selenographic (lunar surface) longitude and latitude of the launch site,

(2) the day of launch,

(3) the lunar powered flight angle from launch to lunar burnout,

(4) the burnout altitude,

(5) the re-entry maneuver downrange angle and maneuver time to touchdown (landing),

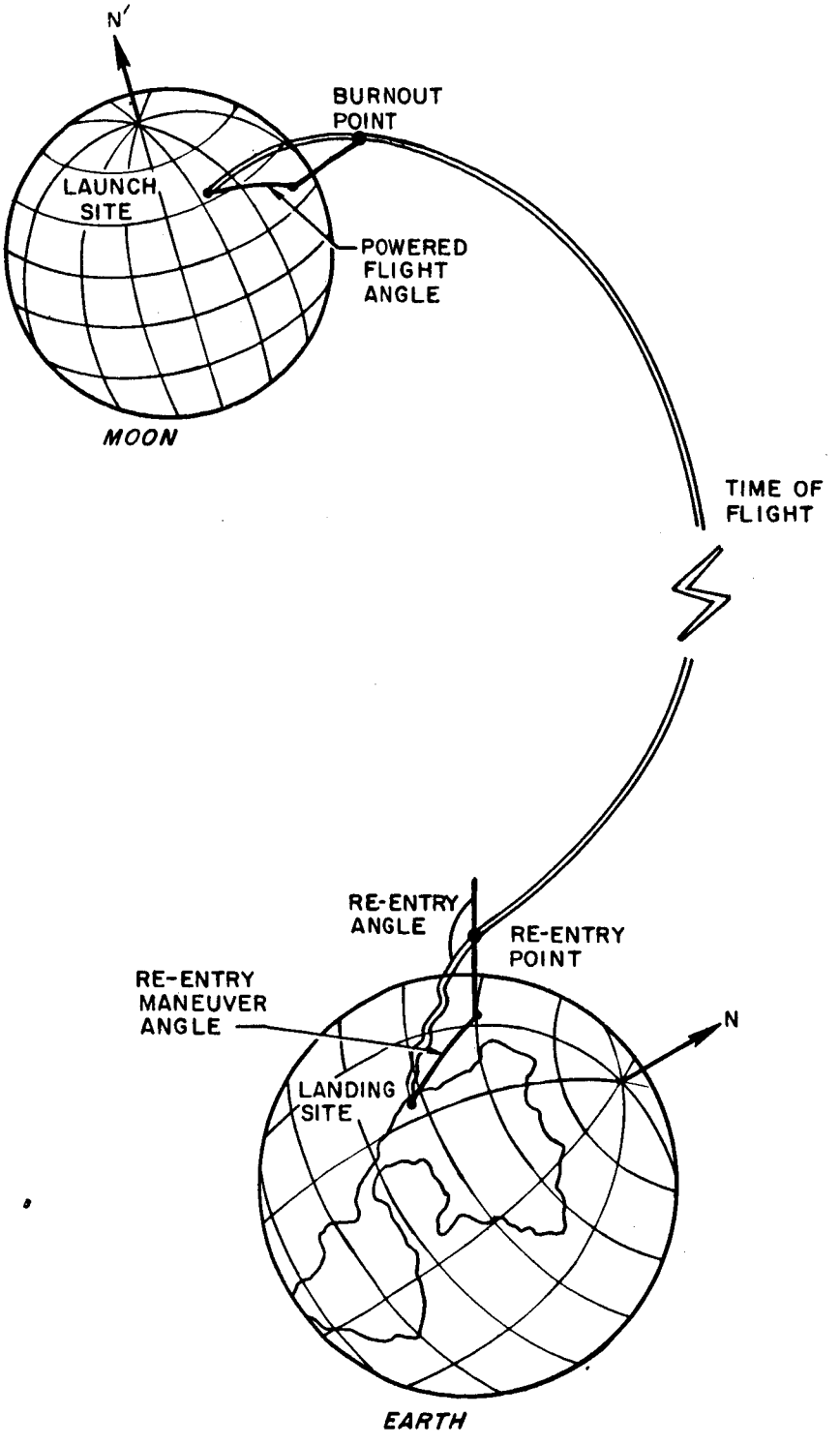

Figure 2. Location of Independent Parameters.

(6) the longitude and latitude of the landing site,

(7) the re-entry flight path angle,

(8) the re-entry altitude,

(9) the total time of flight.

It should be clear that not all of these parameters individually represent degrees of freedom. They are interrelated. The parameters which may be considered essentially independent are:

(1) the launch site latitude

(2) the launch site longitude

(3) the burnout altitude

(4) the landing site latitude

(5) the re-entry flight path angle

(6) the re-entry altitude

(7) the combination of day of launch, landing site longitude and the total time of flight.

To indicate the relationships of the remaining parameters with these: (a) the lunar powered flight angle will simply adjust the selenographic latitude and longitude at burnout, or initiation of free flight, (b) the re-entry maneuver angle will do the same for the termination latitude and longitude of free flight, (c) the maneuver time will adjust the time of free flight.

It is possible to gain some insight into the nature of (7) with the aid of Figure 3. Specifying that the trajectory satisfies all input conditions on a particular day implies that the distance, equatorial latitude and longitude of the moon will change only slightly during the search for that trajectory. Thus, trajectories which are launched on the same day and satisfying all the input quantities except the longitude will be very similar in nature. It should be clear that to do this, i. e., satisfy all conditions but the longitude, it is possible to launch from the moon at any time on the given launch date. In addition, since the earth makes a complete revolution in a single day, it is possible to

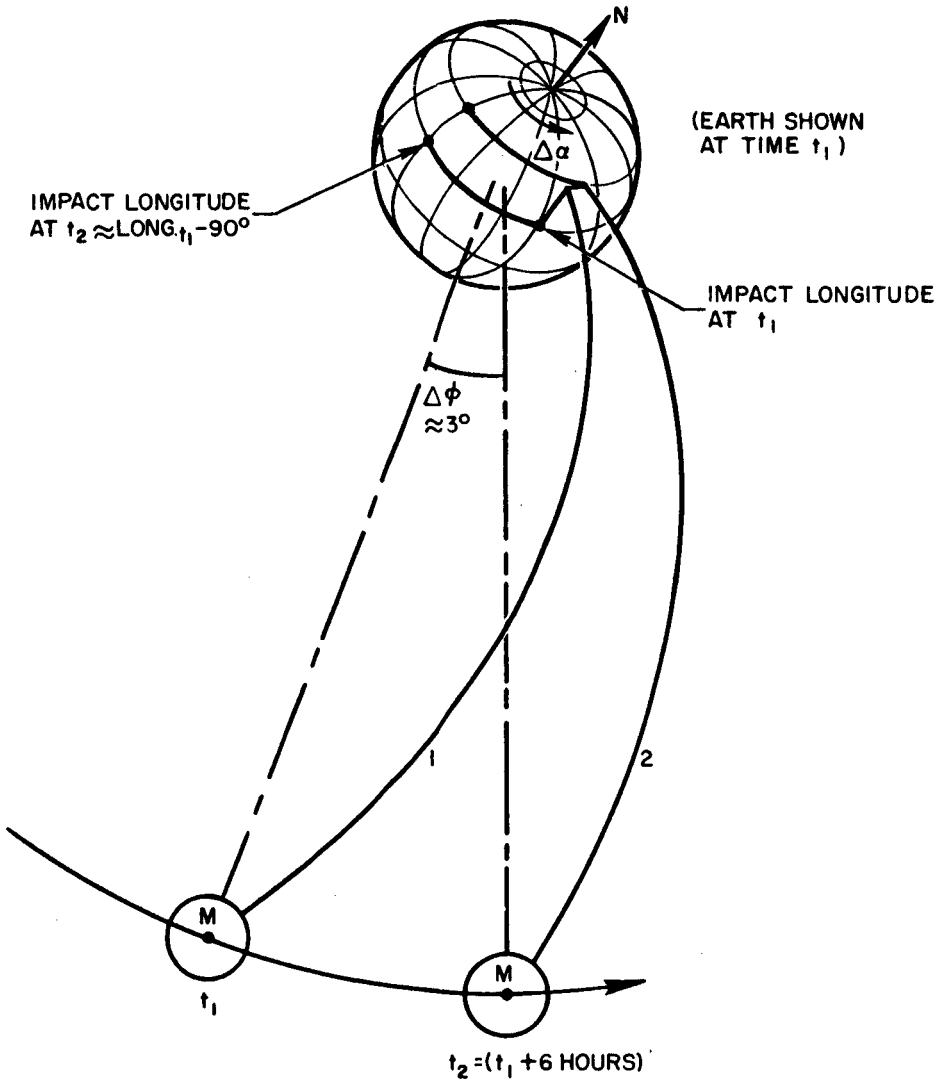

Figure 3. Impact Longitude-Launch Time Relationship.

satisfy the longitude condition by launching from the moon at a specific time of day. This launch time measured from midnight of the launch date will depend on the required longitude, the time of flight and the earth-moon phase relationship on the day of launch.

B. PROGRAM LOGIC

Having established the analytic model, the means by which the positions, velocities and transformations of bodies within the model are to be obtained (i. e., ephemeris tapes), and a set of trajectory input parameters, it is possible to proceed to the problem of building the computer program. If it were possible to begin with the program inputs, and solve the equations explicitly for all of the desired unknown parameters, the program logic would be very simple; however, due to the nature of the equations involved it is not possible to do this. Instead, many of the important conic parameters are implicit in the equations and must be found by iterative methods. The procedure used in this program is a direct iteration method such that whenever a quantity is unknown in value an approximation is assumed and used in succeeding calculations. If when using these approximations certain criteria are not met then succeeding and presumably better approximations are found based on relations which will force these criteria to be met. This procedure had been found previously to work very well in a simple version of an earth-to-moon program. No attempt was made here to determine, a priori, the convergence or rate of convergence of the method for this application, although such an estimation is believed possible.

Consider now the criteria which must be met in obtaining a solution. First, the complete free flight portion of the moon-to-earth trajectory will consist of two conics, one in the moon phase and one in the earth phase, with the position, velocity and time at the moon's sphere of action identical for both conics. The method used in satisfying these conditions is to use the vehicle's earth phase velocity at the MSA to aid in determining the moon phase conic and to use the vehicle's moon phase position at the MSA to aid in determining the earth phase conic. The time of launch from the moon is determined such that the time of the moon phase conic at the MSA will match that of the earth phase conic.

Referring to Figure 4, the sequence of the calculations involved in solving for the trajectory which satisfies the input requirements will now be discussed in detail. Some of the notation used in the figure is explained on page iv under General Notation. The remainder will be defined as the discussion progresses. An enlightening way of representing moon-to-earth trajectories is shown in Figure 4a. To obtain this figure, the moon-to-earth trajectory is first projected onto a non-rotating earth. Figure 4a then represents a Mercator Projection of the earth's surface onto a plane using the equatorial plane as a base plane and the vernal equinox as a reference meridian. The advantage of this figure is that it clearly indicates the location of the earth phase conic elements i, Ω and the point P. Moreover, since the majority of the trajectory will lie in the earth phase, and hence be planar, this figure will aid in solving the "earth phase geometry" of the trajectory by means of spherical triangles. The solution of the earth phase trajectory is also aided by Figure 4b. This figure shows the plane of motion of the earth phase trajectory where the dotted circle represents the re-entry surface to the earth's atmosphere. The determination of the conic elements a (semi-major axis) and e (eccentricity) are based on the parameters shown in this figure.

The sequence of calculations required for the solution of the moon-to-earth trajectory is the following:

1. The conic elements a and e are determined from the four quantities x_r, x_s, β_r and T_{sr} (see Figure 4b). In the first calculation of the earth phase, the distance to the sphere of action x_s and the time of flight from the MSA to re-entry are approximately taken as the distance to the moon and the total time of flight (minus the re-entry maneuver time T_r). Due to nature of Kepler's equations, a and e cannot be solved for explicity in terms of these parameters, however, an iteration scheme has been devised which will provide a rapid solution to the transcendental equations involved [3]. The values of a and e together with the gravitational constant of the earth completely define the in-plane conic from which velocities at S and R, and the angles η_{sr} and η_{pr} may be calculated.

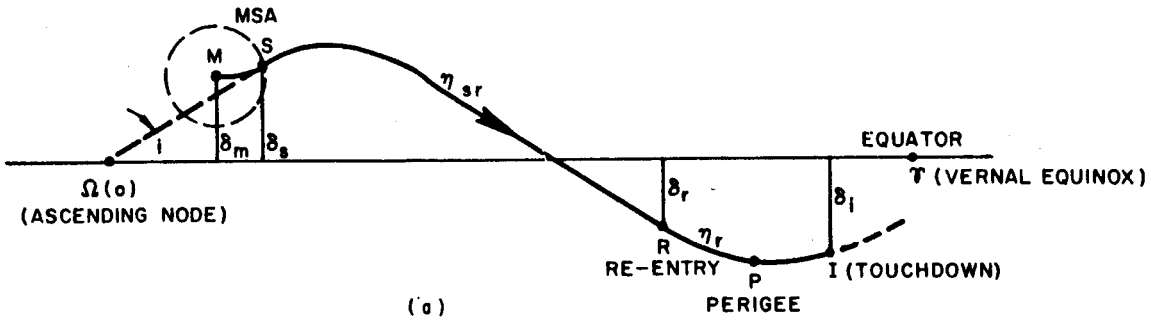

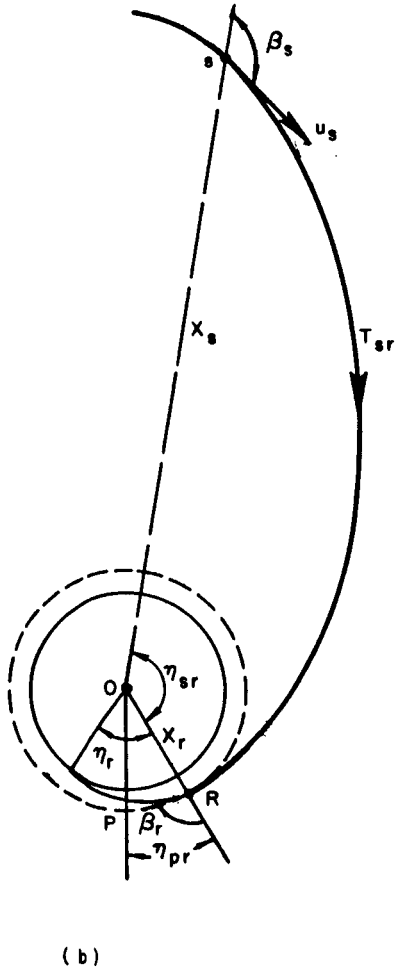

Figure 4. Solution of the Earth Phase Conic.

2. Next, the angular elements i, Ω and ω (angular position of perigee) may be found with the aid of Figure 4a. The given quantities will be δ_i, δ_s, η_r and η_{sr} where η_{sr} (shown in Figure 4b) has been obtained in 1. above. Spherical trigonometry may then be used to solve for the remaining elements of the earth phase conic. The first approximation to the latitude δ_s is taken to be that of the moon.

3. Having found the elements of the earth phase conic, there exists a straightforward procedure for finding the cartesian coordinates of the position and velocity of the vehicle at point S, or the MSA. It is first necessary to set up a rectangular coordinate system in the plane of motion, which is done with the x-axis passing through the ascending node. The position and velocity at S in this coordinate system are easily found knowing the distance x_s and the angles η_{os} and β_s. The transformation of resulting cartesian coordinates may then be found in the equatorial coordinate system by rotating the former system through the inclination angle i and the right ascension of the node Ω.

4. Independent of the calculation of the position and velocity at point S is the calculation of the time of re-entry and hence, by subtracting off the estimated time between point S and R, the time that the vehicle must arrive at point S. This time calculation may be made in the earth phase because the right ascension of point S is approximately known. This, with the solution to the spherical triangles in Figure 4a gives the right ascension of the touchdown point which, knowing the sidereal time of the day of touchdown and the longitude, leads to the Greenwich time of touchdown.

5. Having an estimate of the time that the vehicle is at point S allows one to find the position and velocity there with respect to the moon. This is accomplished by reading the ephemeris tape at time t_s for the moon's position and velocity. Then, the coordinates at point S with respect to the moon will be,

$$\bar{y}_s = \bar{x}_s - \bar{x}_m$$

$$\bar{v}_s = \bar{u}_s - \bar{u}_m$$

where the General Notation is being used for position and velocity. In the first iteration, the values of $\bar{x}_s$ and t_s are only first guesses. Later iterations will cause $\bar{x}_s$ and t_s to converge such that the magnitude of $\bar{y}_s$ will appraoch R_s, the radius of the sphere of action.

In the calculation of the moon phase conic, the velocity of the vehicle at the MSA is assumed to have the direction of $\bar{v}_s$ and a magnitude such that its energy is equal to the vehicle's moon phase energy at point S.

6. This exit velocity vector at the MSA is the only quantity taken from the earth phase computation in calculating the moon phase conic. Before discussing this calculation, it should be noted that the velocity $\bar{v}_s$ will be in a moon centered inertial cartesian coordinate system, whereas the launch site is in the rotating selenographic coordinate system. Since the model assumes that the moon phase conic is fixed in inertial space, the coordinate system most convenient to work with is the inertial selenographic system. The calculation of $\bar{v}_s$ in this system requires the instantaneous transformation from the equatorial coordinate system to the selenographic coordinate system. This transformation has been generated along with the position and velocity of the moon and is available on the ephemeris tapes.

7. Referring to Figure 5 the calculation of the moon phase conic may now be made. The vectorial locations of the launch site and the velocity vector $\bar{v}_s$ will determine the plane of motion. These two vectors also determine the in-plane angle $\bar{\eta}_{bs} + \bar{\beta}_s$ (having subtracted off the powered flight angle $\bar{\eta}_{pf}$). The conic elements $\bar{a}$ and $\bar{e}$ (bars indicate moon phase) may then be determined knowing the two distances y_b and $y_s = R_s$ to the conic, the angle between b and s, and the velocity v_s. The angle $\bar{\eta}_{bs}$ is not known exactly, but may be approximated in the first iteration by setting $\bar{\beta}_s = 0$. These quantities give an explicit solution for $\bar{a}$ and $\bar{e}$. Also, since the vectors $\bar{y}_o$ and $\bar{v}_s$ determine the plane of motion, it is possible, as was done in the earth phase, to find the transformation which takes the in-plane points along the conic to vectors in the inertial selenographic system.

8. The calculations presented thus far almost complete the loop required in the determination of the trajectory satisfying the given input

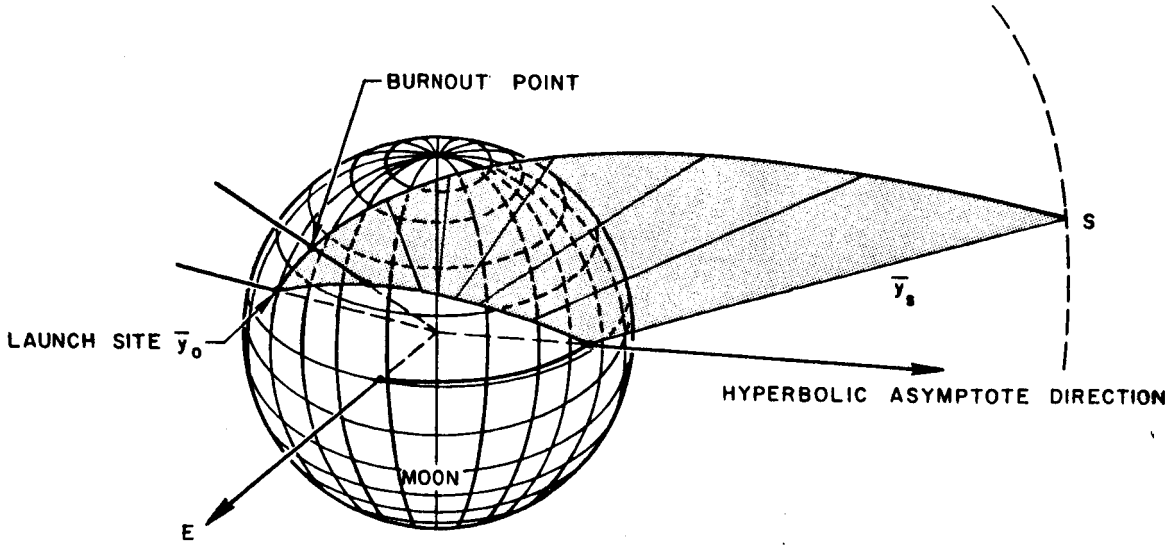

(a)

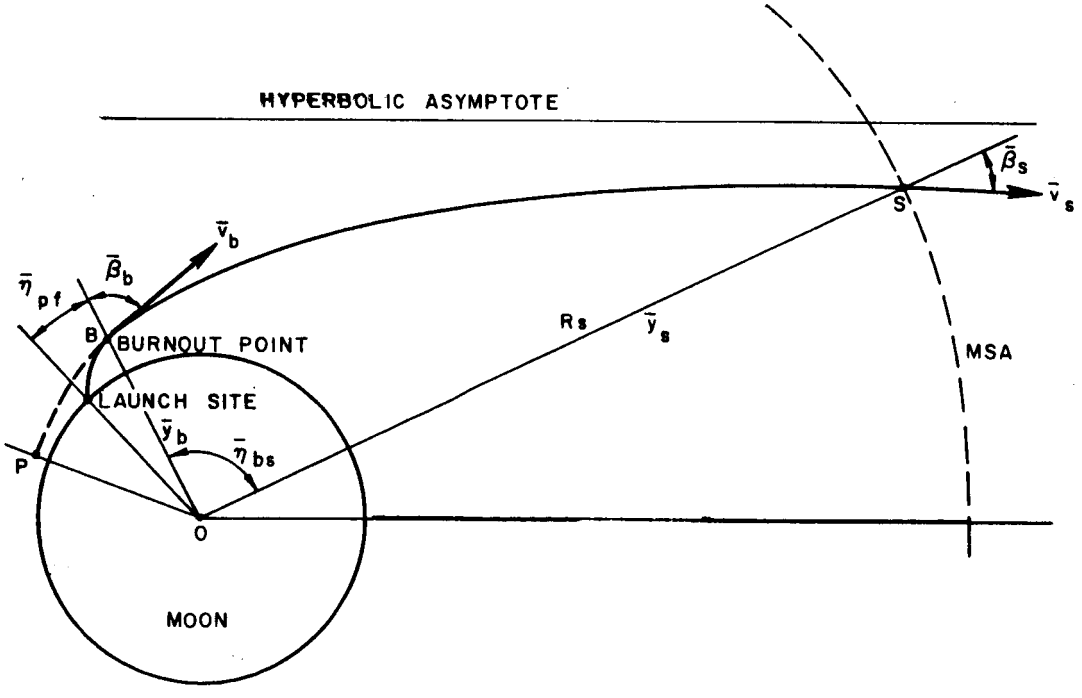

Figure 5. Moon Phase Geometry.

conditions. All that remains is a calculation of the time during which the vehicle is within the sphere of action and the point at which the vehicle penetrates the MSA. These improved values are then used in the second iteration of the earth phase conic. Successive calculations of the earth phase trajectory and the moon phase trajectory continue until given tolerances in the vehicle's position and velocity at the moon's sphere of action are met. It has been found that the total number of loops required for convergence when the tolerances are about 10,000 feet in distance and 2 fps in velocity will range from 4 to 9 as the time of flight varies from 30 hours to 90 hours.

With an understanding of the calculations involved, it is possible to follow the logic charts presented in the next three pages. The General Logic simply re-iterates the calculations and the search loop which have just been discussed. The Earth Phase Logic introduces two things which have not been touched upon. The first is the iteration loop required to solve for the time of impact and hence the time of launch. This iteration is necessary because, although the position of the vehicle at the MSA is known with respect to the moon (since it is calculated in the moon phase), it cannot be found with respect to the earth until the time the vehicle is at the MSA is known. But this time depends on the earth phase geometry which itself depends on the position of S. This "Time of Launch" iteration converges very rapidly due to the slow rotation of the moon around the earth. The second item indicated on this chart is the possibility that no solution exists which will satisfy the input conditions. This possibility corresponds to the most important constraint on the allowable values of the trajectory variables and will be explained in detail in Section IV.

The Moon Phase Logic presented in Figure 8 also indicates the possibility that no solution exists in the calculation of the moon phase conic. This is simply due to the fact that there are sites on the moon from which it is impossible to launch a direct ascent trajectory, such as the back side of the moon. A method for determining specifically when this will be the case is covered in Section IV.

GENERAL LOGIC

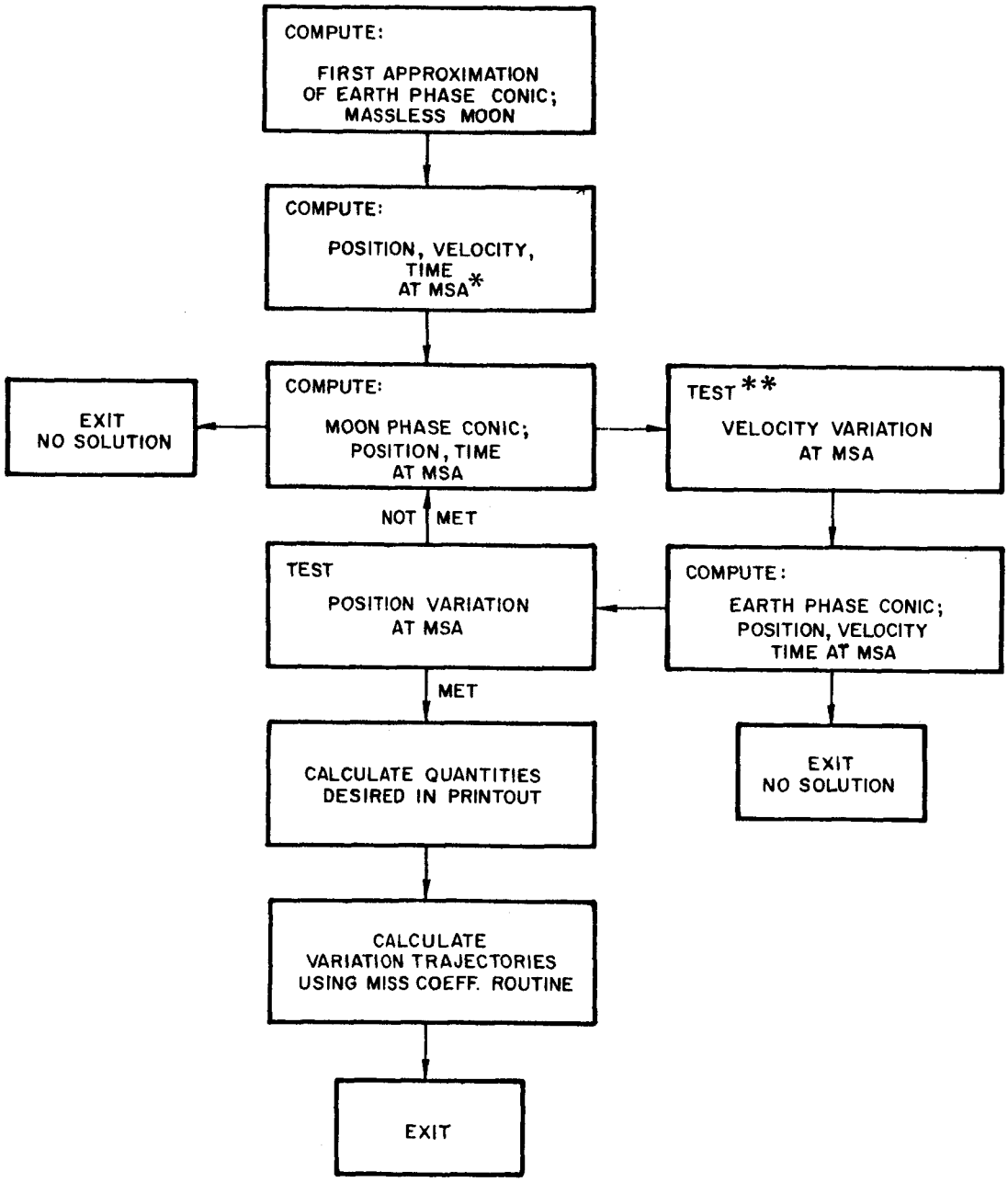

* MSA = MOON'S SPHERE OF ACTION.

** THE SUCCESS OF THIS TEST IS REGISTERED, AND IF THE POSITION TEST IS ALSO SATISFIED, THE PROGRAM EXITS THE SEARCH LOOP.

Figure 6. General Logic Block Diagram.

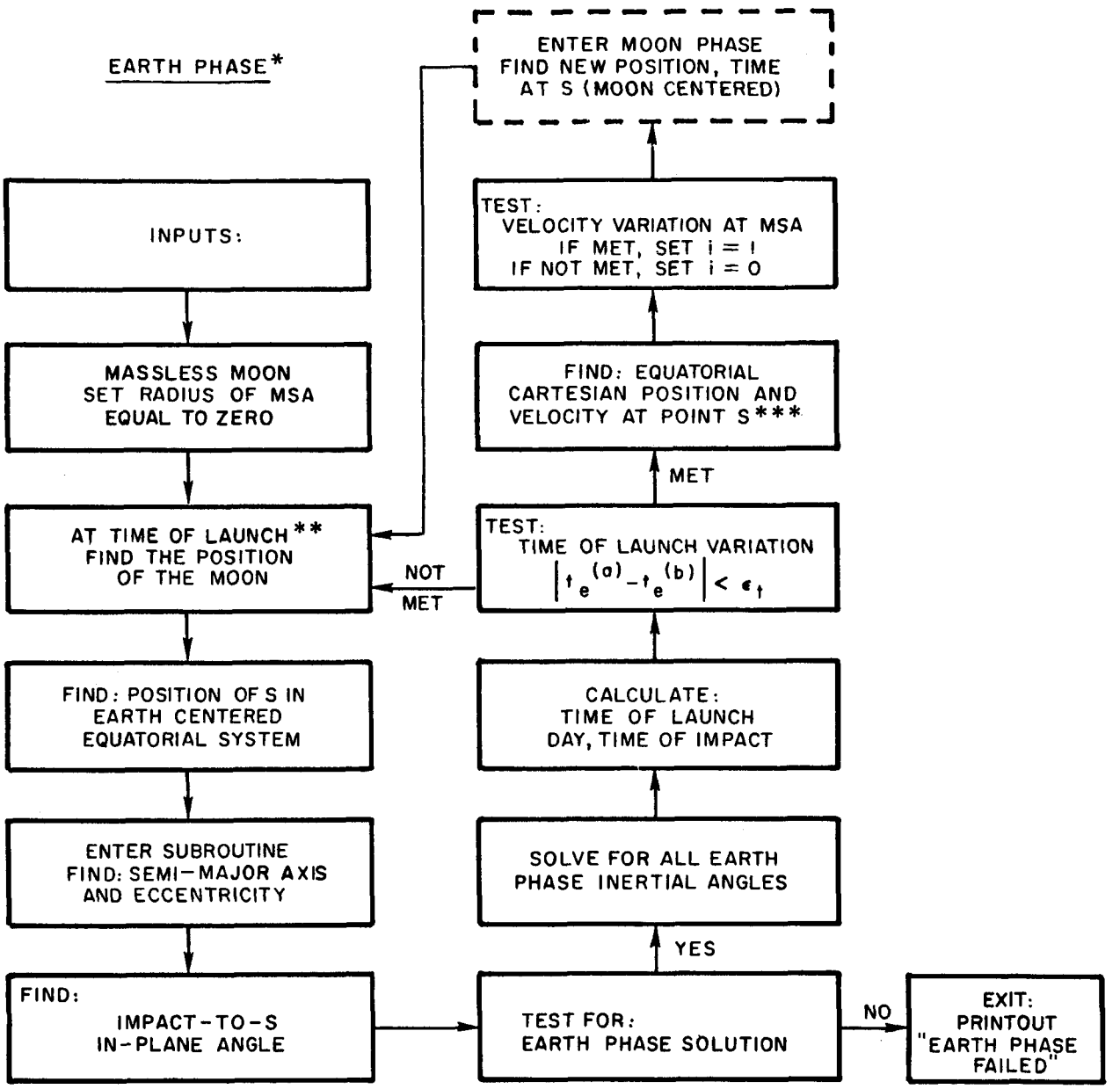

* ALL POSITIONS AND VELOCITIES ARE EARTH CENTERED.

** USE 0^h (GMT) UPON FIRST ENTERING THE LOOP

*** THE EQUATIONS ARE SLIGHTLY DIFFERENT FOR A MASSLESS MOON.

Figure 7. Earth Phase Logic Diagram.

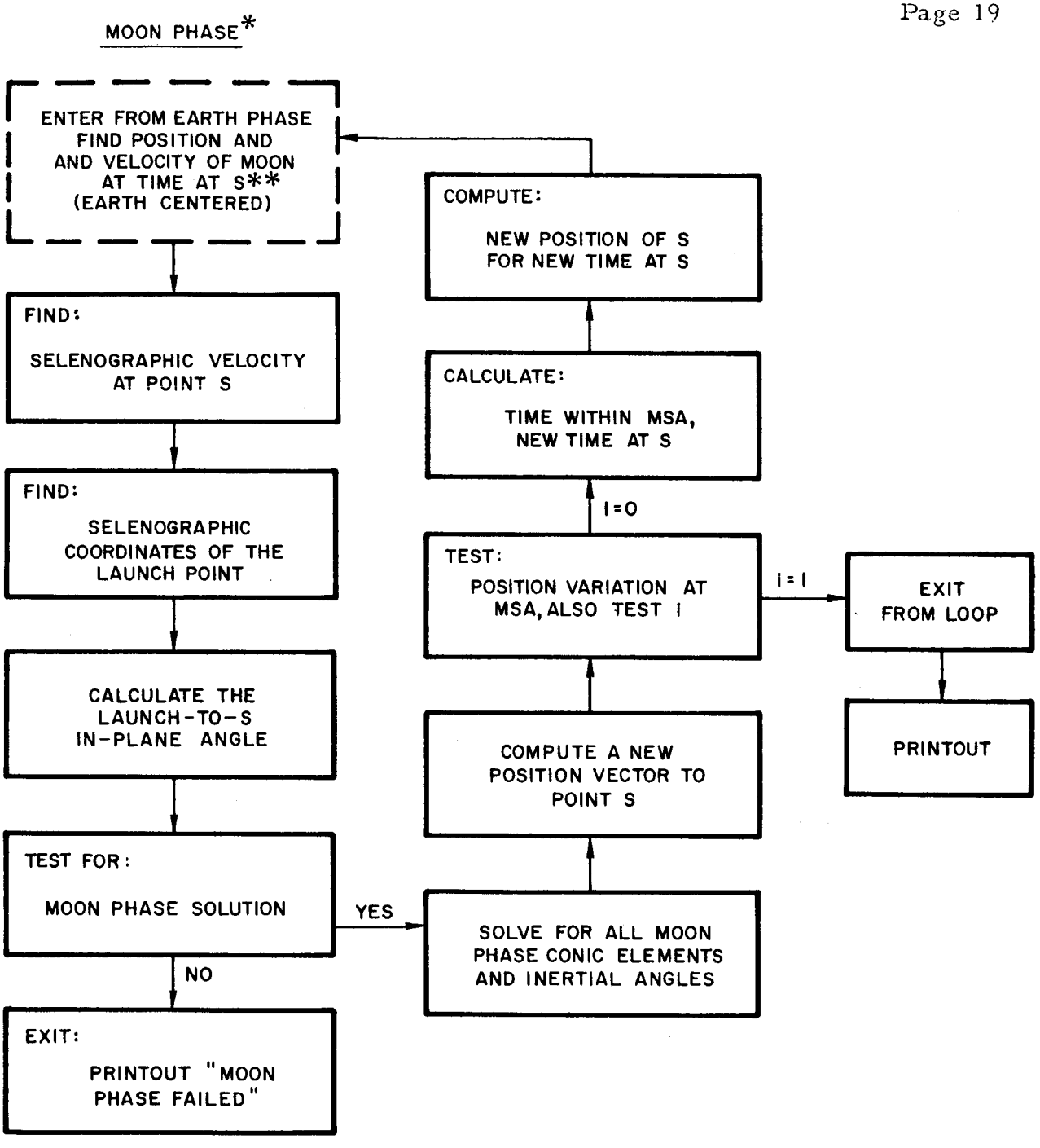

* ALL POSITIONS AND VELOCITIES ARE MOON CENTERED UNLESS OTHERWISE SPECIFIED.

** THE SYMBOL S DENOTES THE POINT OF ENTRY OF THE TRAJECTORY AT THE MSA.

Figure 8. Moon Phase Logic Diagram.

C. SENSITIVITY COEFFICIENT ROUTINE

The analytic program which has just been discussed has been specifically designed to solve the split end-point problem. It is also of interest to calculate various parameters along the trajectory, such as position and velocity and, for the purpose of guidance analysis, to determine sensitivity coefficients of end point parameters with respect to initial or midcourse variables. The logic of this problem is sufficiently different from the search problem just discussed to warrant an independent program.

The inputs to this program, called the Sensitivity Coefficient Routine, are the initial or lunar burnout conditions which may be obtained from the search program. These initial conditions are the day of launch, time of lunar burnout, and six coordinates of position and velocity at the lunar burnout point. The position and velocity may be specified either in the selenographic or equatorial system and in cartesian or polar form.

The preliminary calculation performed by the program consists of finding the terminal conditions from this set of input parameters. This is done simply by solving for the conic elements which, in turn, may be used to find the position, velocity and time of the trajectory at the sphere of action. The position and velocity of the moon are then obtained at this time and used to calculate the position and velocity of the vehicle with respect to the earth. These coordinates are then used to find the earth phase conic elements which may be used to find the re-entry point on the earth.

All of these are straightforward calculations; that is, all quantities may be found from explicit expressions and no iterations are necessary. It is clear that to produce the same terminal conditions that the search program does, exactly the same gravitational model must be used for both. This includes any empirical corrections such as those discussed in the next section.

Once the terminal conditions of the original (or nominal) trajectory have been found, the calculations of sensitivity coefficients and midcourse trajectory parameters may follow. The computation of both is straightforward. Position and velocity at a midcourse maneuver point in the moon phase (or earth phase) may be calculated in exactly the same manner in which the MSA (or terminal) calculation is made. By the nature of Kepler's equation it is convenient to

consider the midcourse distance as the independent variable; otherwise, if time were independent, an iteration would be required to solve for distance. The sensitivity coefficients at the burnout point, or midcourse points, are found by independently perturbing one of the position and velocity coordinates by some increment and then recalculating the terminal conditions. Subtracting the perturbed terminal conditions from the nominal conditions will then yield the terminal sensitivity coefficients for that particular coordinate variable. This may be done as soon as the midcourse (or initial) position and velocity coordinates have been found.

If the increments discussed above are small, then the sensitivity coefficients will approach the partial derivatives of the terminal conditions with respect to the coordinate variable. If they are large, then the sensitivity coefficients may represent difference ratios for some expected midcourse position or velocity correction. Aside from this possibility this method of differencing, by choosing different magnitudes of the increments, may be used to find approximations to higher order derivatives or to study directly the non-linearity characteristics of the sensitivity coefficients themselves.

III. PROGRAM ACCURACY

A. PRELIMINARY STUDY

The usefulness of any analytic model depends directly upon the accuracy with which it yields the true conditions which are being simulated. For this reason, it was necessary to carefully analyse a broad range of results obtained from the model and compare them with exact results. In addition, through study of the behavior of the deviations of the approximate from the true results it was possible to find a method by which the basic model may be made to yield greater accuracy. This section presents first, a comparison of the results from the original model to those from the exact model; second, the arguments which led to an empirical correction scheme; and finally, a comparison of the true results with those from the corrected model.

The preliminary results obtained from the original model are shown in Table 1. The "exact program" mentioned here solves for the exact trajectory (which includes earth, sun, moon, vehicle and oblateness perturbations) as a function of time by numerically integrating the second order differential equations of motion using Encke's method. Several trends may be noted. First, faster flight times result in greater overall accuracy. This may be expected since the size of the perturbations on the trajectory will be directly proportional to the duration of time in which they act. The second noticable trend is that the greater the re-entry angle (steeper) the more accurate the results. This, of course, is due to the nonlinear effect of the trajectories intersecting the spherical earth. It is expected that the same perturbation acting on a trajectory having a shallow re-entry as acting on one having a steep re-entry may cause the former to miss the earth completely while indicating fair accuracy for the latter. Also, if one looks carefully at the impact longitudes obtained from the exact program, he will notice that in all cases the actual re-entry point is east of the desired re-entry point. A later examination into the nature of the lunar perturbation will explain why this is so. Next, although not enough cases are presented in Table 1 to indicate this, the accuracy is dependent on the lunar date of launch and, in particular, on

Table 1. Comparison of Results from Original Model with Results from an Integrating ("Exact") Program

Analytic Program				Integrating Program*				
Time of Flight (hr)	Re-entry Latitude (deg)	Re-entry Longitude (deg)	Re-entry Angle (deg)	Time of Flight (hr)	Re-entry Latitude (deg)	Re-entry Longitude (deg)	Re-entry Angle (deg)	Perigee (E. R.)
50	30	-104	170	50.2	29.9	-94.1	163.7	----
60	30	-104	160	60.5	23.8	-90.1	149.4	----
60	30	-104	140	60.6	16.4	-90.8	127.5	----
60	30	-104	120	60.7	-5.2	-84.1	97.0	----
60	30	-104	100	60.5	----	----	----	1.28
75	30	-104	140	75.9	4.5	-79.6	116.8	----
75	30	-104	120	75.9	----	----	----	1.08
90	30	-104	170	90.6	19.5	-67.8	148.7	----
90	30	-104	140	91.0	13.6	-76.8	121.4	----
90	30	-104	120	91.0	----	----	----	1.19
90	30	-104	110	89.2	22.9	-21.0	141.0	----**

*All cases shown have counterclockwise re-entry.

**Different launch date.

the distance of the moon from earth. Finally, the one parameter which indicates best results for the cases shown in Table 1 is the total flight time.

To improve the accuracy of the basic model, it was first necessary to determine the specific source and size of the perturbations not accounted for in the analytic model and then attempt a correction. The procedure followed in doing this is summarized for two sample cases in Table 2. Here, the analytic program and the integration (exact) program are used in such a manner as to extract the information being sought. The desired trajectory conditions shown in the first row are inputs into the analytic program, and therefore, are satisfied for that model. The first run is identical to those of Table 1, i. e., the lunar burnout conditions as calculated in the analytic program are used in the exact program and the re-entry results tabulated in the four center columns. This run integrates the equations of motion numerically and includes the four bodies, sun, earth, moon and vehicle and the earth's oblateness. The second run is a repeat of the first except that the earth's oblateness term is removed from the equation's of motion. The lack of any difference (to three places at least) between runs 1 and 2 indicates that the perturbative effects of earth's oblateness on the trajectory are negligible. Run 3, again a repeat of run 1 also has the sun removed from the equations of motion. The results in this case when compared to run 2 are not negligible but still quite small when compared with the total differences of the exact run and the analytic run. At this point, the conclusion may be drawn that the major part of the perturbations not included in the analytic model are due to the earth-moon system itself.

Runs 4 and 5 were made to determine the effects of the earth on the moon phase (within the MSA) portion of the trajectory and the effects of the moon on the earth phase portion of the trajectory respectively. That is, run 4 integrates the complete equations of motion up to the penetration of the sphere of action and then removes the sun and moon for the remaining part of the trajectory. This is equivalent to including only the earth's central force field in the earth phase. Run 5, on the other hand takes the position and velocity of the vehicle at the MSA as calculated in the analytic program and integrates the complete equation's of motion to re-entry. The resulting trajectory then

Table 2. Earth-Lunar Perturbation Summary

RUN	DESCRIPTION OF RUN	Flight Time (min)	Re-entry Longitude (deg)	Re-entry Latitude (deg)	Path Angle (deg)	EXPLANATION OF RESULTS
-	Desired Trajectory Conditions	3600	-104	30	140	These are the inputs to the analytic run
1	Integration Run with the Analytic Input at Burnout	3626 (3600)*	-90.4 (-81.6)	17.6 (40.6)	128.8 (150.3)	This integration run includes all bodies and Earth's oblateness
2	Integration Run with Earth's Oblateness Omitted	3626 (3600)	-90.4 (-81.6)	17.6 (40.6)	128.8 (150.3)	This run indicates that the effect of oblateness is negligible
3	Integration Run with Sun Omitted	3624 (3600)	-90.8 (-82.6)	18.3 (40.2)	129.1 149.9	This run indicates that the effect of the Sun is small
4	Integration Run with the Sun and Moon Removed from the MSA to Re-entry	3589 (3571)	-93.9 (-96.8)	26.5 (30.4)	136.2 (139.5)	This indicates the effect ofthe Earth's perturbation in the Moon phase
5	Integration Run Using the Analytic Input and Starting at the MSA	3647 (3622)	-100.3 (-91.1)	20.3 (38.2)	131.4 (148.6)	This run indicates the effect of the Moon's perturbation in the Earth phase
6	Integration Run Using the Analytic Input and Starting at the MSA; No Sun and Moon	3600 (3600)	-103.5 (-103.1)	30.2 (30.0)	140.0 (140.0)	Verification that the integration and analytic results are the same if the same model is used

*Values in parentheses correspond to clockwise re-entry, other values to counterclockwise re-entry.

has only the moon's force field in the moon phase. A glance at the results obtained from these two runs (and others made but not shown here) indicates that the effect of the moon on the earth phase trajectory is 2 to 3 times as great as the effect of the earth on the moon phase trajectory. Knowledge of this fact is helpful in the analysis made in the next paragraph. Run 6 is identical to run 5 except that the sun and moon are removed from the exact integration. This run simply verifies that the results from the integration will be identical to those from the analytic program if the gravitational models are identical.

B. CORRECTION SCHEME

The preliminary study just discussed points out that any effort in correcting the basic analytic model should be centered about the earth-lunar perturbational effects. In this regard, several schemes were contemplated, including explicit analytic expressions which would periodically correct the osculating conic elements in the moon and earth phases. This scheme was quickly discarded for two reasons. First, the expressions themselves and the transformations required were so lengthy that the computer running time would be more than doubled. The second, and more important reason is that, as frequently is true for expressions of this kind, difficulty would arise for the special cases of near parabolic and in-plane motion (in-plane meaning that the conic element Ω becomes undefined). Other attempts at theoretically correcting the perturbational effects included a correction or variation of the vehicle's potential energy at the MSA, however, none of these methods gave consistent results.

Finally, it was decided that the best approach would be to correct empirically for the bias type error that existed in all of the runs made with the analytic program. The nature of this bias may be seen more clearly with the aid of Figure 9a. As indicated in the previous analysis, the greater perturbation is that due to the moon on the earth phase trajectory; but, as shown in the figure, the moon at this time has rotated in its orbit and will always lie to the east of the trajectory (as seen from the earth). The bias, then, is simply due to the moon pulling the trajectory eastward. A simple method of correcting this is shown in Figure 9b. An explanation of the

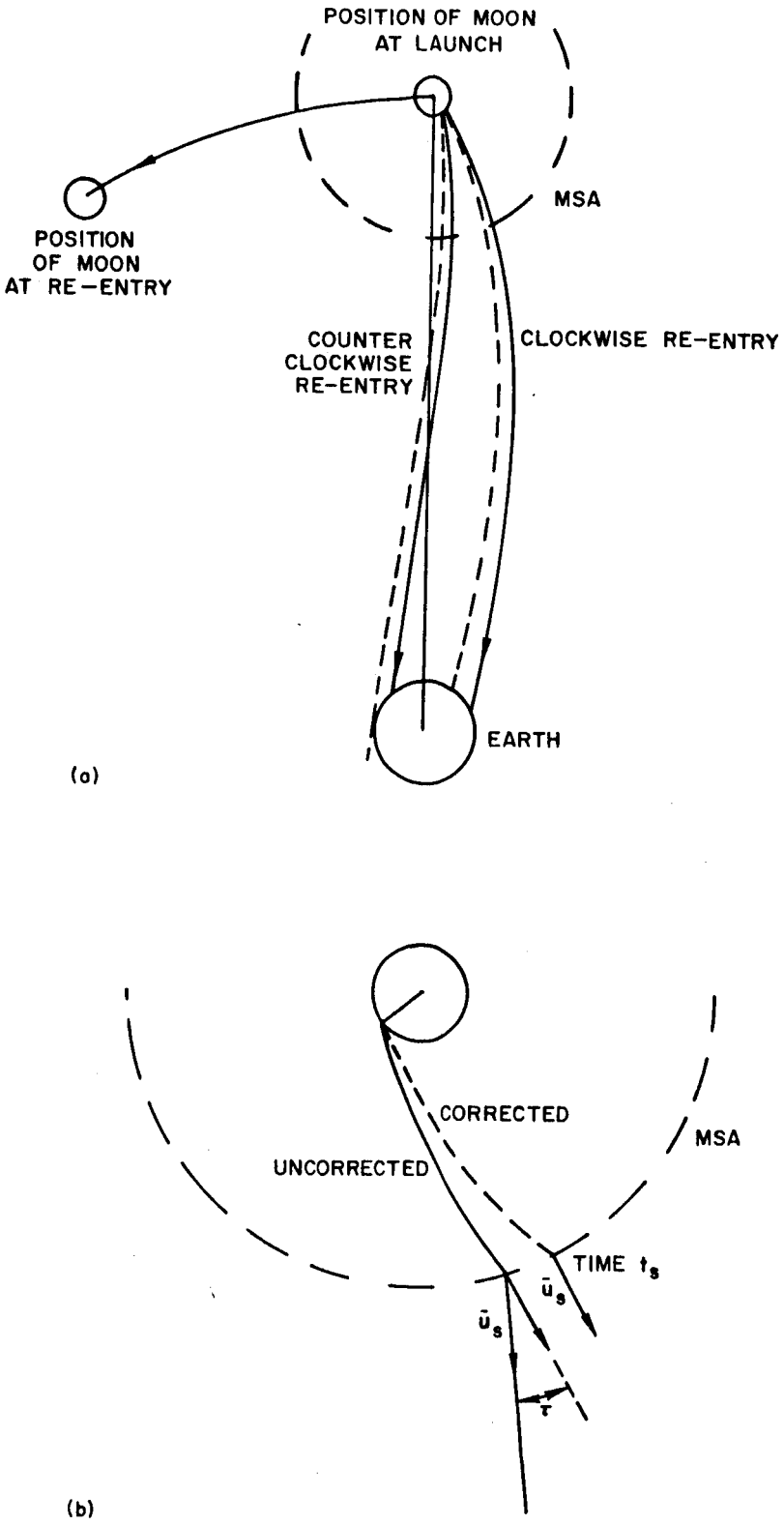

Figure 9. Tau Correction Scheme.

correction must be made in the context of the search method used in the analytic program. First, as discussed in Section II, the analytic program calculates an approximation to the earth phase portion of the trajectory. Then, the earth phase velocity at the MSA, as shown in Figure 9b, is computed and used, after subtracting off the moon's velocity at the time t_s, to calculate the moon phase conic. The correction is applied to this earth phase velocity. Specifically, the velocity is first projected into the earth-moon orbit plane and this projection rotated through the empirical angle τ. Thus, only that component of $\bar{u}_s$ which lies in (or parallel to) the moon's orbit plane is rotated. This rotation to counteract the unidirectional bias will always be counterclockwise. The effect of the rotation is primarily an adjustment of the moon phase conic as shown in Figure 9b. The earth phase conic will be only slightly changed with additional iterations. The justification for this correction is the fact that the perturbational effects on the earth phase trajectory will be primarily in the earth-moon plane and, more strongly, the fact that the correction does yield satisfactory results.

C. EVALUATION OF TAU

Investigations were next carried out to determine, first, the trajectory parameters on which the correction angle τ depends and second, an empirical expression which approximates this dependence. The procedure used in carrying out these investigations was first to allow τ to be an independent input into the analytic program. The lunar burnout conditions which the program calculated for various values of τ were then fed into the exact program and the results tabulated. Those trajectories whose re-entry conditions, as obtained from the exact program, most closely correspond to the desired entry conditions were considered to have used the optimum τ correction angle.

The variation of τ with respect to the following trajectory parameters was studied:

a) total time of flight,
b) re-entry approach; clockwise and counterclockwise,
c) re-entry angle,

d) lunar launch site location,

e) declination of the moon at launch (with the equator)

f) earth-moon distance at launch.

Table 3 presents some results on the study of the variation of τ with the time of flight. Here, the estimation of optimum τ is based primarily in obtaining the best value of the re-entry angle and then, of latitude and longitude respectively. In all cases, an attempt was made to choose τ such that the tolerances on the re-entry angle and the latitude were ±5 degrees and the longitude ±15 degrees. As expected, the value of τ is more sensitive to the time of flight than to any other parameter.

The study on all parameters was first made for counterclockwise re-entry. It was found that the location of the launch site had the least effect on the value of τ and that the lunar declination and the re-entry angle had only minor effects. These parameters were then considered to be invariant with respect to angle τ. This left the value of τ dependent only on the flight time and the earth-moon distance.

The expression for optimum τ with respect to the time of flight was then determined for the average earth-moon distance. The results are shown graphically in Figure 10a. Also shown in this graph is the variation of τ with the time of flight for clockwise re-entry. The results in this case were sufficiently different as to warrant a separate study. Following the study for clockwise and counterclockwise re-entry, it was found that both sets of empirical data could be easily approximated by quadratic expressions.

The effects of τ on the distance to the moon was then studied for trajectories having a total flight time of 90 hours. The results in this case, shown in Figure 10b, indicate a linear dependence of τ on the earth-moon distance. Again separate studies were required for clockwise and counterclockwise re-entry. The product of the quadratic and linear expressions resulted in the following expressions for the evaluation of optimum τ:

Table 3. Variation of τ with Total Time of Flight

	τ	Time of Flight (hr)	Re-entry Latitude (deg)	Re-entry Longitude (deg)	Re-entry Angle (deg)	Re-entry Direction	Optimum τ
Desired Values	-	50	30	-104	170	ccw	
	0.5	50.2	30.8	-100.0	166.9	ccw	0.5
	1.0	50.2	31.3	-106.7	169.8	ccw	
Desired Values	-	60	30	-104	140	ccw	
	1	60.3	25.1	- 99.6	135.6	ccw	
	2	60.1	31.5	-108.6	141.7	ccw	1.4
	3	59.9	37.1	-117.9	147.2	ccw	
Desired Values	-	80	30	-104	140	ccw	
	5	80.0	26.7	- 99.9	137.6	ccw	
	6	79.9	30.4	-104.7	141.2	ccw	5.9
	7	79.7	33.7	-109.8	144.7	ccw	
Desired Values	-	90	30	-104	170	ccw	
	6	90.0	27.4	- 91.2	162.9	ccw	
	8	90.1	28.9	-100.3	167.2	ccw	
	10	90.1	29.8	-110.0	171.2	ccw	9.4
Desired Values	-	60	30	-104	140	cw	
	1	60.1	35.5	- 94.9	145.3	cw	
	2	60.3	29.5	-108.4	139.7	cw	1.9
	3	60.5	22.7	-122.7	133.3	cw	
Desired Values	-	80	30	-104	140	cw	
	5	79.9	45.1	- 67.2	155.2	cw	
	6	80.9	27.5	-118.8	138.9	cw	5.5
	7	81.2	23.4	-128.9	135.3	cw	
Desired Values	-	90	30	-104	170	cw	
	8	90.5	30.4	-105.6	172.6	cw	8.0
	10	90.7	29.1	-117.8	169.1	cw	
	12	91.3	27.3	-130.5	165.2	cw	

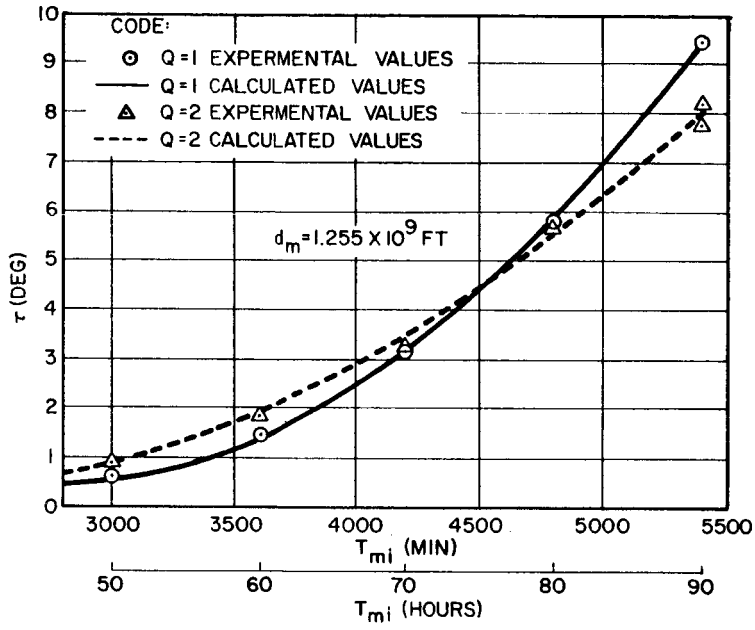

Figure 10a. Variation of τ with Time of Flight.

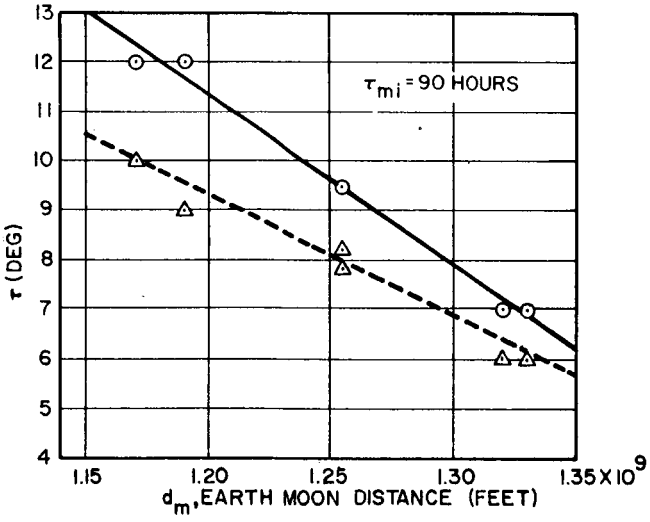

Figure 10b. Variation of τ with Earth-Moon Distance.

For counterclockwise re-entry and time of flight greater than 45 hours,

$$\tau = (5.5246 - 3.6052 \times 10^{-9} x_m)$$

$$\left(9.881 - 0.69055 \times 10^{-2} T_{mi} + 1.2639 \times 10^{-6} T_{mi}^2\right)$$

For clockwise re-entry and time of flight greater than 35 hours,

$$\tau = (4.7957 - 3.0245 \times 10^{-9} x_m)$$

$$\left(3.1834 - 0.28483 \times 10^{-2} T_{mi} + 0.69247 \times 10^{-6} T_{mi}^2\right)$$

where x_m (ft) = distance to the moon and T_{mi} (min) = time of flight. The value of τ is taken as zero for flight times shorter than these.

D. FINAL ACCURACY

The results obtainable with the τ-corrected program are very good in comparison with those of the uncorrected program. A glance at Table 3, for example, indicates that the most important three quantities, re-entry latitude, longitude and flight path angle behave with respect to τ in such a manner as to be corrected simultaneously. Incorporating the expressions for τ developed in the last paragraph into the analytic program yields the results shown in Table 4 for a few sample cases. As expected, the results compare most favorably with the exact integration program when the time of flight is the shortest and when the re-entry angle is the steepest and compare the least favorably for long flight times and shallow re-entry.

It may be possible, by extending this method of analysis, to find expressions for τ, and/or some other angle, which will result in even greater accuracy in the terminal conditions, however, it should be remembered that this method improves primarily the end point conditions and does not correspondingly correct other parameters or coordinates along the trajectory.

Intermediate values of position and velocity (midcourse), however, compare favorably with exact results as are shown for a specific case in Table 5.

Table 4. Results of the τ-corrected Analytic Program

τ-corrected Analytic Program				Exact Program				
Time of Flight (hr)	Re-entry Latitude (deg)	Re-entry Longitude (deg)	Re-entry Angle (deg)	Time of Flight (hr)	Re-entry Latitude (deg)	Re-entry Longitude (deg)	Re-entry Angle (deg)	Re-entry Direction
50	15	-40	175	50.1	15.7	-36.4	173	ccw
50	15	-40	135	50.1	15.4	-34.1	130.8	ccw
50	-29	184.1	96	49.8	-30.9	178.0	98.5	ccw
60	30	-104	140	60.2	27.7	-103.2	138.0	ccw
60	30	-104	140	60.3	29.9	-107.5	140.0	ccw
90	--	-150	175	90.5	- 1.0	-156.9	175.4	ccw
90	30	-104	170	90.2	29.6	-107.3	170.1	ccw
90	30	-104	170	90.6	30.4	-105.6	172.6	ccw
90	15	-40	135	88.9	15.3	-25.3	135.6	ccw
90	30	-104	110	90.7	28.0	-95.2	113.0	ccw
90	30	-104	110	91.4	29.4	-114.4	114.3	ccw
90	-6	173.4	96	88.1	- 7.0	176.9	106.7	ccw

Table 5. Midcourse Comparison between the τ-corrected Analytic and Exact Programs

R (ft)	t (min)	α (deg)	δ (deg)	V (fps)	β (deg)	A (deg)
0.1216×10^{10}	0	-0.757	-5.80	6288	149.6	245.3
	(0)*	(-0.757)	(-5.80)	(6288)	(149.6)	(245.3)
0.1158×10^{10}	360	-1.03	-5.98	2460	176.0	86.3
	(360)	(-1.03)	(-5.98)	(2472)	(175.8)	(85.5)
0.1104×10^{10}	720	-0.734	-5.93	2572	172.6	77.2
	(720)	(-0.723)	(-5.92)	(2619)	(172.1)	(76.4)
0.1045×10^{10}	1090	-0.165	-5.77	2837	169.4	74.1
	(1080)	(-0.267)	(5.80)	(2850)	(171.0)	(74.9)
0.9815×10^{9}	1452	0.471	5.58	3130	169.8	74.0
	(1440)	(0.302)	(-5.65)	(3127)	(170.6)	(74.2)
0.9115×10^{9}	1812	1.20	-5.38	3464	170.1	73.9
	1800	(0.99)	(-5.45)	(3453)	(170.4)	(73.8)
0.8339×10^{9}	2171	2.05	-5.13	3856	170.3	73.8
	(2160)	(1.82)	(-5.21)	(3841)	(170.3)	(73.6)
0.7473×10^{9}	2529	(3.08)	(-4.83)	4334	170.3	73.8
	(2520)	(2.86)	(-4.90)	(4318)	(170.3)	(73.4)
0.6492×10^{9}	2888	4.41	-4.45	4948	170.2	73.7
	(2880)	(4.20)	(-4.50)	(4931)	(170.1)	(73.2)
0.5358×10^{9}	3247	6.25	3.90	5801	169.9	73.5
	(3240)	(6.08)	(-3.93)	(5785)	(169.7)	(73.0)
0.3998×10^{9}	3606	9.23	-3.02	7178	169.1	73.3
	(3606)	(9.12)	(-3.00)	(7164)	(168.8)	(72.8
0.2211×10^{9}	3965	16.25	-0.90	10415	166.3	73.1
	(3960)	(16.30)	(-0.76)	(10404)	(166.0)	(72.6)
0.2133×10^{8}	4200	80.0	15.0	36073	135.0	82.0
	(4196)	(83.1)	(15.8)	(36078)	(133.7)	82.6

*Quantities in parentheses are from the Exact Program.

The τ-correction introduces a velocity discontinuity at the sphere of action and this is noted in this example for the distance $R = 0.1045 \times 10^{10}$ feet. Here the variation in the β-angle, for example, jumps from -0.5 degrees at the previous point to 2.7 degrees at this point (the value of τ is 3.7 degrees). For 90 hour flight times where the value of τ may reach 10 degrees, as shown in Figure 10a, the midcourse velues at the MSA will deviate from the exact results by this corresponding amount, and will be reflected either in the β-angle, as in the example above, or in some other angular quantity; or the deviation will be distributed among all angular quantities.

The final comparison of results that may be made with the exact program are the sensitivity coefficients obtainable from the Sensitivity Coefficient Routine. Table 6 presents these results for two cases; 50 hour and 90 hour times of flight. The results were obtained from the exact program in exactly the same manner as from the analytic program, i.e., each burnout parameter was varied independently by the increment shown and the trajectory was then integrated to re-entry. The differences between the resulting terminal values and the unperturbed nominal values are those shown in the tables.

It is clear that the τ-correction will not appreciably affect the values of the sensitivity coefficients generated by the program since this correction simply involves a rotation of the velocity vector at the MSA. Both of the cases shown are for steep re-entry. It is expected that the analytic program will give similar accuracy for trajectories having shallow re-entries. One stipulation in producing a valid comparison of miss coefficients resulting from the exact and analytic programs is that both trajectories have the same terminal conditions. Thus, it is clear that a comparison is not being made with an exact trajectory whose burnout conditions are exactly identical to those of the τ-corrected program.

In summary, using the τ-corrected program:

(1) The adjustment required in the burnout conditions of the analytic program to produce the desired conditions on an "exact" program will be of the order of a few tenths of a degree in β and A or a few fps in velocity. This adjustment may be made by incorporating a linear search routine in the exact program.

Table 6. Sensitivity Coefficient Comparison Between the Analytic and Exact Programs

Total Time of Flight = 50 Hours
Re-entry Flight Path Angle = 163 Degrees
Increments*

Terminal Parameters	Δr (50,000ft)	Δλ (1 deg)	Δμ (1 deg)	Δv (50 fps)	Δβ (1 deg)	ΔA (1 deg)
Re-entry Time	-21.4	19.9	-.065	-35.2	28.0	.11
	(-21.3)**	(20.5)	(-.300)	(-35.1)	(28.8)	(.30)
Latitude	-.051	3.33	1.41	.389	2.69	-15.21
	(.003)	(3.20)	(1.24)	(.451)	(2.52)	(-15.1)
Longitude	4.72	-20.2	.692	4.93	-28.1	-3.52
	(4.50)	(-19.9)	(.735)	(4.56)	(-27.8)	-3.25
Re-entry Angle	.291	5.81	-.49	1.75	8.03	1.59
	(.386)	(5.70)	(-.56)	(1.89)	(7.90)	(1.50)

Total Time of Flight = 90 Hours
Re-entry Flight Path Angle = 169 Degrees
Increments

Terminal Parameters	Δr (50,000ft)	Δλ (1 deg)	Δμ (1 deg)	Δv (50 fps)	Δβ (1 deg)	ΔA (1 deg)
Re-entry Time	-48.4	68.4	-3.6	71.0	100.2	-6.67
	-44.5)	(71.9)	(-4.3)	(-65.0)	(103.9)	(06.0)
Latitude	1.24	1.13	7.98	1.34	-1.00	-7.05
	(1.17)	(1.00)	(7.86)	(1.22)	(-1.13)	(-7.16)
Longitude	-1.72	-20.8	3.29	-4.67	-30.8	-0.55
	(-2.79)	(-21.1)	(3.17)	(-6.50)	(-30.8)	(0.68)
Re-entry Angle	3.82	1.05	-3.14	4.18	2.43	1.58
	(3.95)	(.90)	(-2.96)	(4.30)	(2.13)	(1.50)

*The values in the tables represent actual variations in the terminal parameters and have not been divided by the indicated increments.

**Quantities in parentheses are from the Exact Program.

(2) The sensitivity coefficients obtained from the analytic program are generally within 10 per cent of those obtained from an exact program.

Thus, the results obtained from the analytic program should be satisfactory for all general mission studies other than final mission trajectories and firing tables.

IV. TRAJECTORY ANALYSIS

The purpose of this section is to present a qualitative and quantitative analysis of moon-to-earth trajectories. This will be accomplished by first reviewing the general characteristics of such trajectories, under the hypotheses set forth concerning the gravitational model, and then determining which parameters in the earth phase most affect the moon phase conic and, conversely, which parameters in the moon phase most effect the earth phase conic. In this manner, it will be possible to conveniently separate the analyses of the earth phase and moon phase portions of the trajectory.

A. EARTH PHASE ANALYSIS

In Section II, (as shown in Figure 4a) it has been pointed out that the majority of the total trajectory will be the earth phase conic. In fact, it can be easily shown that the angle subtended by the radius of the moon's sphere of action as seen from the earth is about 8.5 degree. The perigee distance of the conic will be close to the radius of the earth, or less, and its apogee distance (if the conic is an ellipse) must be greater than the distance to the MSA. A simple calculation will show that this implies that the minimum eccentricity the earth phase conic may have is about 0.96. The earth phase conic, then, must be a section of a highly eccentric ellipse; or else be hyperbolic or parabolic.

Returning to Figure 4a, the trajectory as drawn, with the moon on the left and the re-entry point on the right, will cause the vehicle to re-enter the atmosphere in the same direction as the rotation of the earth, i.e., in a counterclockwise manner. It is possible to find a trajectory which satisfies all of the input conditions stipulated in Section II and which approaches the earth in a clockwise manner. This implies that in solving for a moon-to-earth trajectory, one must indicate which manner of approach at re-entry is desired. Figure 11 illustrates this more clearly.

Refering now to Figure 4b of Section II, it is interesting to see what input parameters will affect the in-plane conic elements and related quantities. It has already been noted that the conic section will be determined directly

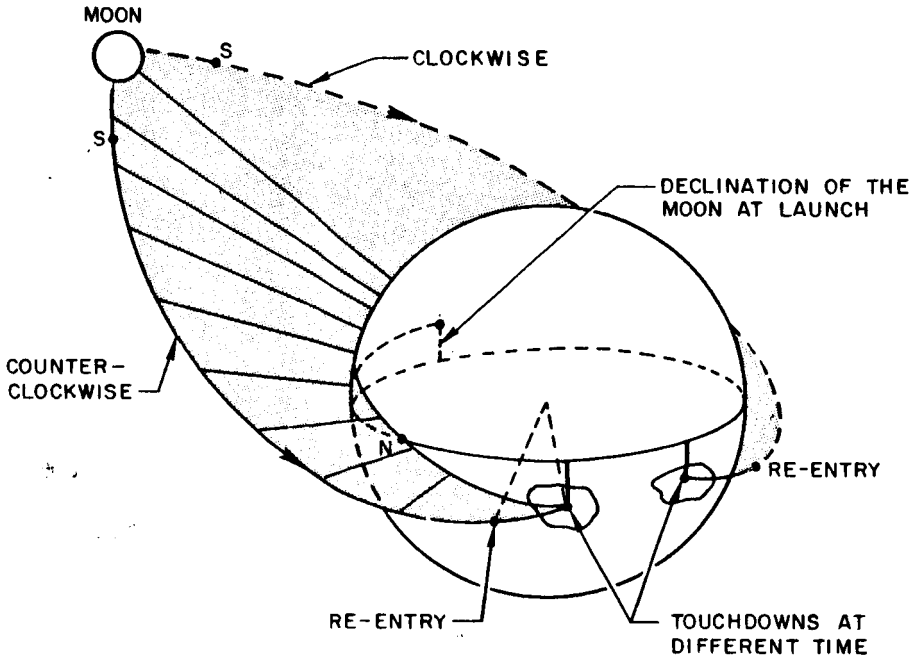

Figure 11a. Earth Phase Geometry (Rotating Earth).

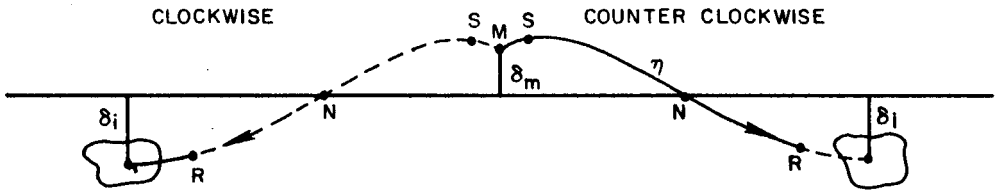

Figure 11b. Mercator Projection.

by the quantities x_r, x_s, β_r, and T_{sr} where x_s and T_{sr} are strongly dependent on the distance to the moon at launch and the total time of flight, respectively. During a lunar month, the distance to the moon will vary by about 7.5 earth radii. It turns out that for trajectories with a fixed total flight time, the time T_{sr} remains fairly constant. Thus, for fixed flight times, vehicles launched on those days when the moon is farthest from the earth must have higher energies than those launched when the moon is closest to the earth. This observation is born out by Figure 12 which plots the re-entry velocity for a re-entry altitude of 400,000 feet versus the total time of flight for different earth-moon distances.

It should be pointed out that all of the data plotted on this and ensuing graphs (unless otherwise stated) were obtained from the Analytic Lunar Return Program. Therefore, they include the lunar and three dimensional effects on the trajectories. In Figure 12, for example, it was discovered by means of additional trajectory runs that the effects of the re-entry angle β_r and clockwise or counterclockwise re-entry on the re-entry velocity are negligible. One would not expect that the locations of the lunar launch site or the landing site will have much affect on this velocity, and this has also been checked.

In a similar manner, referring to Figure 13, it is possible to determine the variations of the velocity and the flight path angle at the sphere of action with the input parameters. As with the re-entry velocity these parameters depend primarily on the time of flight and the distance to the moon. In the case of the velocity u_s, however, a significant variation is evident with respect to the re-entry angle. This is indicated in Figure 13a where the velocity versus the time of flight for near extreme cases of vertical and horizontal re-entry are plotted. Values of u_s for intermediate re-entry angles will lie between these curves. The indication that steeper re-entry angles have lower velocities at the MSA may be explained by the fact that these trajectories re-enter on the side of the earth facing the moon whereas shallow re-entry trajectories come in on the back side to the earth. The steep re-entry trajectories, then, may have a distance of as much as two earth radii less to travel than shallow re-entry trajectories, and therefore require less energy to accomplish this in the same amount of time.

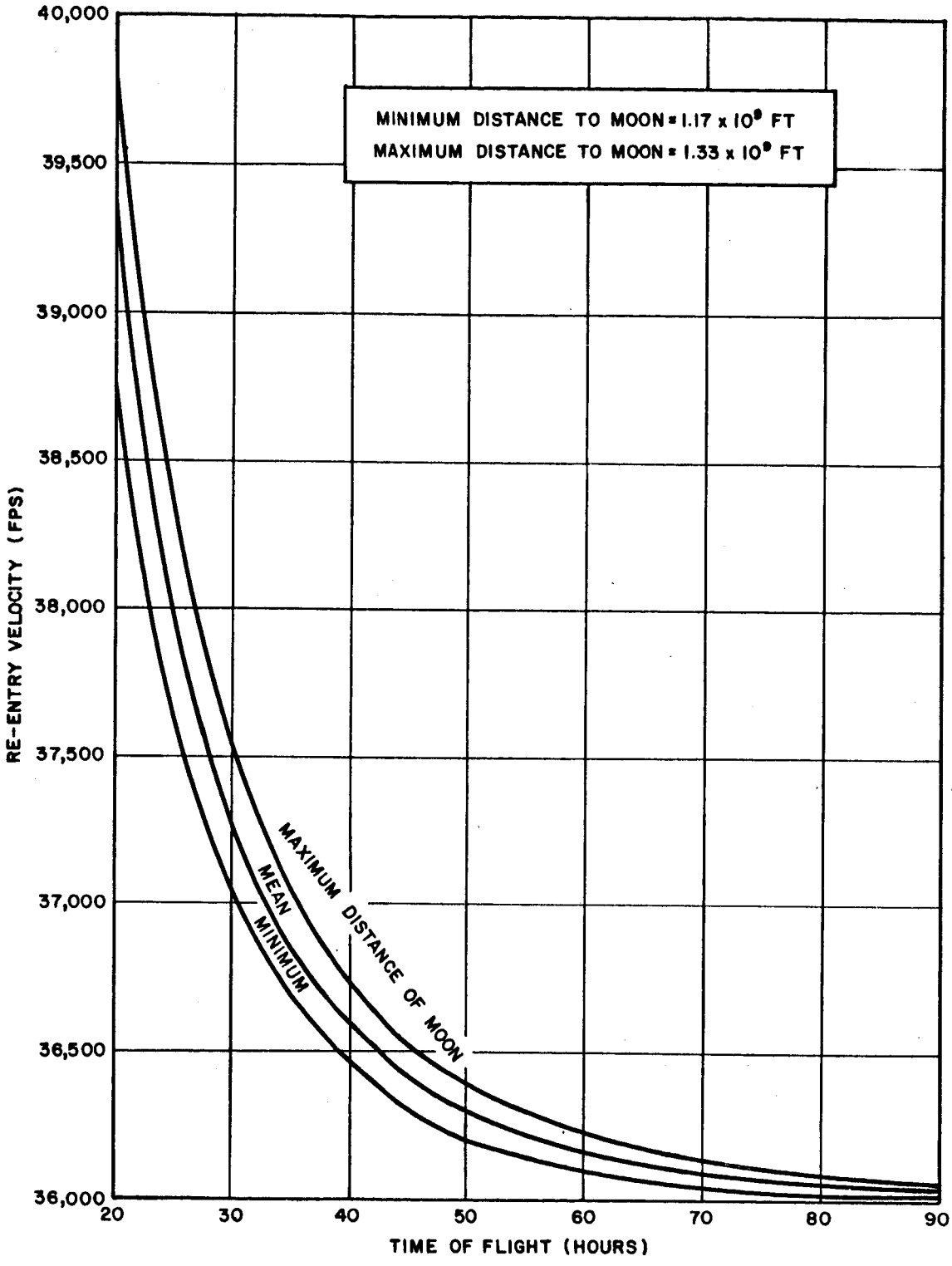

Figure 12. Re-entry Velocity (Altitude = 4000,000 Feet) versus Total Time of Flight for Various Distances to the Moon.

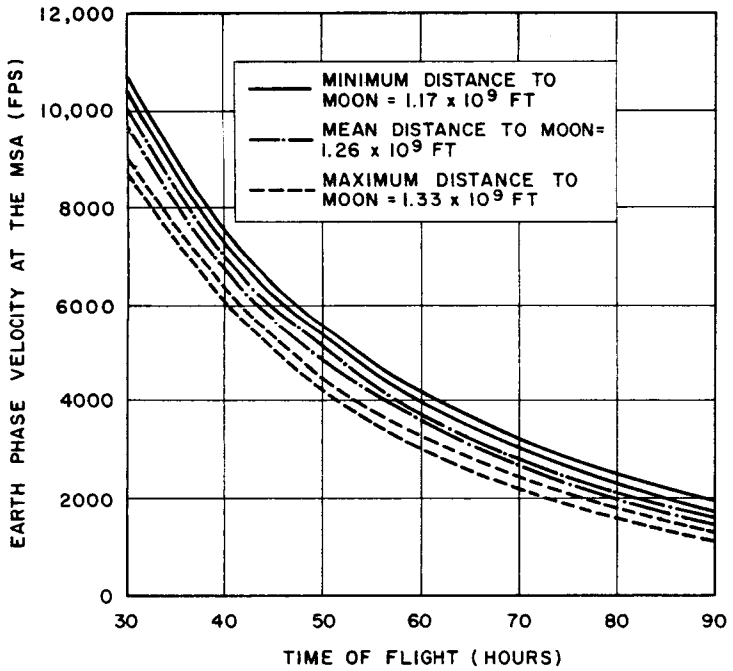

Figure 13a. Earth Phase Velocity at the Sphere of Action versus Total Time of Flight for Various Distances to the Moon. The Upper Curves Represent a Re-entry Angle or 96° and the Lower Curves a Re-entry Angle of 175°.

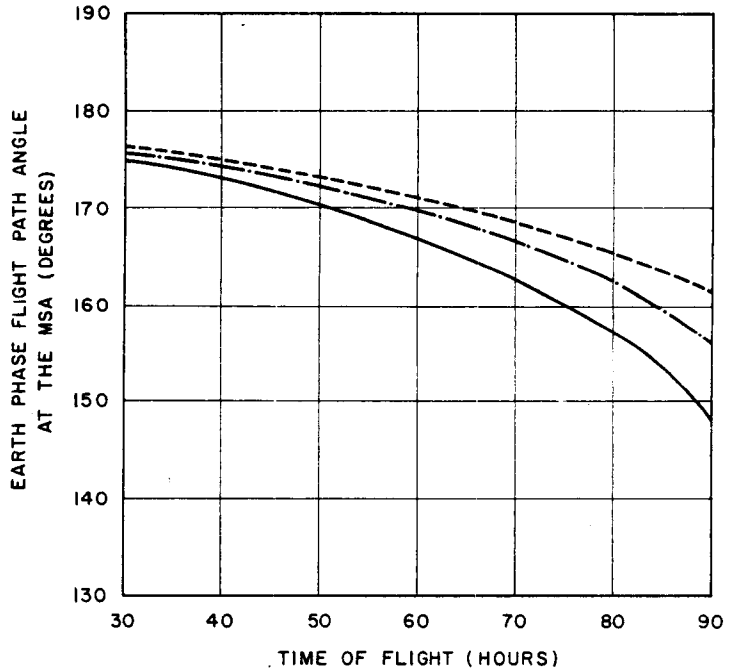

Figure 13b. Earth Phase Flight Path Angle at the Sphere of Action versus Total Time of Flight for Various Distances to the Moon. Re-entry Angle = 96°.

Figure 13b presents the flight path angle versus the time of flight for various distances to the moon and for a re-entry angle of 96 degrees. These curves represent the lower limits of the flight path angles for those trajectories having greater re-entry angles and similar distances to the moon.

To round out the discussion of the earth phase conic, it is of interest to plot the intermediate time and velocity relationships, and this has been done in Figure 14a and b. The data shown was obtained from three exact integration runs for a launch date in which the moon is at a mean distance from the earth. No attempt has been made to acquire a complete set of parametric relationships for these quantities.

Having analysed the in-plane characteristics of the earth phase conic, it is possible to derive some properties of the three dimensional earth phase geometry of moon-to-earth trajectories. First it has already been stated that the earth phase conic, as seen on a Mercator projection of the earth such as in Figure 11b, begins at most 8.5 degrees from the moon. The difference in the latitudes of the moon and the vehicle at the MSA is much less than this. In fact, observations of many moon-to-earth trajectories indicate that the two declinations will always be within 1.5 degrees of one another. Another important observation is that the in-plane angle between point S and point r, or η_{sr}, remains essentially dependent upon the total time of flight and the re-entry angle β_r. The next important parameter affecting this angle is, as mentioned above, the distance to the moon. This effect, however, is consistantly less than 4 degrees. Referring to Section II Figure 4b, then, the in-plane angle η_{sr} is essentially a function of only the total time of flight and β_r. The parameter η_{sr} has been plotted in Figure 15 and will be called the moon-to-re-entry in-plane angle.

Returning to our first observation concerning the declination of the vehicle at the MSA being within 1.5 degrees of that of the moon, it is also true that the right ascension of the moon at launch and point S are within this value. This is true in spite of the fact that the radius of the MSA subtends an arc of 8.5 degrees. The reason for this is the fact that just after

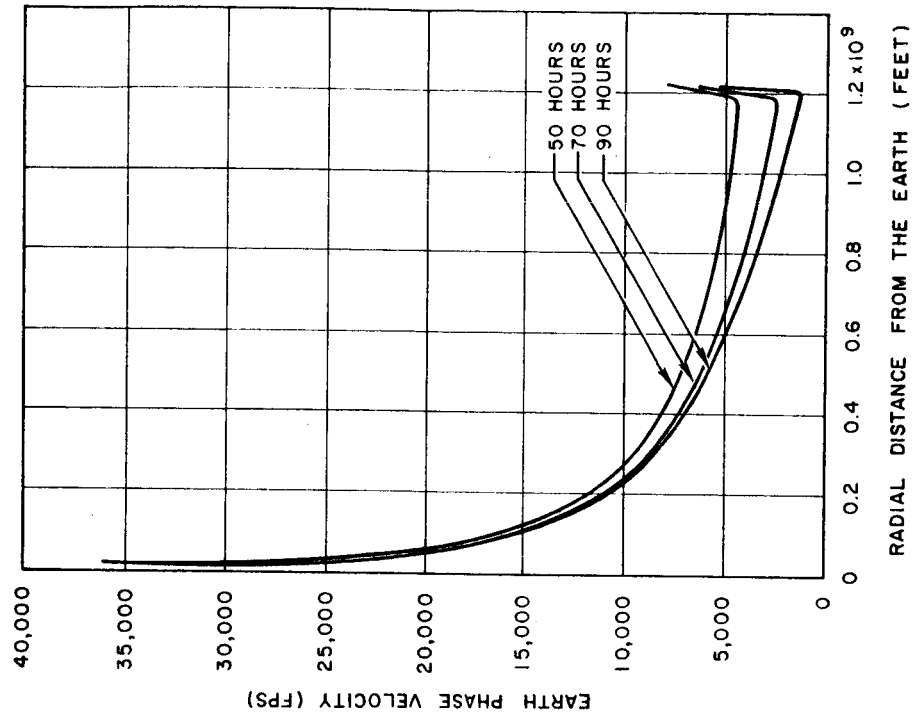

Figure 14b. Earth Phase Velocity of the Vehicle versus its Radial Distance from the Earth for 50, 70, and 90 Hour Total Flight Times.

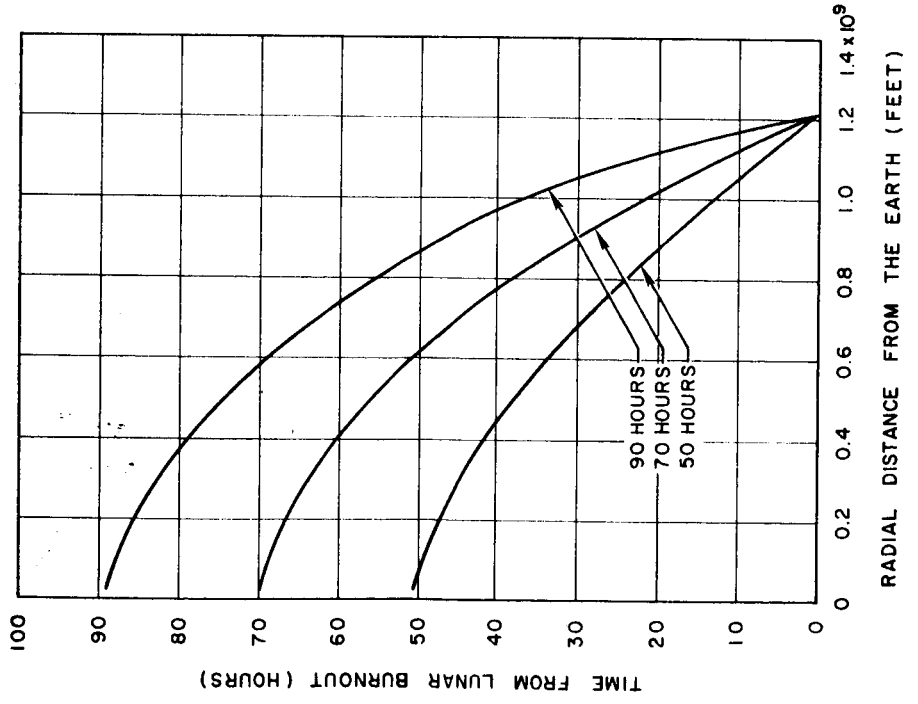

Figure 14a. Time from Lunar Burnout versus Vehicle's Radial Distance from the Earth for 50, 70, and 90 Hour Total Flight Times.

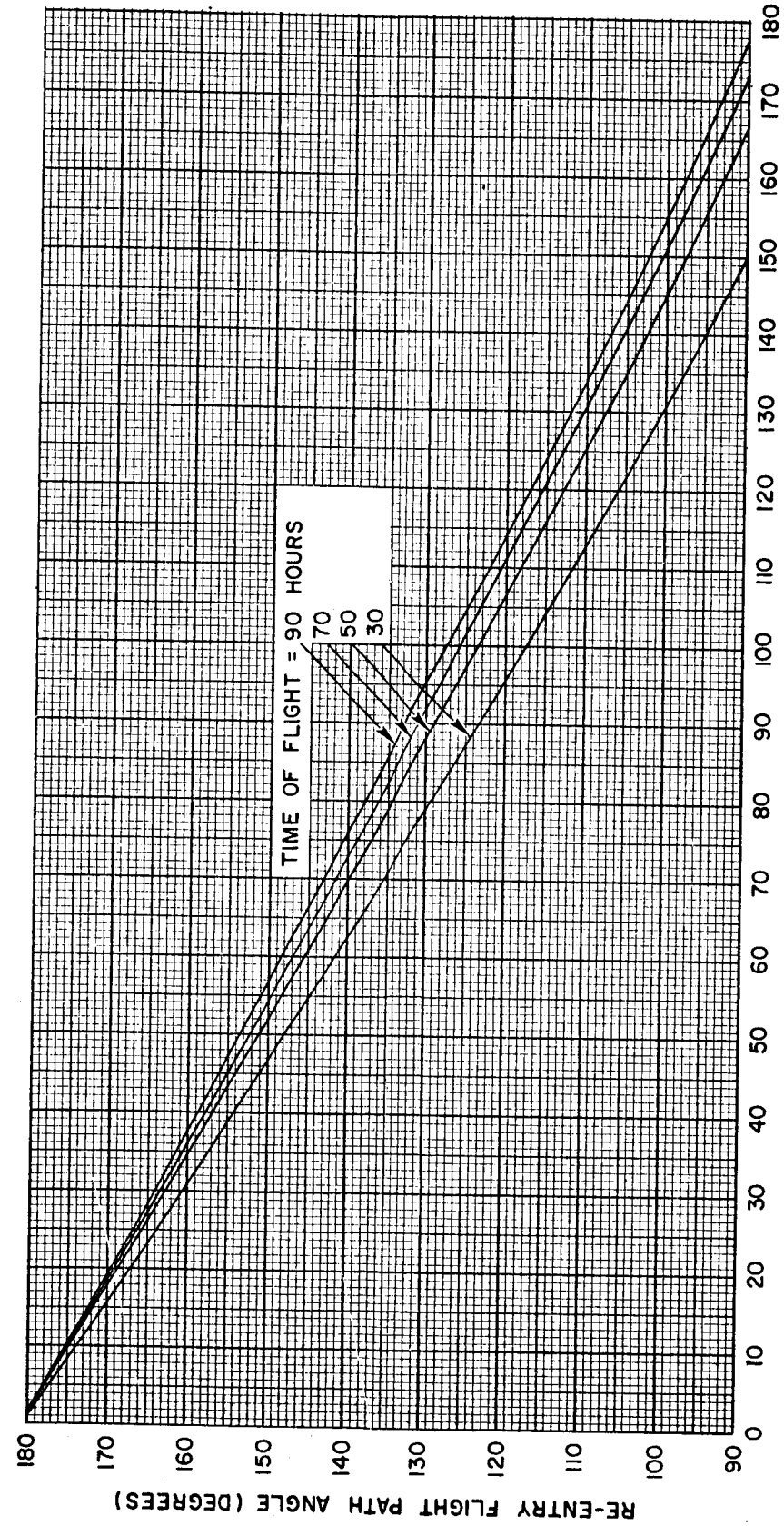

Figure 15. Re-entry Flight Path Angle versus Moon-to-Re-entry In-Plane Angle for Various Total Times of Flight.

lunar burnout the vehicle very nearly cancels the angular velocity of the moon causing its angular position with respect to an inertial earth centered system to remain nearly fixed,out to the point S.

On the basis of these observations, it is possible to define what may be called a "touchdown cone" as shown in Figure 16. This cone may be generated as follows:

(1) For a given total flight time and a given re-entry flight path angle the in-plane angle η_{sr} will be fixed and determined by Figure 15. With the arguments given above, this angle will be essentially the in-plane angle from the moon to re-entry.

(2) The re-entry maneuver angle, if non-zero, may now be added to η_{sr} to produce the total in-plane angle from the moon to touchdown.

(3) With this total in-plane angle fixed, it is possible to generate all possible earth phase conics which are launched from a certain declination of the moon, i.e., on a certain day, and which have a given total flight time, re-entry flight path angle and re-entry maneuver angle. These trajectories may be generated by rotating the in-plane conic about the earth-moon line at launch producing the touchdown cone shown in Figure 16a. It is clear that as re-entry progresses from shallow to steep angles, the angular radius of the cone will increase to a maximum of 90 degrees and then decrease, on the moon side of the earth, down to zero for a rectilinear trajectory. The allowable declination for this trajectory will be, as expected, identical to the declination of the moon at launch.

One question which can now be asked is: what restrictions does this process place on allowable landing sites? Certainly there will be no restriction on the landing site longitude since any longitude may be obtained by launching from the moon at the proper time of day. There are restrictions on the allowable landing site latitudes, however, and this is shown in

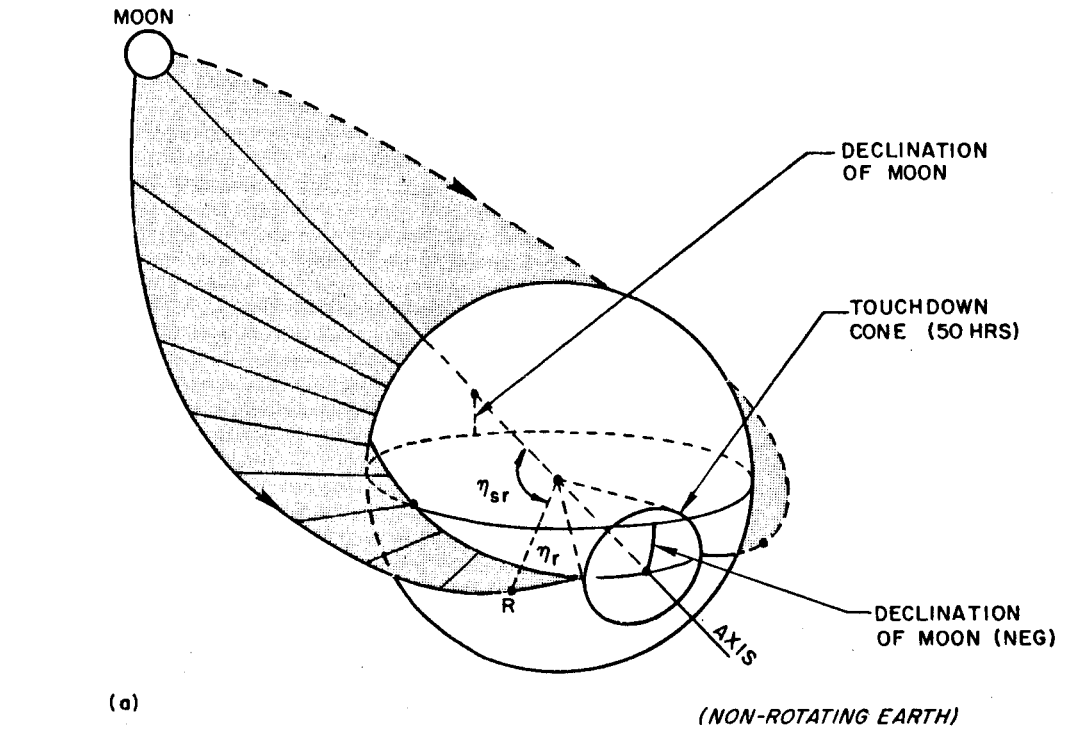

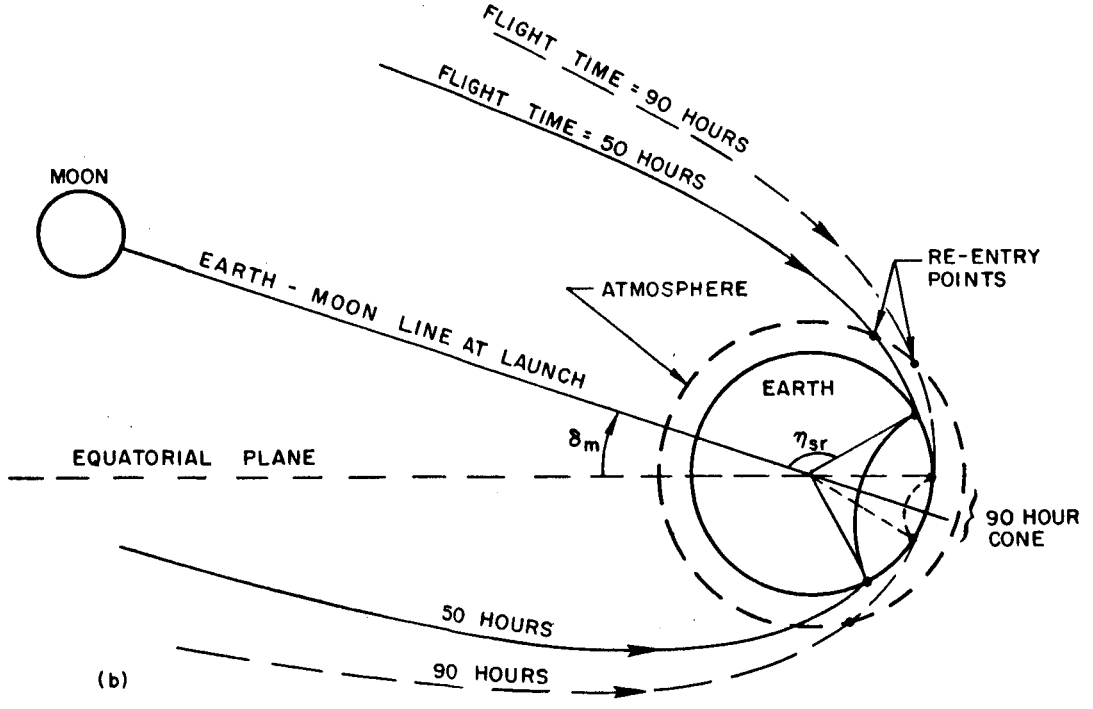

Figure 16. Allowable Touchdown Cones for a Fixed Re-entry Angle and Two Flight Times.

Figure 16b. As indicated on this diagram, the landing site must be within a certain angular distance of the earth-moon axis as measured from the center of the earth. The maximum allowable latitude will be attained for the trajectory passing over the north pole whereas the minimum latitude will be for a trajectory passing over the south pole. These are shown in the figure for 50 hour and 90 hour flight times. Simple linear relationships may be obtained from this figure giving these optimum latitudes as a function of the total in-plane angle and the declination of the moon. These are presented graphically in Figure 17. The manner in which this graph may be used is first to decide what the total in-plane angle is, based on the total time of flight, the re-entry flight path angle and the re-entry maneuver angle (with the aid of Figure 15) and second to determine the declination of the moon on the day of launch. The allowable touchdown latitudes will then lie within the parallelogram for the given lunar declination and total in-plane angle.

This graph may also be used to answer the following question: for a given landing site latitude, total time of flight and re-entry flight path and maneuver angles, what are the allowable declinations of the moon (which is equivalent to days of the lunar month) for which a trajectory is possible? This question is easily answered by determining what lunar declination parallelograms will cause the desired touchdown latitude to lie within them for a fixed total in-plane angle.

The following two examples are given for illustration.

a) Simple lunar sample return mission:

Total time of flight = 70 hours
Re-entry flight path angle = 175 degrees
Re-entry maneuver angle = 0 degrees

From Figure 15, the moon-to-re-entry in-plane angle will be about 10 degrees. This will also be the moon-to-touchdown angle. If the desired landing site latitude is 20 degrees, then from Figure 17, the allowable declinations of the moon will be between 10 degrees to 30 degrees.

b) Apollo manned return mission:

Total time of flight = 70 hours
Re-entry flight path angle = 96 degrees
Re-entry maneuver angle = 40 degrees

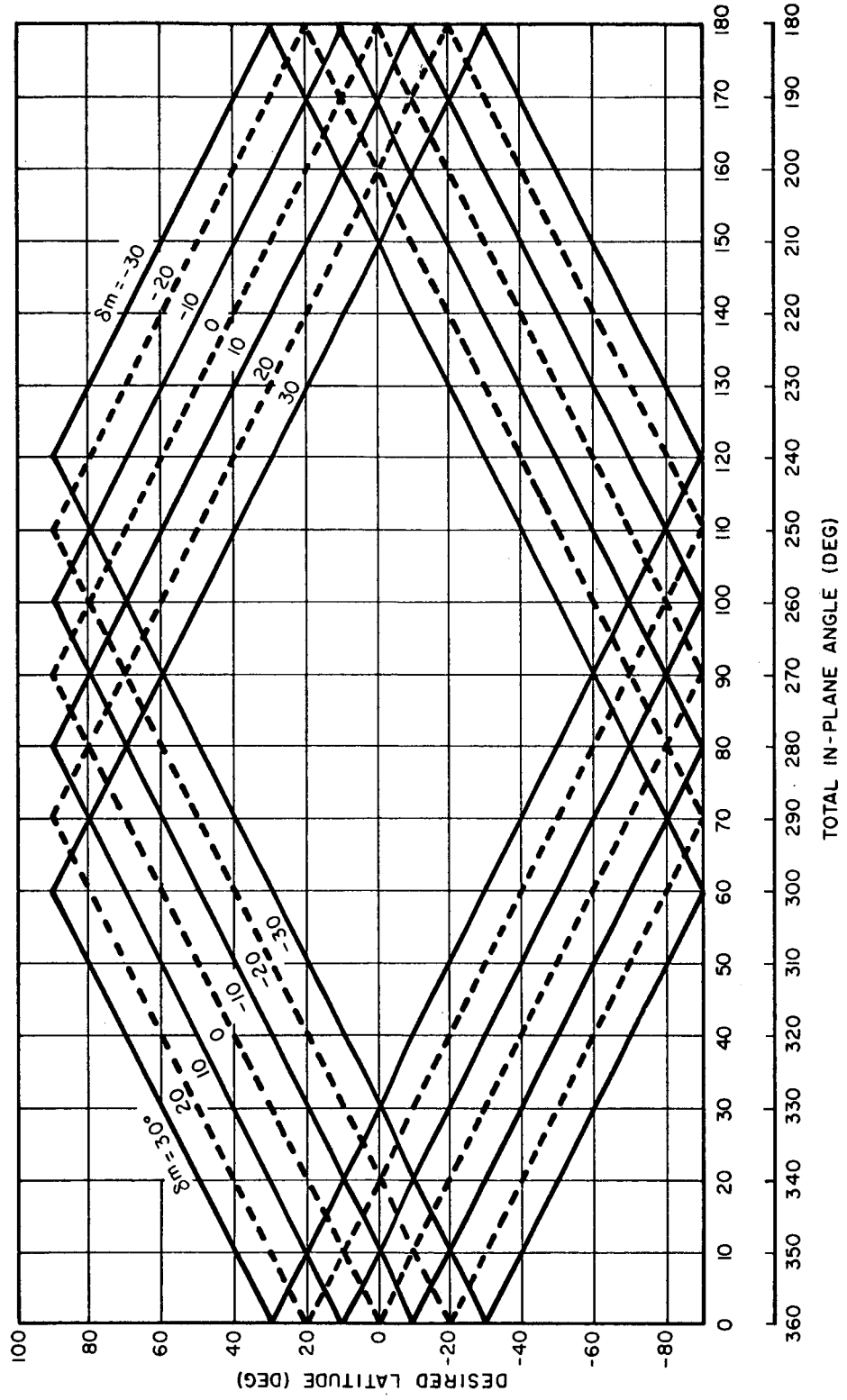

Figure 17. Touchdown Latitude versus Total In-Plane Angle from Moon to Touchdown for Various Declinations of the Moon. (Read allowable declinations within the closed figures)

From Figure 15, the moon-to-re-entry in-plane angle will be about 160 degrees. Adding on the maneuver angle will make the total moon-to-touchdown angle equal to 200 degrees. (This angle will produce the same cone as one whose angle is 360 degrees -200 degrees = 160 degrees). Again if the desired landing site latitude is 20 degrees then, from Figure 17, the allowable declinations of the moon will lie between 0 degrees and -30 degrees.

The reduction of the number of significant variables that enter into the calculation of the earth phase conic also makes it possible to graphically determine some of the angular quantities involved. For example, referring to Figure 4a, the declinations of the moon and landing site and the total in-plane angles between these points will determine the orientation of the earth phase conic. Figures 18 and 19 present the inclination of the conic and the azimuth at touchdown respectively for specific total in-plane angles. Graphs for a complete range of in-plane angles have been drawn, however, only these are presented for illustrative purposes. For the Sample Return mission presented above where the declination of the moon is 15 degrees, Figures 18a and 19a indicate the inclination and azimuth to be about 36 degrees and 120 degrees respectively. In the case of the Apollo Return for a declination of the moon of -10 degrees, the inclination and azimuth by Figures 18b and 19b are 34 degrees and 62 degrees respectively.

It is also possible to generate other variations of restriction curves such as those shown in Figures 20 and 21. These curves were generated from data obtainable from Figures 15 and 17 and present the available launch dates for a given month in 1963. All of these graphs assume that the re-entry maneuver angle is 0 degrees. These graphs may be easily redrawn if this angle has some other value. Each graph represents the latitude restrictions for a given re-entry flight path angle. For a given launch date and total time of flight, the available touchdown latitudes will lie between the corresponding upper and lower curves. The situation is similar for determining the available launch dates for a given landing site latitude.

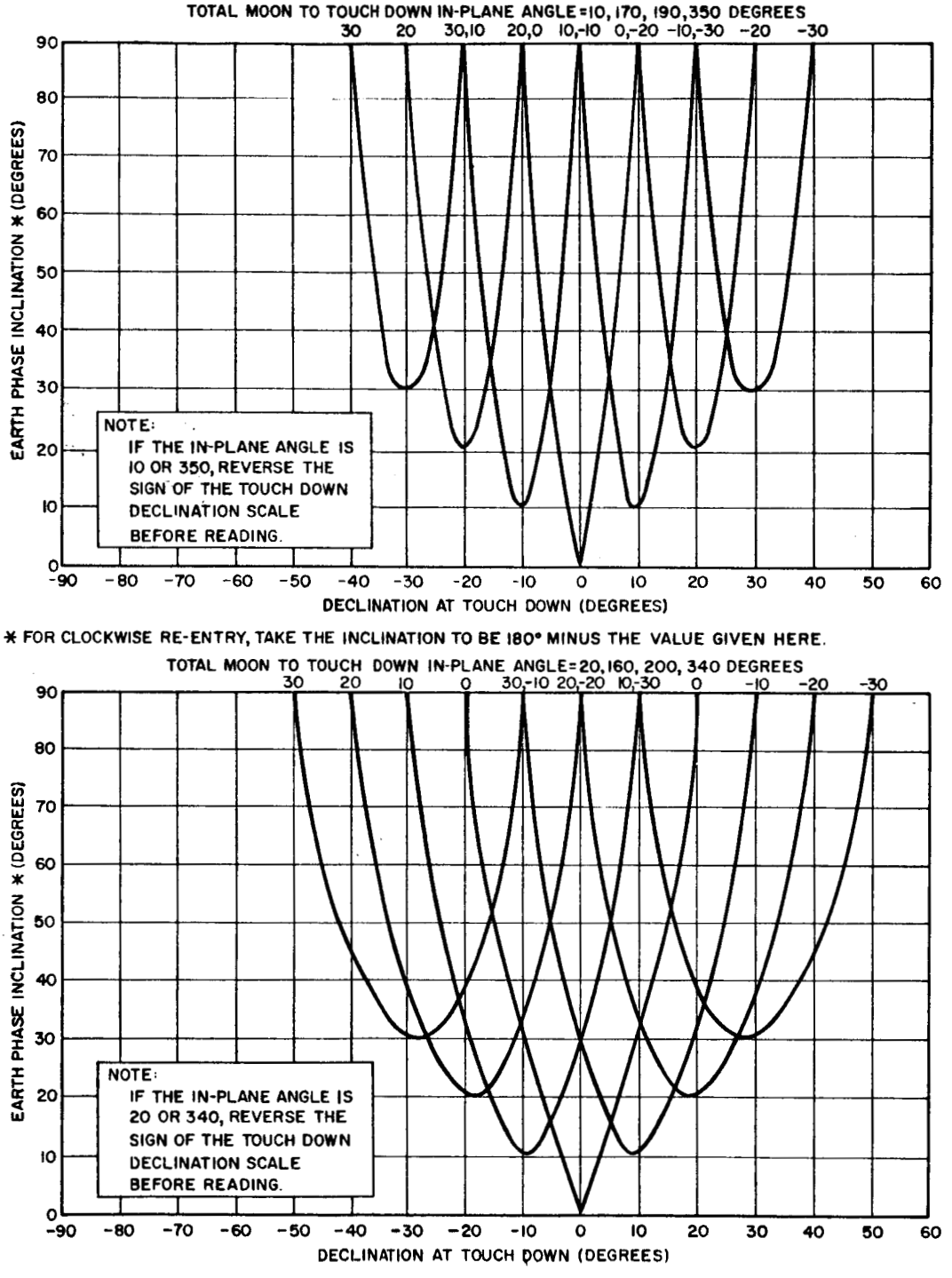

Figure 18. Earth Phase Inclination* with the Equator versus the Declination at Touchdown for Various Declinations of the Moon.

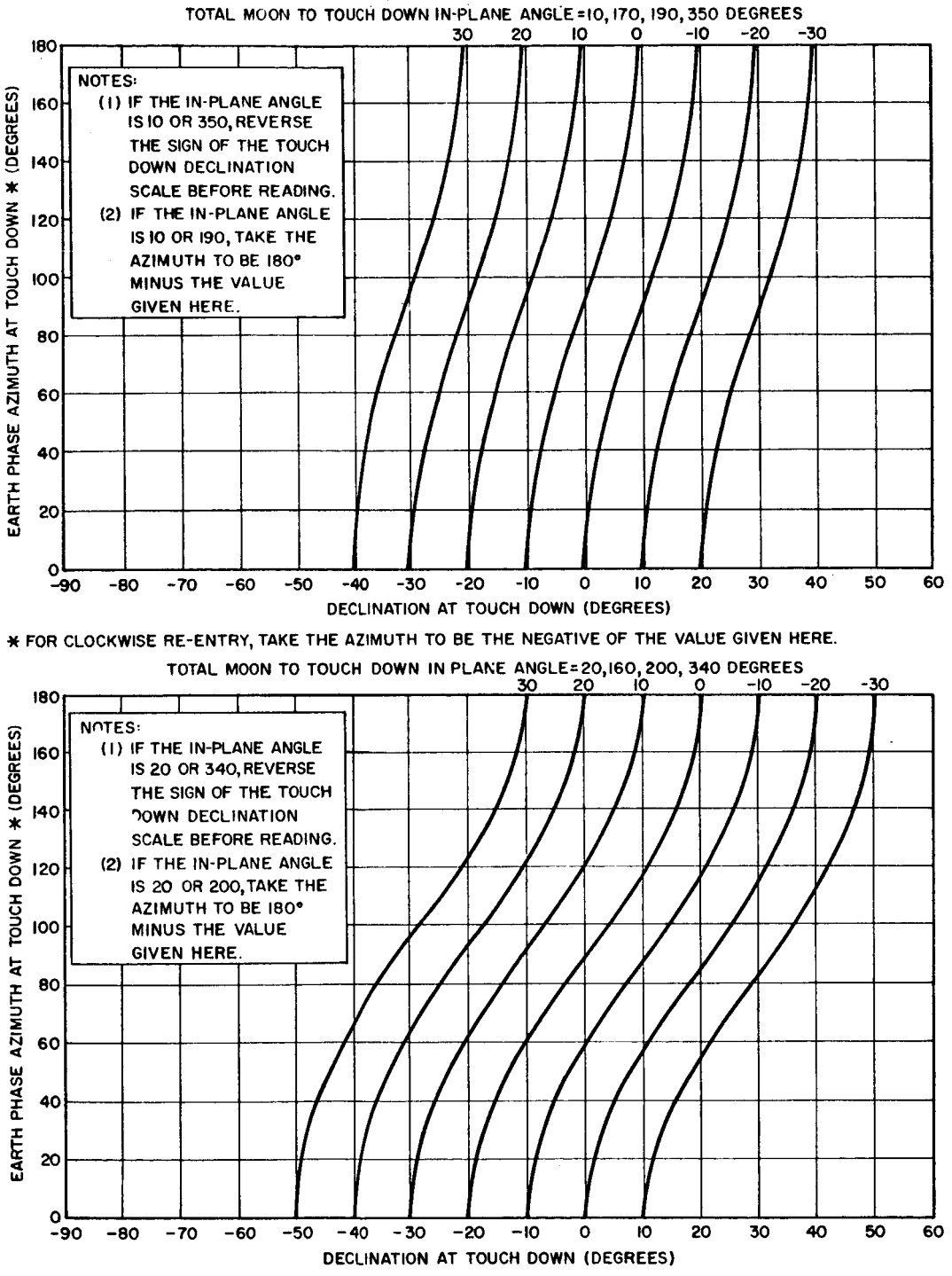

Figure 19. Earth Phase Azimuth* at Touchdown versus the Declination at Touchdown for Various Declinations of the Moon.

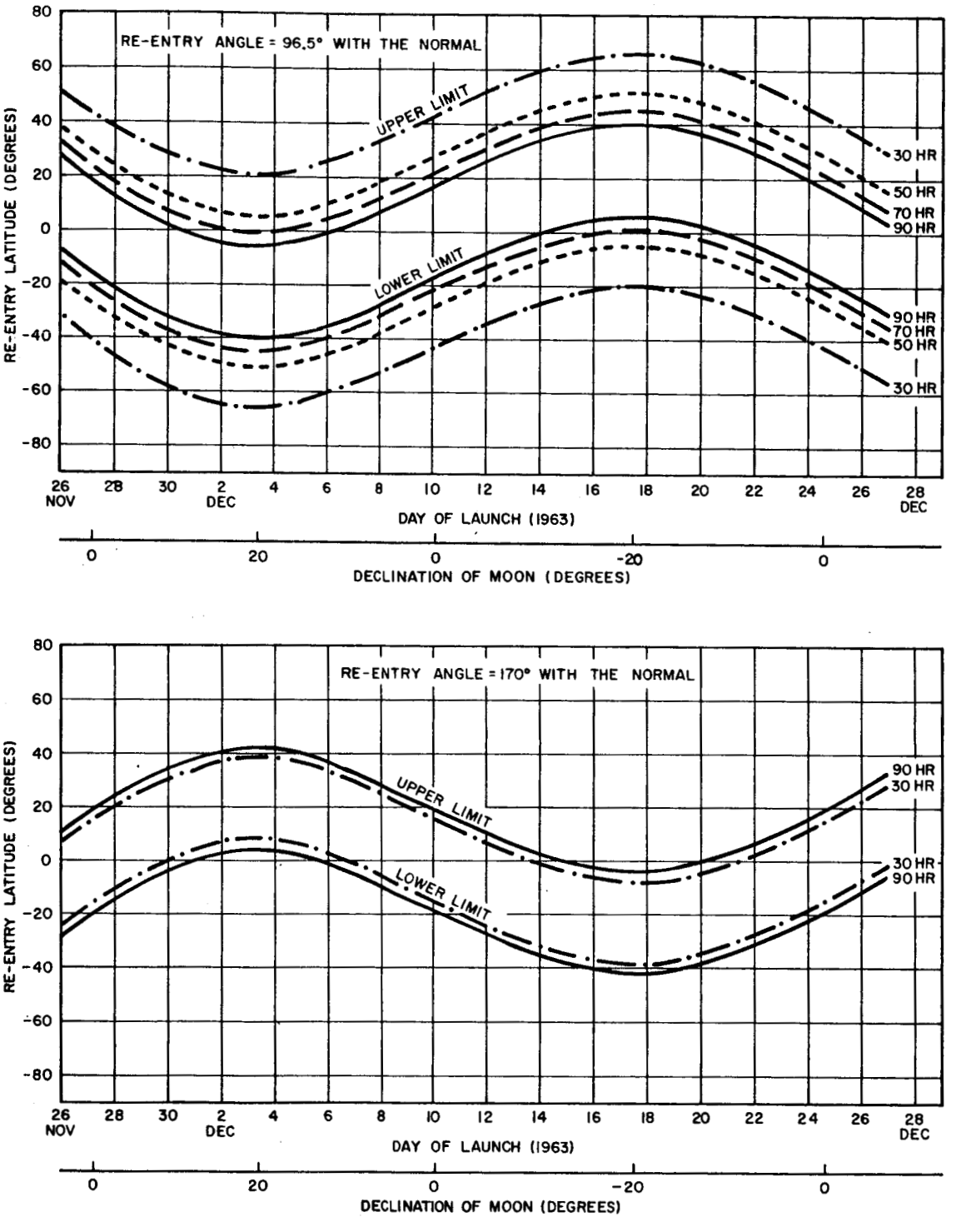

Figure 20. Allowable Re-entry Latitudes versus Time of Lunar Month for Various Flight Times and Re-entry Angles.

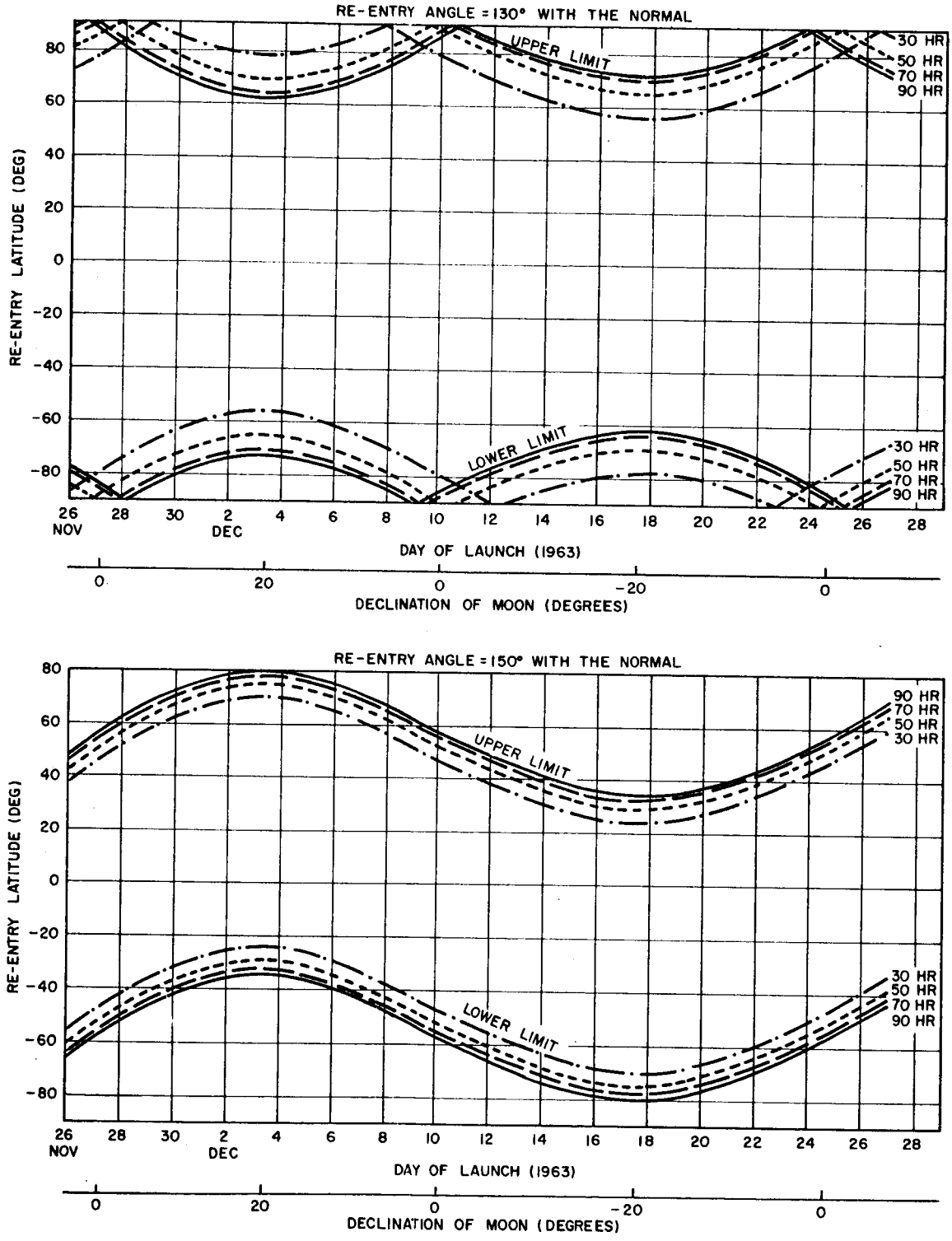

Figure 21. Allowable Re-entry Latitudes versus Time of Lunar Month for Various Flight Times and Re-entry Angles.

B MOON PHASE ANALYSIS

The earth phase analysis has been based primarily on the fact that many independent parameters at the moon have little effect on the earth phase conic. To a certain extent, the reverse is also true. It is possible to see more clearly what the relation is between the two phases by analysing the velocity vectors of the trajectory at the sphere of action. Referring to Figure 1 of Section I, it is seen that the moon's velocity vector must be added to the vehicle's velocity at the MSA to obtain the vehicle's velocity with respect to the earth. The velocity vector of the moon, however, is very nearly perpendicular to the earth-moon line and its magnitude (about 3500 fps) is of the order of the earth-phase velocity for a 60 hour flight (Figure 13a). This implies that for a direct impact on the earth, the vector diagram will be very nearly a right triangle and, specifically, for a 60 hour flight time, the vehicle's velocity vector with respect to the earth will be pointed about 45 degrees to the right of the moon-earth line. If the return trajectory were not a direct impact on the earth, then the earth phase velocity can deviate from this direction. The most it may deviate will be the earth phase flight path angle at the MSA for tangential re-entry which is shown approximately in Figure 13b. For example in the 60 hour case discussed above, this angle will be about $180^{\circ} - 170^{\circ} = 10^{\circ}$. Thus the earth phase velocity and hence the moon phase velocity at the MSA will not vary greatly from its vertical impact direction. Analysis of many moon-to-earth trajectories which have been run on the analytic program indicates that the moon phase velocity of the vehicle at the MSA will always be directed to the east of the moon-earth line (as seen on the moon).

Before presenting some of the quantitative results of these runs, it is possible to deduce some qualitative properties of the velocity at the MSA by visualizing the class of all moon-to-earth trajectories for a given flight time and a given re-entry angle. As deduced in the earth phase analysis, this may be done without involving the shape or orientation of the moon phase conic. Figure 22a shows such a class of trajectories. In this figure, no positions will be designated on the sphere of action. Instead, only the velocity vector $\overline{v}_s$, projected from the center of the moon, will be drawn. As will be seen later, the directions of these velocity vectors will represent very nearly the direction of the hyperbolic asymptote of the moon phase conic.

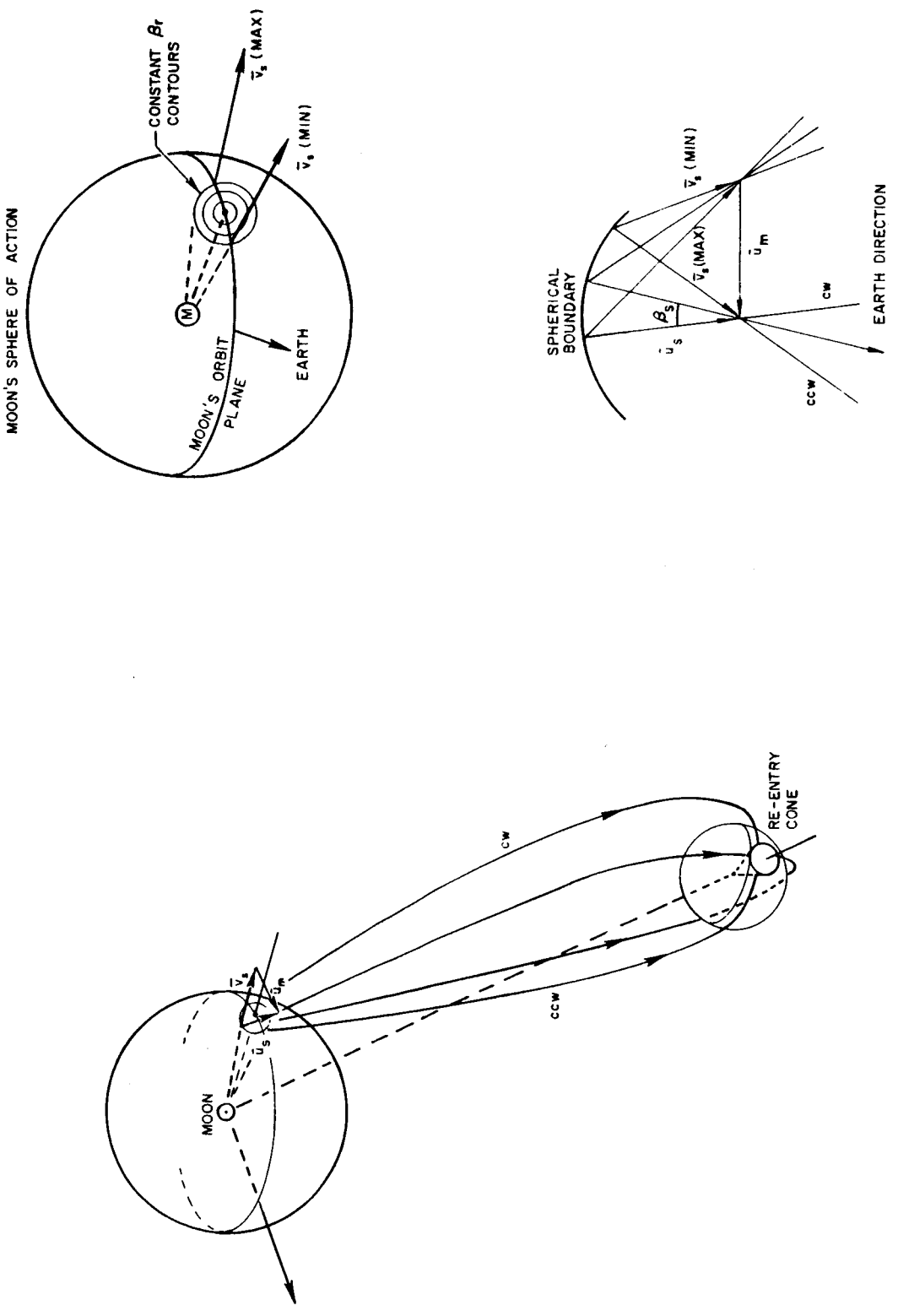

Figure 22. Geometry at Moon's Sphere of Action.

Continuing with Figure 22a, the earth phase conic has been drawn with respect to inertial space where $\bar{u}_s$ and $\bar{u}_m$ are the velocities of the vehicle and the moon respectively at the MSA relative to the earth. For a fixed day of launch, flight time, and re-entry flight path and maneuver angles, it is possible to draw the re-entry cone indicated. Shown on this figure are trajectories which approach the earth in extreme clockwise and counterclockwise manners and over the north and south poles. All other trajectories will form a surface passing through these four. If as assumed above, the time of flight and the re-entry flight path angle are fixed then, as shown in the earth phase analysis, the velocity magnitude u_s and the flight path angle β_s will be constant. Also, since the vector $\bar{u}_m$ is fixed and the velocity

$$\bar{u}_s = \bar{v}_s + \bar{u}_m ,$$

the class of earth phase velocity vectors may be drawn as radii of a sphere whose radius is u_s and whose center is located at the tip of the $\bar{u}_m$ vector. This is called the spherical boundary in Figure 22b where the velocity vector additions for extreme clockwise and counterclockwise re-entry are shown.

On visualizing the class of all possible vector additions, it is seen that the extreme clockwise re-entry will generate the maximum possible moon phase velocity $\bar{v}_s$ and the extreme counterclockwise re-entry will generate the minimum possible velocity $\bar{v}_s$. Thus, it has been shown that although the energy of the vehicle for various trajectories may be identical in the earth phase, the energy in the moon phase will differ. Analysis of extreme clockwise and counterclockwise re-entry trajectories computed by the analytic program indicates that the difference may be considerable. An attempt was made to find the bounds on the energy and this is shown in Figure 23. Here the lunar burnout velocity has been plotted against the total time of flight for various distances to the moon. To obtain extreme trajectories a re-entry flight path angle of 96 degrees was chosen for all cases.

By means of the vis-viva integral, it is possible to convert these velocities to equivalent velocities v_s at the sphere of action. The results are shown in Figure 24. Also plotted here are the hyperbolic excess velocities, and these

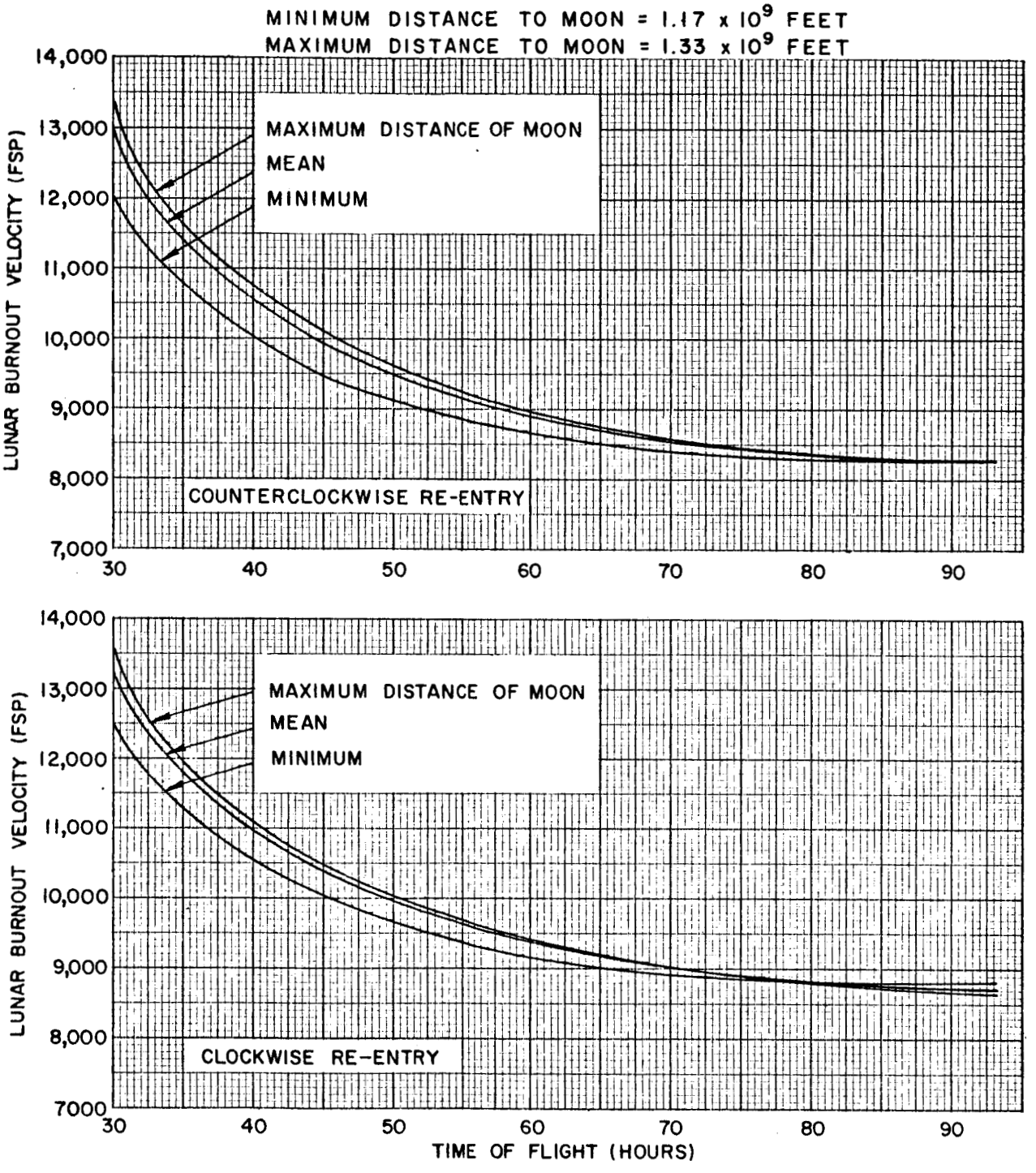

Figure 23. Lunar Burnout Velocity (Altitude = 100,000 Feet) versus Total Time of Flight for Various Distances of the Moon.

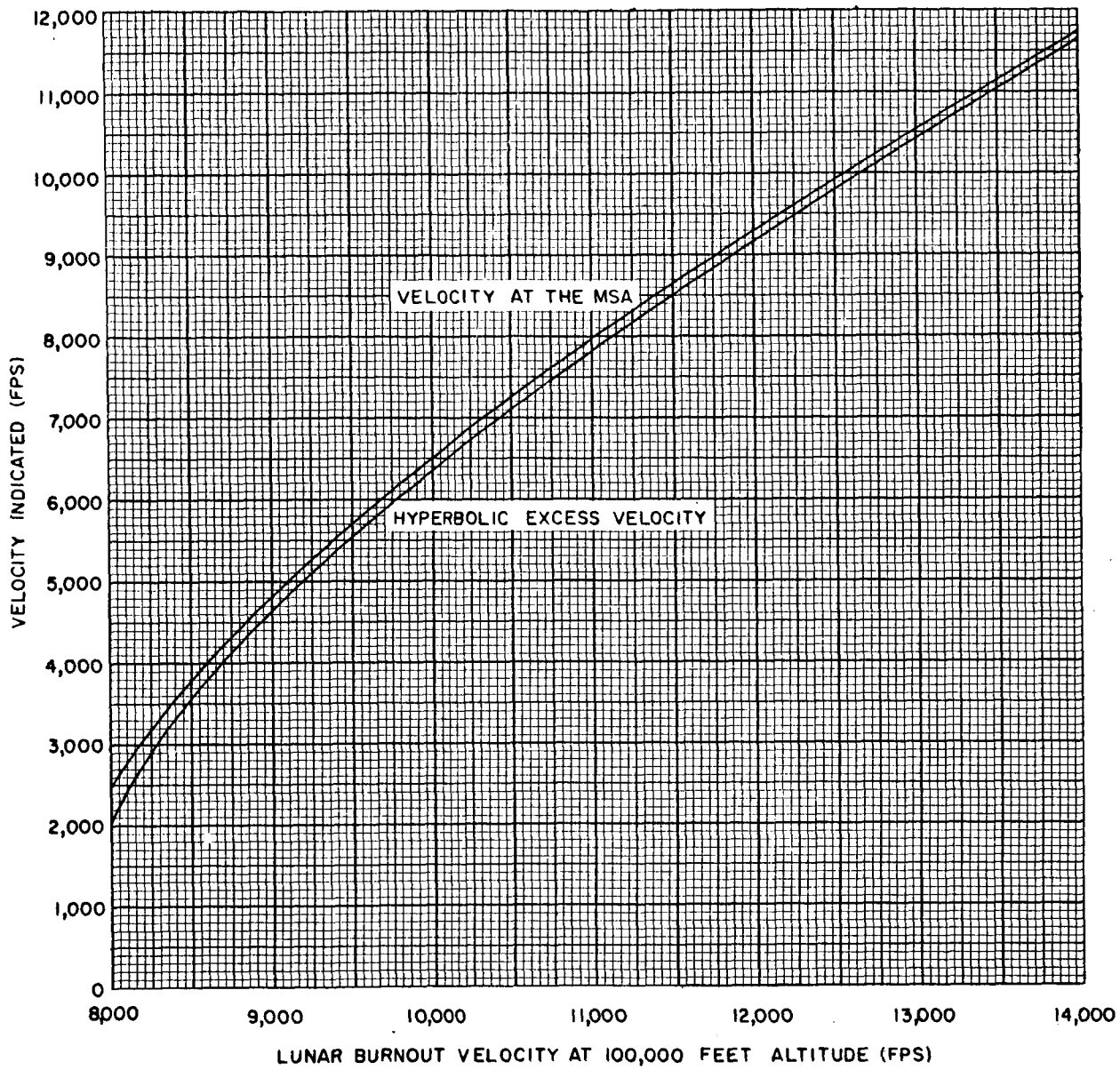

Figure. 24. Hyperbolic Excess Velocity and Velocity at the Moon's Sphere of Action versus Lunar Burnout Velocity at 100,000 Feet Altitude Above the Surface of the Moon.

are within 100 fps to 300 fps of the velocities v_s. It can be shown that the direction of the hyperbolic asymptote is within 0.1 degrees (order of magnitude) of the direction of $\overline{v}_s$.

Finally, Figure 25 presents the time that the vehicle will remain within the sphere of action versus the total time of flight. This time is primarily a function of the energy and so will have the same parametric dependence. These curves are presented for the purpose of indicating upper and lower bounds on the time spent within the MSA.

As mentioned previously, the direction of the velocity vector $\overline{v}_s$ (and equivalently the hyperbolic asymptote) always lies to the east of the moon-earth line. It will be shown shortly that this angle plays a very important part when the launch site location is introduced into the analysis. Therefore, it is convenient to know the direction of $\overline{v}_s$ with respect to the surface of the moon.

Under the assumptions made in Section I concerning the gravitational model, the moon phase conic may be considered as stationary in inertial space (for an observer on the moon) from the moment that it leaves its surface. Therefore, although the moon will rotate in this system, the direction of the velocity vector $\overline{v}_s$ may be found with respect to the surface of the moon at launch. This angle, measured from the earth-moon line is presented in Figure 26. It is called earth-moon-probe angle (EMP) and will depend upon the same set of parameters on which the magnitude of $\overline{v}_s$ depends. Again the data was taken from analytic runs representing extreme re-entry conditions at the earth ($\beta_r = 96^\circ$) and for various distances to the moon. It is seen from this graph that this angle varies considerably in going from counterclockwise to clockwise re-entry. Also, as expected from the velocity vector diagram shown in Figure 22b, the angle EMP is greater for clockwise re-entry than for counter-clockwise re-entry. For example, for a 60 hour total flight time and a mean distance to the moon the angle will vary between 40 degrees (ccw re-entry) and 49 degrees (cw re-entry).

Concerning the moon, it is well known that except for librations which amount to about 7.5 degrees in the east-west direction and about 6.5 degrees in the north-south direction, the face of the moon directed towards the earth

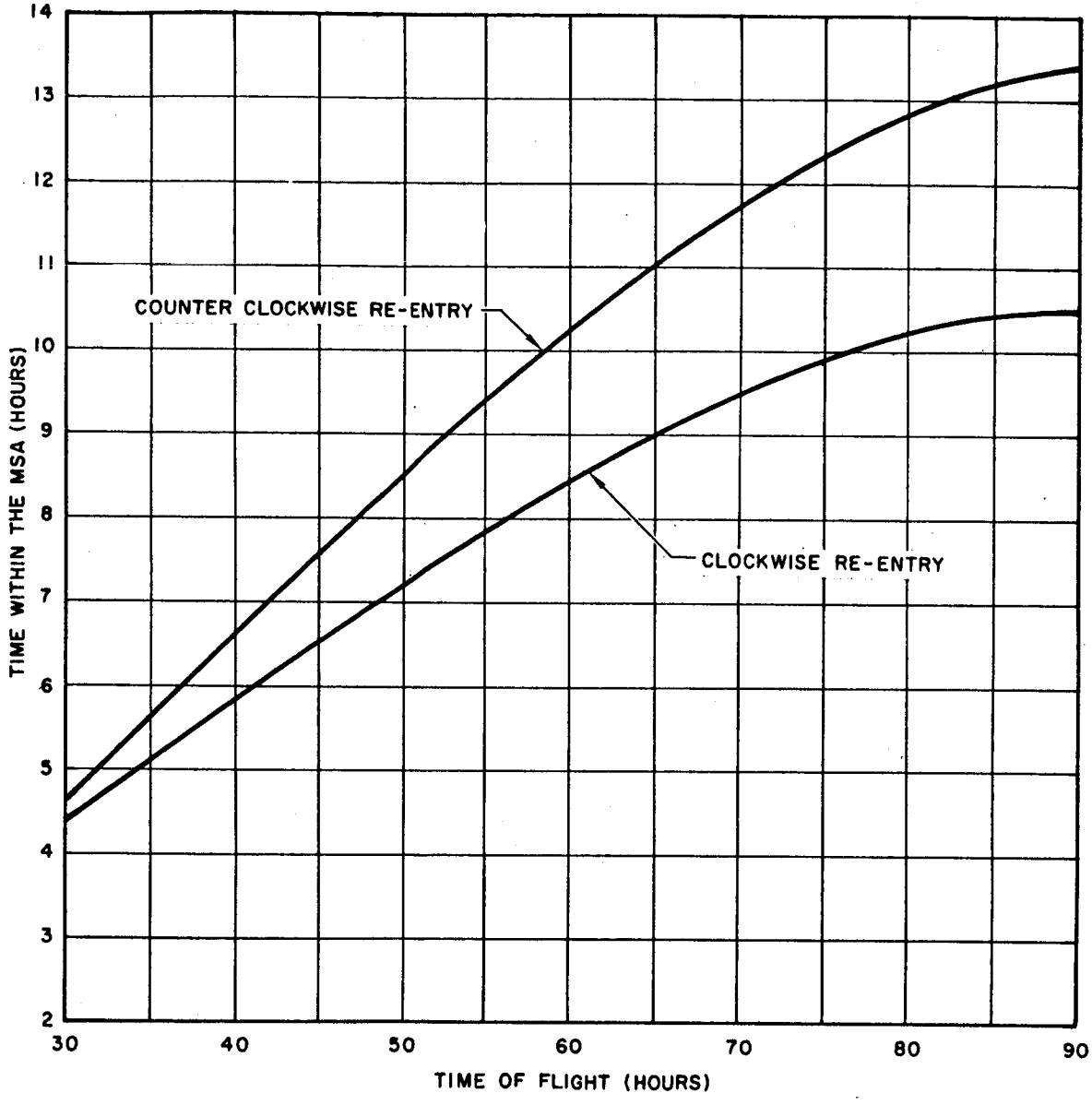

Figure 25. Time During Which the Vehicle is Within the Sphere of Action versus Total Time of Flight.

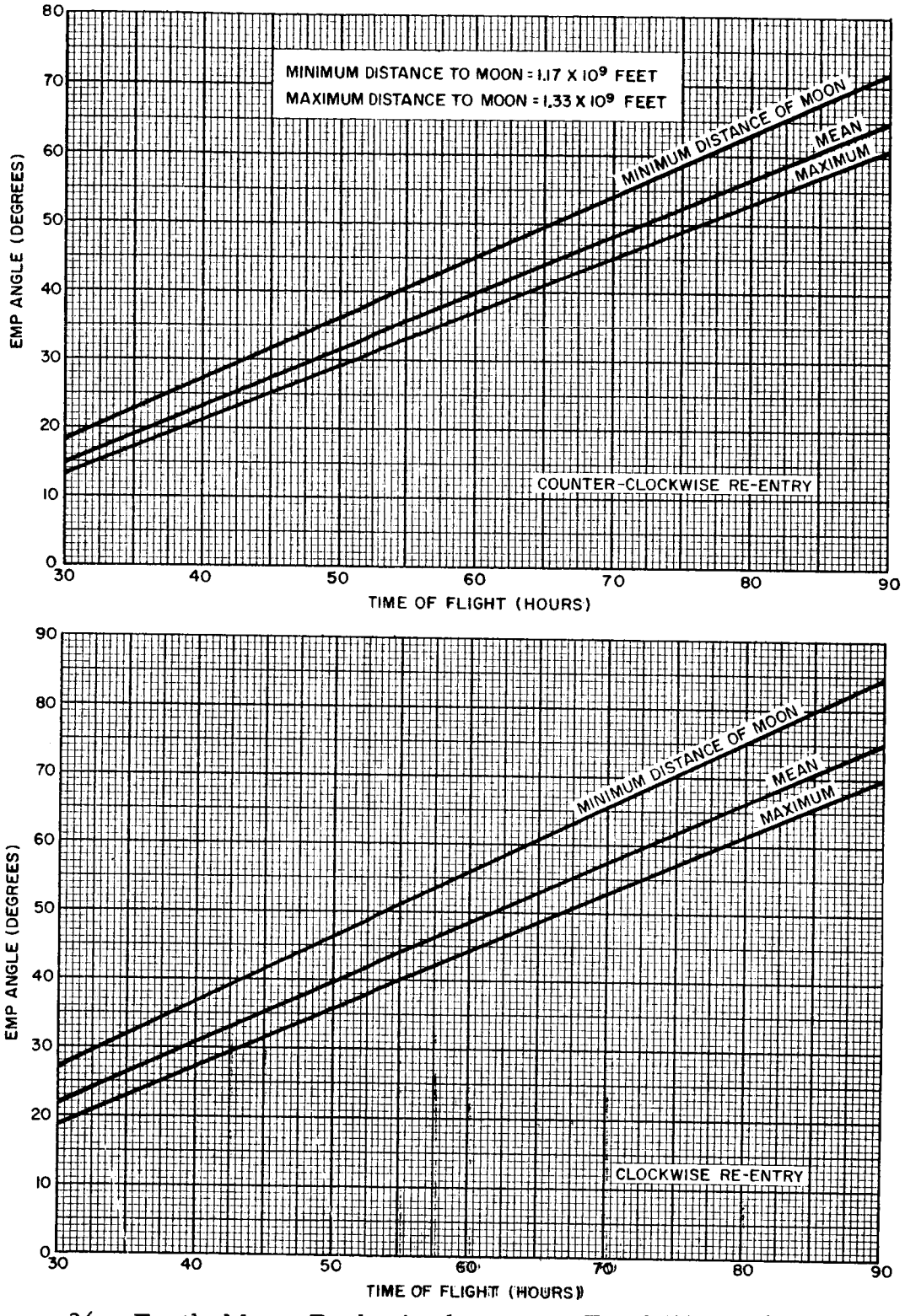

Figure 26. Earth-Moon-Probe Angle versus Total Time of Flight for Various Distances of the Moon.

remains relatively fixed. The selenographic coordinates set up on the moon are such that the surface's "mean" position on the earth-moon line represents zero latitude and longitude. Also, the moon's axis of rotation lies very nearly perpendicular to its plane of motion around the earth. Thus, its equatorial plane will nearly contain the moon's velocity vector $\bar{u}_m$. This implies that the vector $\bar{v}_s$ will be very close to the selenographic equator and in fact upon observing the results of many analytic runs, it does consistently come within 10 degrees of the moon's equator. Since this angle is of the same order of magnitude as the librations of the moon, and since the librations will be ignored in the discussion that follows, it will be assumed that the vector $\bar{v}_s$ does in fact lie in the moon's equator.

We shall consider now a graphical method which may be used to solve approximately for some of the remaining parameters used in the moon phase geometry. This approach has the dual purpose of providing a method for the practical determination of some of the important moon-to-earth parameters while at the same time indicating the parametric relationships involved in the moon phase. The data used in generating these graphs have been obtained in some cases from the analytic program and in others from solutions of simple spherical triangles.

(1) First, it is assumed that all the parameters required to solve the earth phase have been decided upon and that the analysis has progressed to the point where the magnitude and direction of the $\bar{v}_s$ vector has been found; with the EMP angle representing the direction of this vector relative to the selenographic coordinate system.

(2) Then, referring to Figure 27, the specification of the selenographic latitude and longitude (μ_o and λ_o respectively) will determine the orientation of the moon phase conic since it must pass through the $\bar{v}_s$ vector and the launch site vector. The right spherical triangle shown in this figure with the sides μ_o and $(\lambda_o - \text{EMP})^*$ may then be

*Remember that longitudes measured west of (0, 0) are negative.

solved for the inclination of the moon phase trajectory, the launch azimuth and the in-plane angle from launch to the $\bar{v}_s$ vector. The inclination is given in Figure 28 versus the longitude minus the EMP angle for the specified launch site latitude.

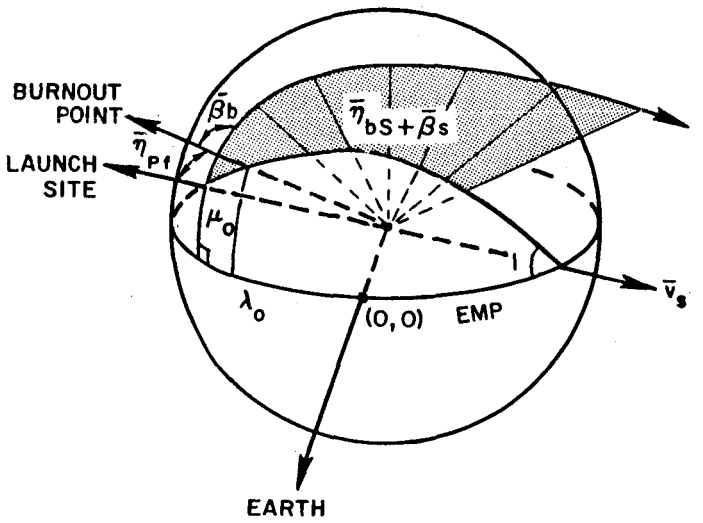

Figure 27. Moon Phase Geometry.

(3) The launch azimuth may be found from Figure 29 which is also plotted versus the longitude minus the EMP angle and for various launch site latitudes.

(4) The in-plane angle from the launch site to the vector $\bar{v}_s$ (which also indicates the direction of the hyperbolic asymptote) is composed of the sum of the powered flight angle and the in-plane burnout to asymptote angle; indicated by $\bar{\eta}_{pf} + \bar{\eta}_{bs} + \bar{\beta}_s$ in Figure 27. This angle is presented in Figure 30 and also plotted versus the longitude minus the EMP angle for various launch site latitudes.

(5) The partial in-plane angle $\bar{\eta}_{bs} + \bar{\beta}_s$ may now be used to solve for the burnout flight path angle $\bar{\beta}_b$. To see how this may be done, reference is made to Figure 5b in Section II. Here it is seen that the moon phase conic will be completely determined if the burnout

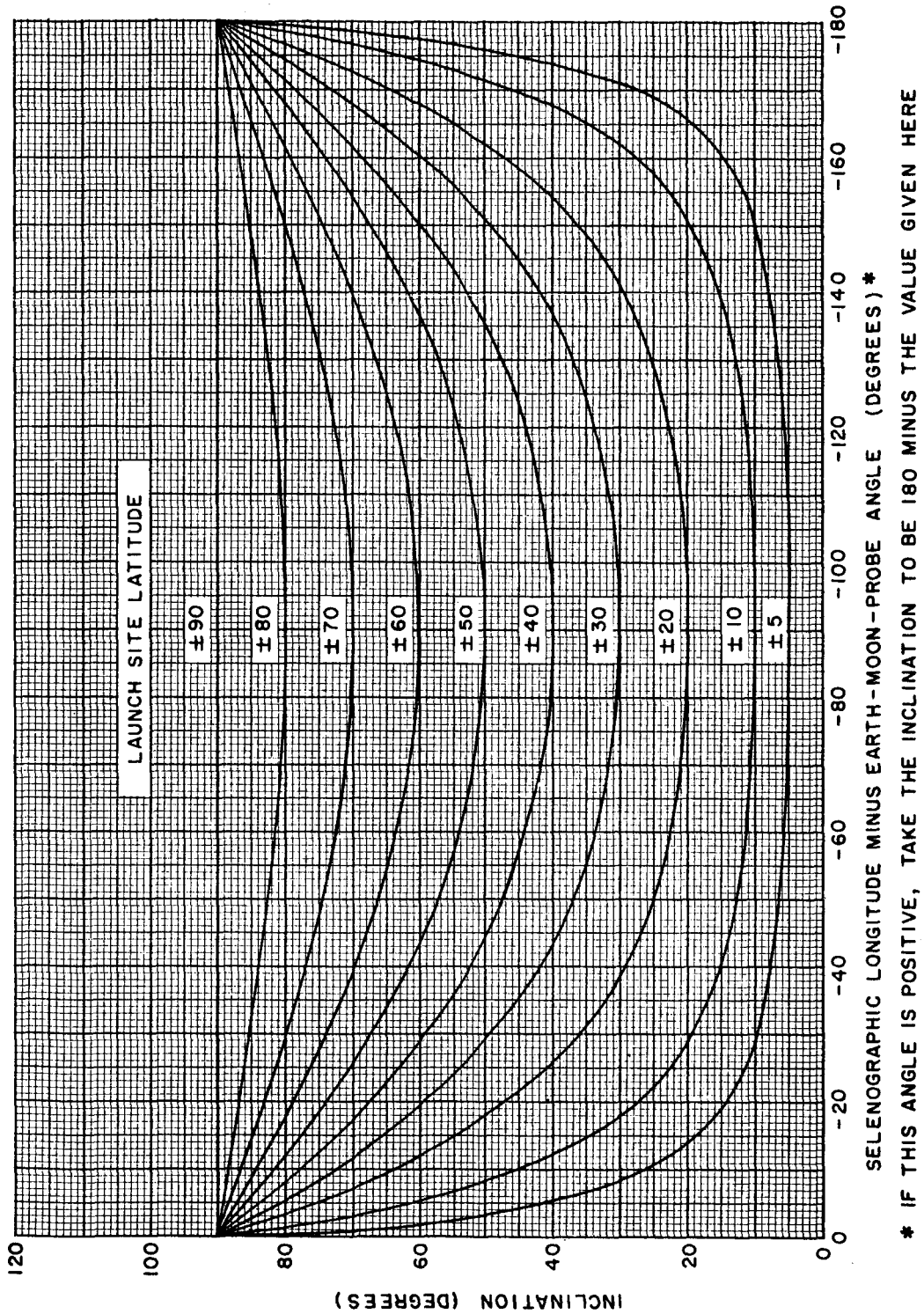

Figure 28. Inclination of the Hyperbolic Plane versus Longitude Minus Earth-Moon-Probe Angle for Various Launch Site Latitudes (Selenographic).

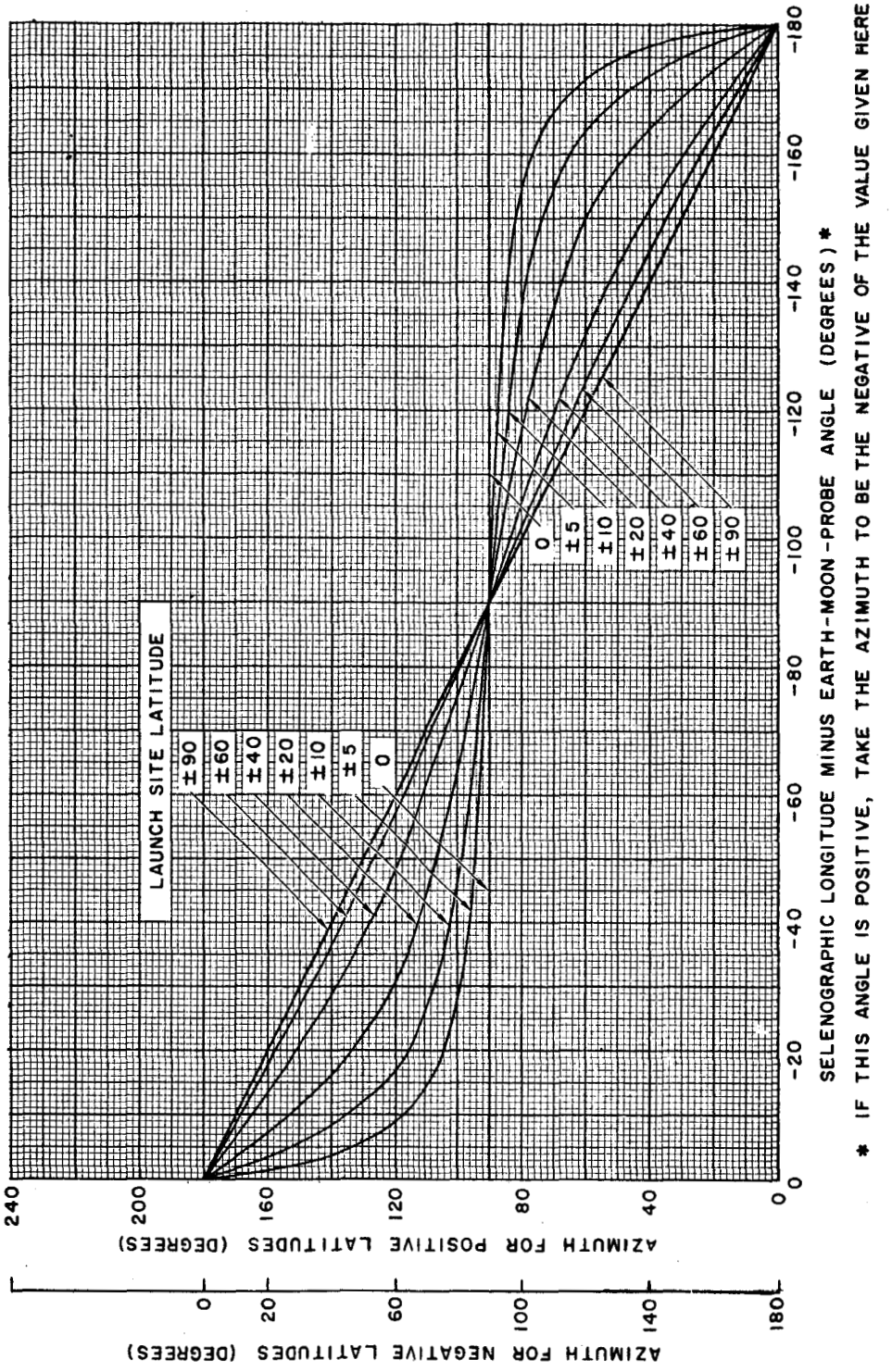

Figure 29. Lunar Burnout Azimuth versus Longitude Minus Earth-Moon-Probe Angle for Various Launch Site Latitudes (Selenographic).

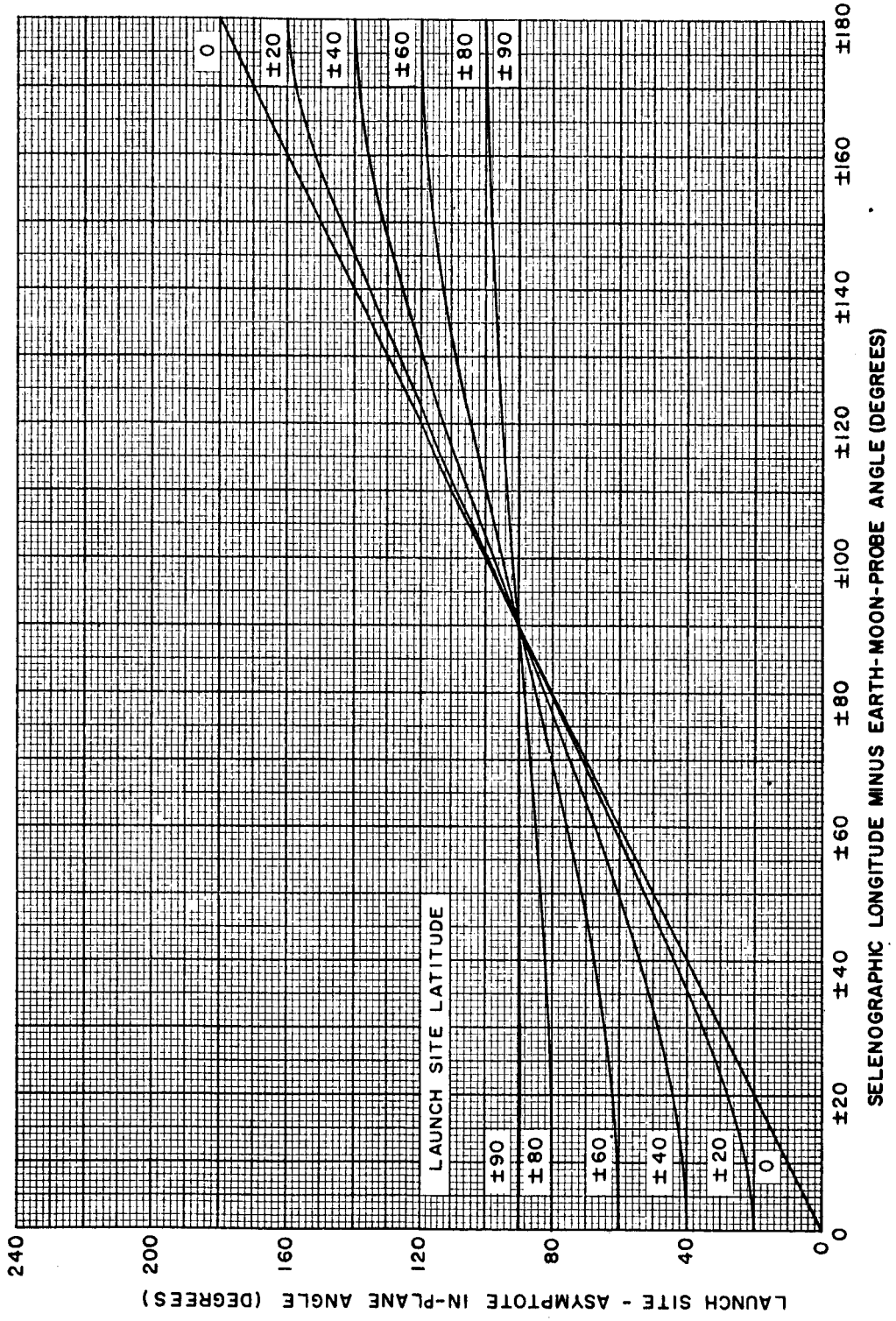

Figure 30. Launch Site-Asymptote In-Plane Angle (Hyperbolic Plane) versus Longitude Minus Earth-Moon-Probe Angle for Various Launch Site Latitudes (Selenographic).

parameters of altitude, velocity and flight path angle are specified. Then it would be possible to solve for the angle $\ddot{\imath}\iota_{bs} + \overline{\beta}_s$ given R_s, the radius of the sphere of action. These parameters have been plotted in Figure 31 for a fixed burnout altitude of 100,000 feet and may be used to solve for $\overline{\beta}_b$.

To illustrate this procedure, consider the following example:

Total time of flight = 90 hours
Distance of the moon at launch $\cong 1.33 \times 10^{10}$ feet (max)
Type of re-entry = counterclockwise
Launch site latitude = 5^o
Launch site longitude = 25^o
Burnout altitude = 100,000 feet
Powered flight angle = 3^o

With this information and the foregoing graphs, the following information may be obtained.

Lunar burnout velocity $\cong$ 8250 fps (Figure 23)
Velocity at the sphere of action $\cong$ 3200 fps (Figure 24)
Hyperbolic excess velocity $\cong$ 2900 fps (Figure 24)
Time in the sphere of action $\cong$ 13.4 hours (Figure 25)
Earth-moon-probe (EMP) angle $\cong 61^o$ (Figure 26)
Longitude - EMP angle = 25 - 61 = -36^o
Trajectory inclination = 9^o (Figure 28)
Launch azimuth = 97^o (Figure 29)
Launch site - asymptote in-plane angle = 37^o (Figure 30)
Burnout - asymptote in-plane angle = $37^o - 3^o = 34^o$
Burnout flight path angle = 23^o (Figure 31)

Since it was not necessary to specify the day of the month on which the vehicle was launched (except that it must be on a day when the distance to the moon specified above is satisfied) the determination of the moon phase by this method is independent of the declination of the moon. It has already been made clear that the moon phase is essentially independent of the terminal conditions at the earth (except for cw or ccw re-entry).

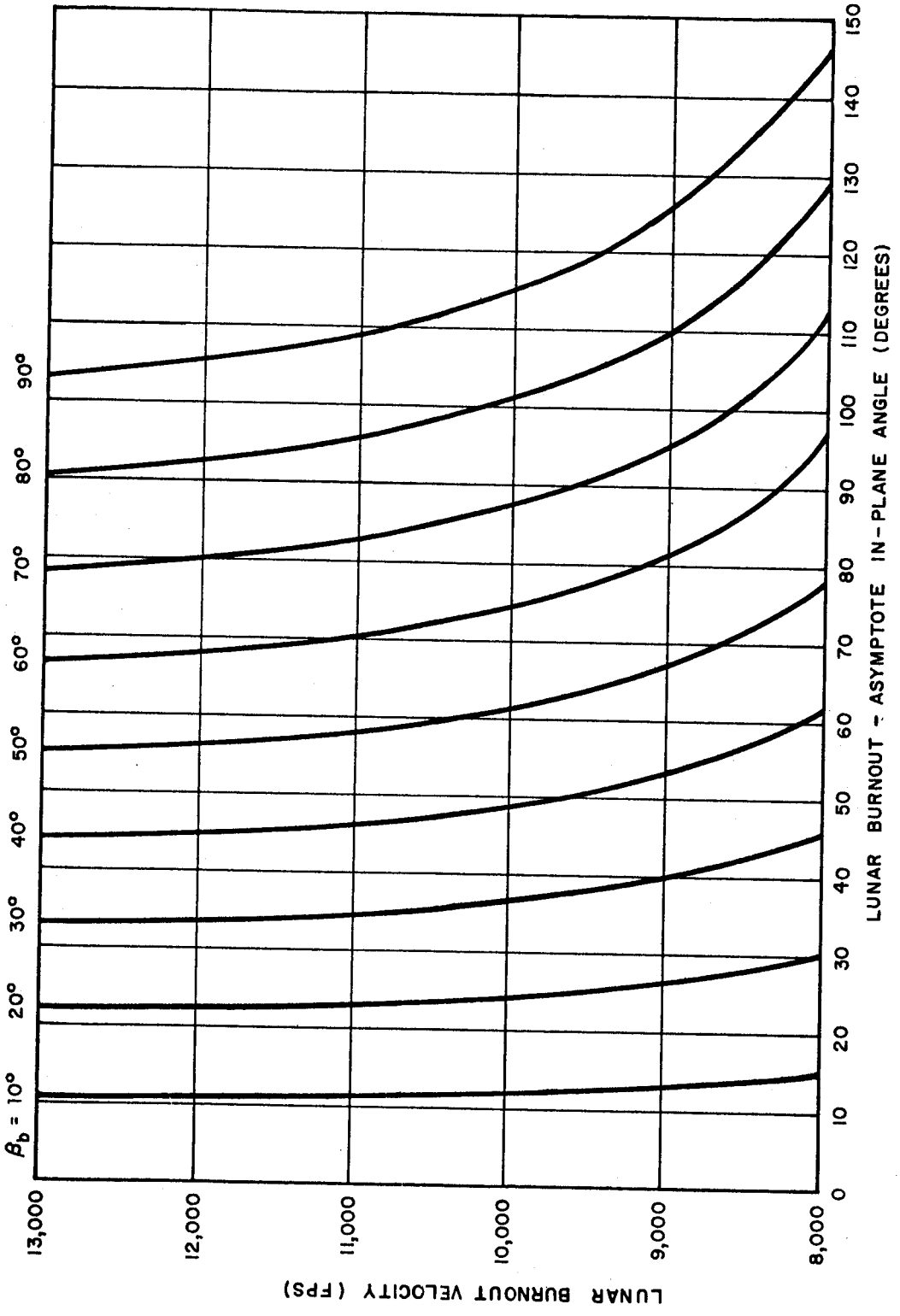

Figure 31. Lunar Burnout Velocity (Altitude = 100,000 ft) versus Lunar Burnout - Asymptote In-Plane Angle for Various Lunar Burnout Flight Path Angles.

It is realized that all of these values are approximate and that the greatest uncertainty enters in the clockwise-counterclockwise decision. The two are not completely independent since in the earth phase there is a continuous transition from one type of re-entry to the other. For the example above, better results may have been obtained by first solving for the inclination of the earth phase trajectory and on this basis interpolating between clockwise and counterclockwise values. One should also be aware of the two other assumptions made; the first being the neglect of the lunar librations (mentioned previously) and the other the restriction of $\bar{v}_s$ to lie in the moon's equatorial plane.*

Aside from using these graphs to obtain approximate values of moon phase parameters in specific situations, it is possible to generate restriction curves as has been done in the earth phase analysis. Returning to Figure 27 (and also Figure 5b), for example, it is clear that the in-plane angle $\bar{\eta}_{bs} + \bar{\beta}_s$ is dependent only on the velocity magnitude v_s and the burnout flight path angle $\bar{\beta}_b$. Thus, for a given day of launch and time of flight, and for specific earth phase conditions, the selenographic position and velocity of $\bar{v}_s$ will remain essentially fixed. The in-plane angle $\bar{\eta}_{bs} + \bar{\beta}_b$ will then be <u>only</u> a function of $\bar{\beta}_b$. In this situation it is possible to draw constant $\bar{\beta}_b$ contour curves on the surface of the moon as shown in Figure 32 where each point on a given contour is displaced by the corresponding $\bar{\eta}_{bs} + \bar{\beta}_s$ angle from the $\bar{v}_s$ vector.

Such contours have been generated with the analytic program by running trajectories with different launch sites but having all remaining input parameters equivalent. The results of these runs are presented in Figure 33 which plots, by interpolation, the constant $\bar{\beta}_b \cong \beta$) and constant azimuth curves. These curves are <u>not</u> everywhere orthogonal. The restricted region shown here and in Figure 32 simply implies that it is impossible to launch a <u>direct ascent</u> moon-to-earth flight from these sites, for the earth phase parameters considered, without first passing through the pericynthion of the moon phase conic.

---

*It should be noted that these simplifying assumptions are <u>not</u> made in the analytic Lunar Return Program, but were only made in the qualitative graphical analysis discussed above and illustrated in Figures 26 through 30.

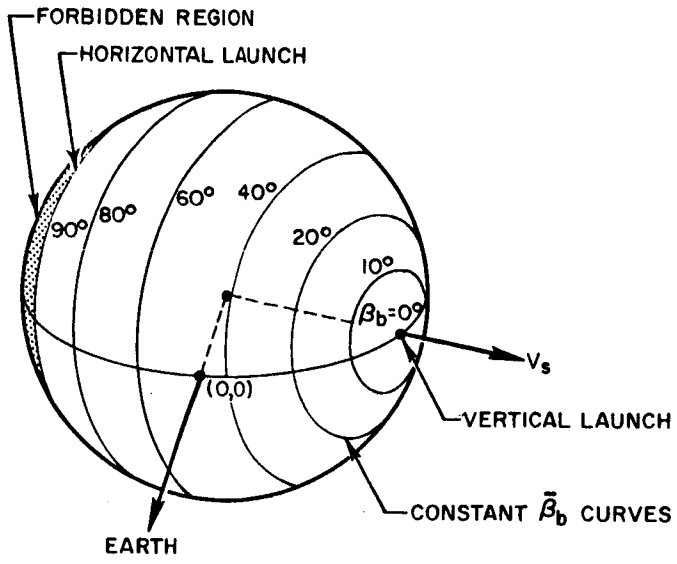

Figure 32. Constant Burnout Flight Path Angle Contours.

With the aid of Figures 23 and 31, and restricting the class of moon-to-earth trajectories to those having a mean distance to the moon and a steep re-entry angle, it is possible to generate the graph shown in Figure 34. This figure and Figure 26 may be used to generate data required to plot constant β_b contours and forbidden launch regions.

C. SENSITIVITY COEFFICIENT ANALYSIS

The Sensitivity Coefficient Routine provides a method of computing quite accurate sensitivity coefficients at a very rapid rate (0.1 sec per perturbed trajectory) and therefore makes it possible to generate extensive burnout or midcourse sensitivity data. This data, some of which is presented in the following graphs, may then be used to show the dependence of sensitivity coefficients on launch site location, energy, time of flight, etc., and the results may be examined for general trends. However, the most meaningful results will be obtained when a specific launch guidance system (i.e., set of burnout errors) is considered, since it is the resultant errors at re-entry—or more complex, the midcourse correction requirements—which are

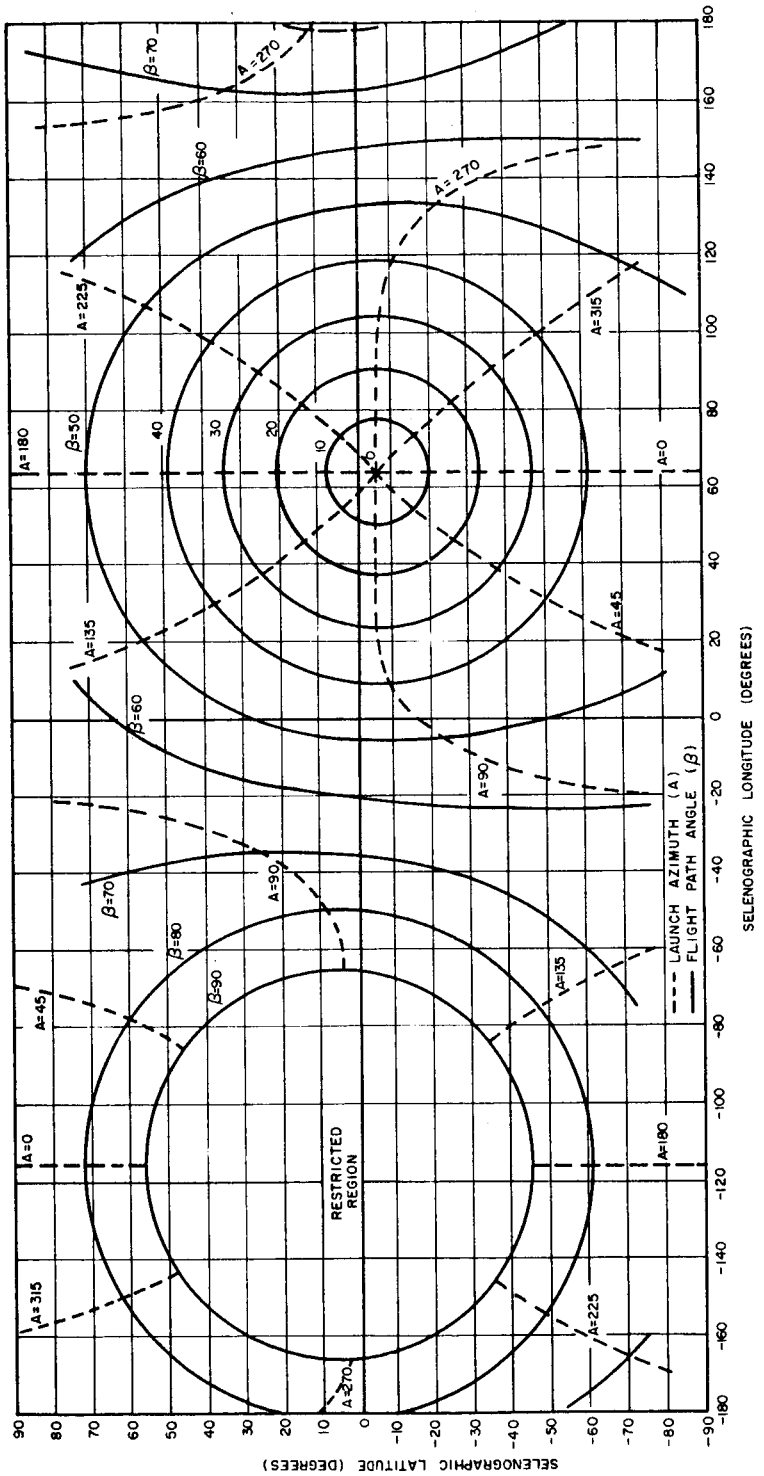

Figure 33. Launch Azimuth and Flight Path Angle Contours Mapped on the Surface of the Moon (Including Lunar Librations). Vehicle Launched on December 4, 1963 to Re-enter Gulf of Mexico with a Re-entry Angle of 175°. Total Time of Flight = 70 Hours.

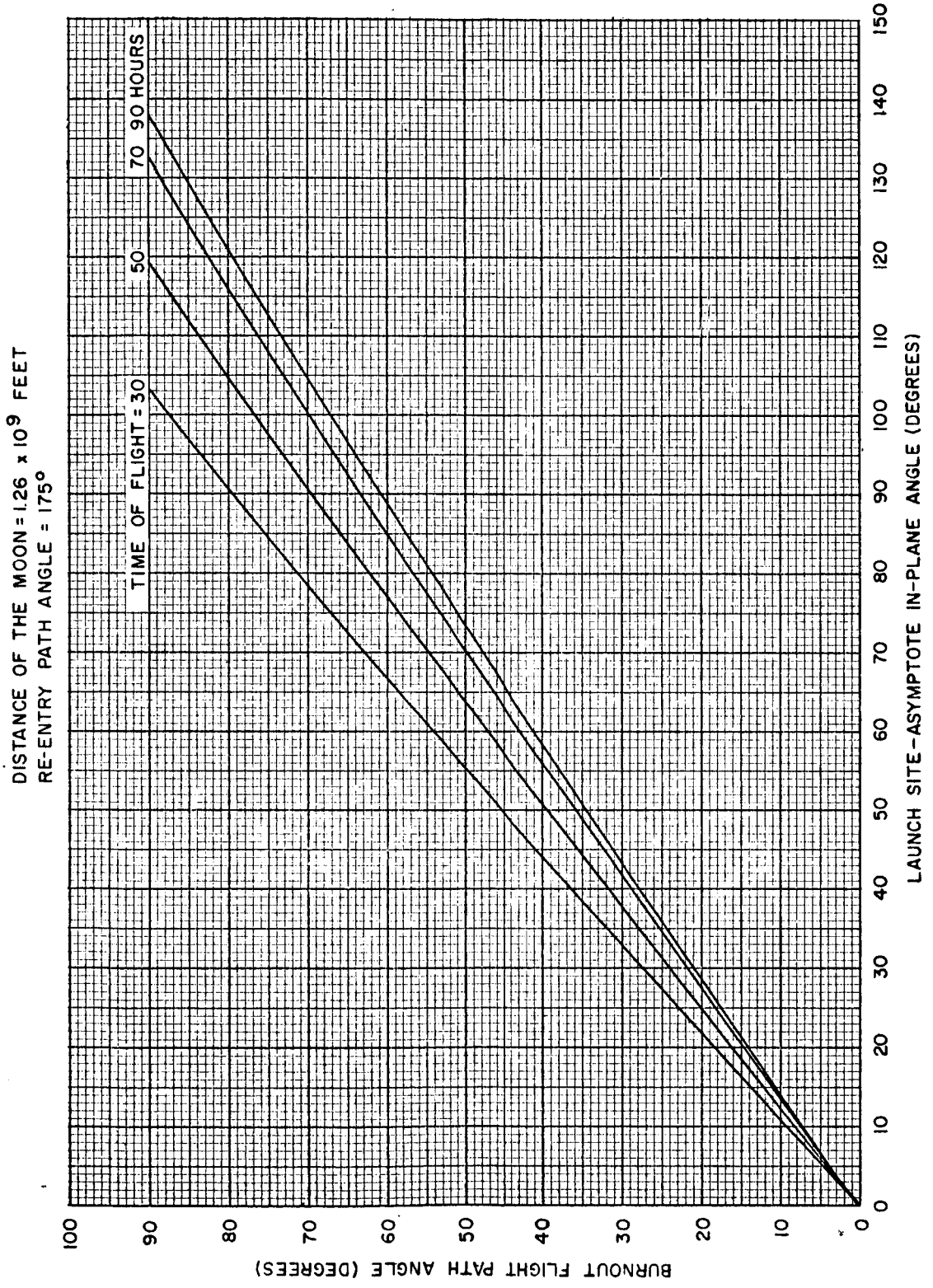

Figure 34. Lunar Burnout Flight Path Angle versus In-Plane Angle (Hyperbolic Plane) from Launch Site to the Hyperbolic Asymptote for Various Total Times of Flight.

significant rather than either the burnout errors produced by the guidance system or the sensitivity coefficients. The methods for carrying out such an over-all guidance analysis are described in [4].

In this report no attempt is made to conduct an extensive analysis of sensitivity coefficients, but rather, material is presented which will indicate (1) the general behavior with respect to burnout and landing site variables, and (2) the general magnitudes of these coefficients for various flight times and re-entry conditions. Let us begin then with Figures 35, 36, and 37. Here we have plotted the sensitivity coefficients of latitude, longitude, flight path angle and time of re-entry with respect to the lunar burnout velocity, burnout flight path angle and launch azimuth. In the corresponding analytic runs, it was assumed that the powered flight angle was zero. This term has no appreciable affect on the results. The sensitivity coefficients were plotted against the selenographic longitude of the launch site (latitude is zero) for three times of flight.

Looking at these graphs and the following three Figures, i.e., 38, 39, and 40 which have a shallow flight path angle, the following observations may be made:

(1) As expected, trajectories with slow flight times yield greater sensitivity coefficients than those with faster flight times. This is true among all of the burnout variables.

(2) Also, it is possible to discern some general trends when the coefficients with respect to the three burnout variables are plotted versus longitude. Specifically, the coefficients with respect to velocity seem to vary linearly with longitude. The coefficients with respect to the flight path angle has a tendency to remain constant in magnitude but change signs near the longitude corresponding to vertical launch. Finally, with respect to the burnout azimuth, there seems to exist a sinusoidal type symmetry of the sensitivity coefficients with respect to the launch site longitude.

(3) Returning to the quantitative properties of the sensitivity coefficients, it is seen that their magnitudes in latitude, longitude and flight path angle with respect to burnout velocity increase as the launch site sweeps from the west side of the moon to the east side of the moon. Both sets of curves indicate the opposite effect on the time of re-entry sensitivity with respect to launch site longitude. In this case, the coefficient magnitude decreases as the launch site moves from west to east; except for the 50 hour case in which it remains nearly constant.

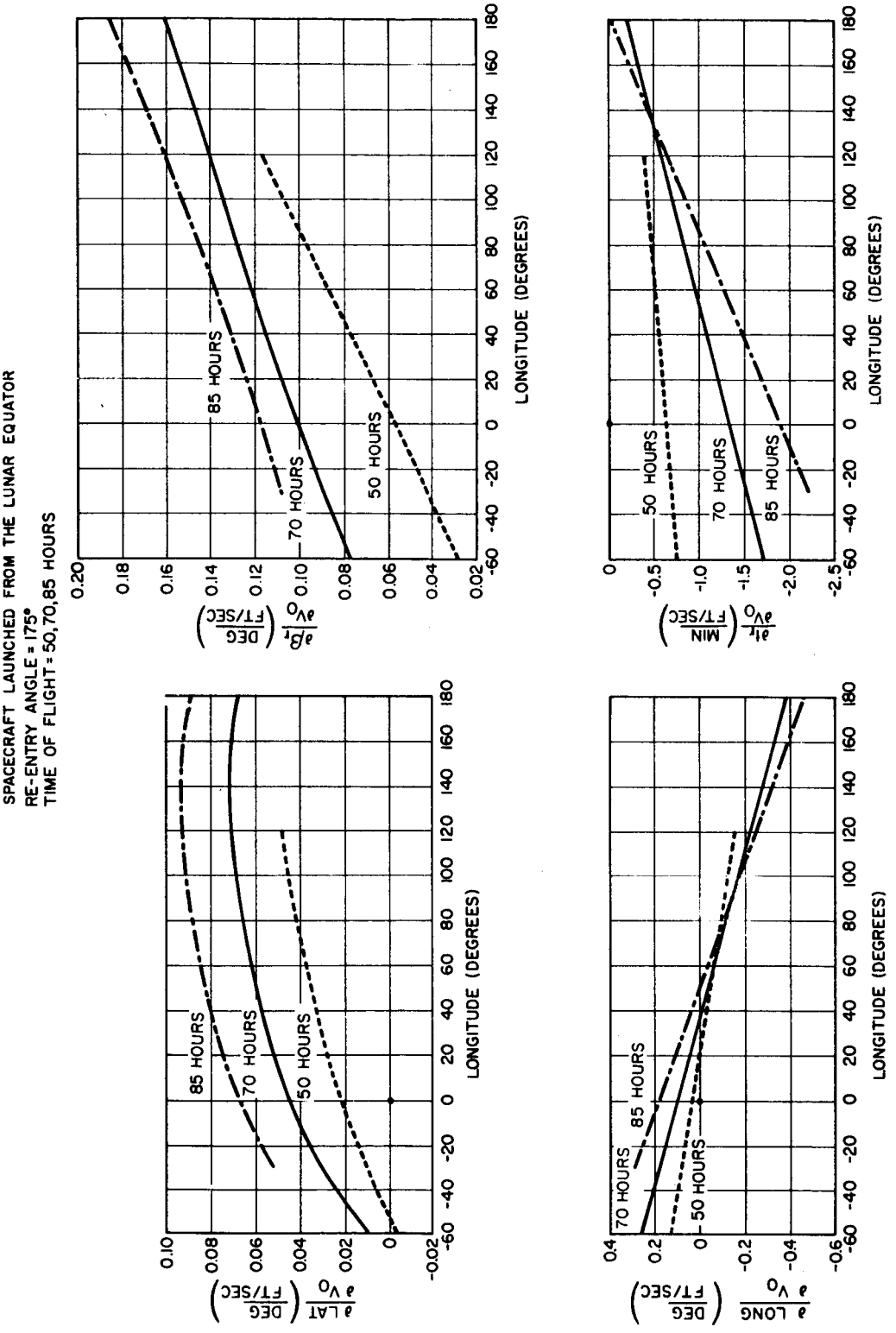

Figure 35. Sensitivity Coefficients at Re-entry to Burnout Velocity versus Selenographic Burnout Longitude.

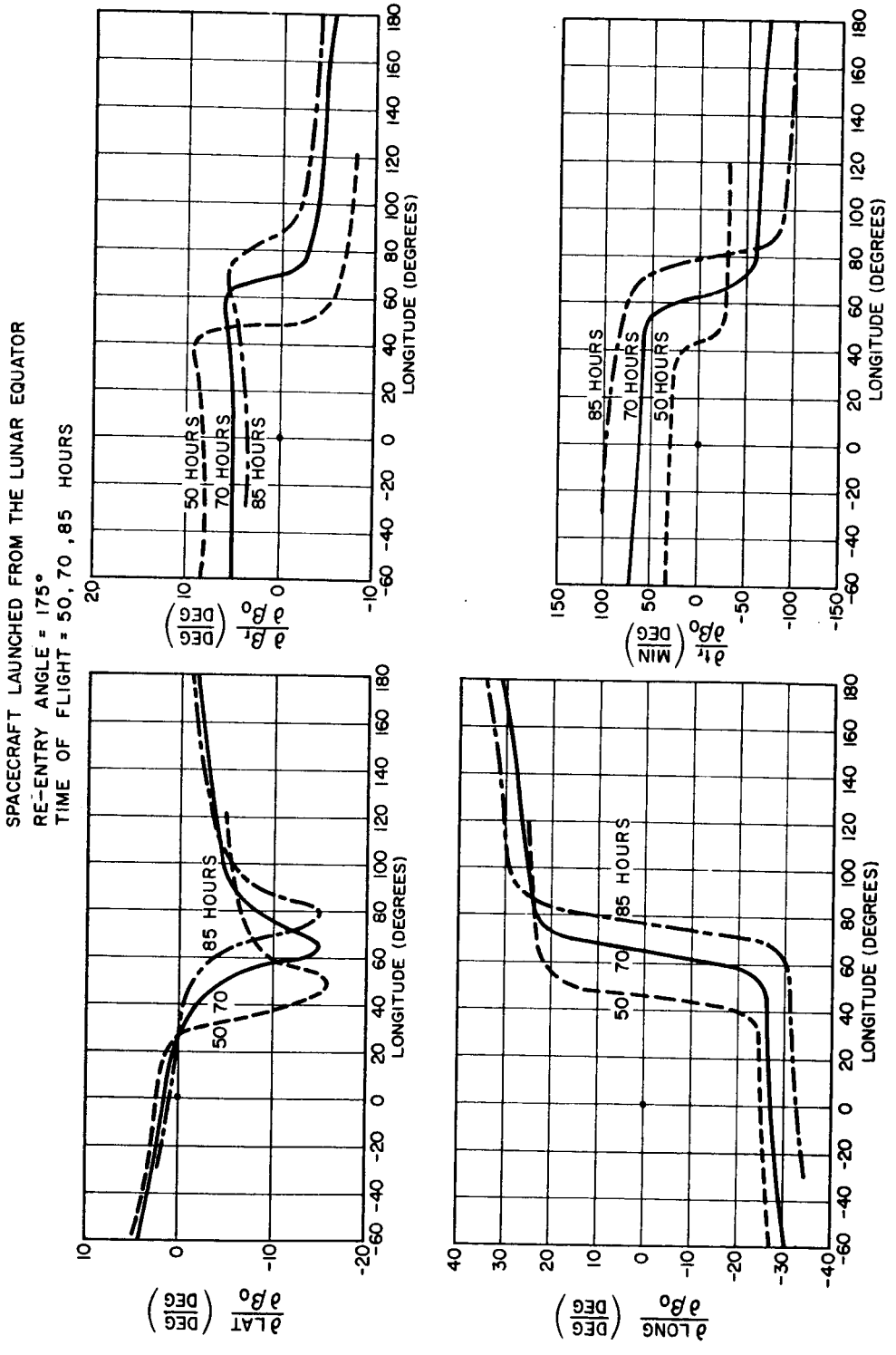

Figure 36. Sensitivity Coefficients at Re-entry to Burnout Flight Path Angle versus Selenographic Burnout Longitude, [illegible] Indicated Variables.

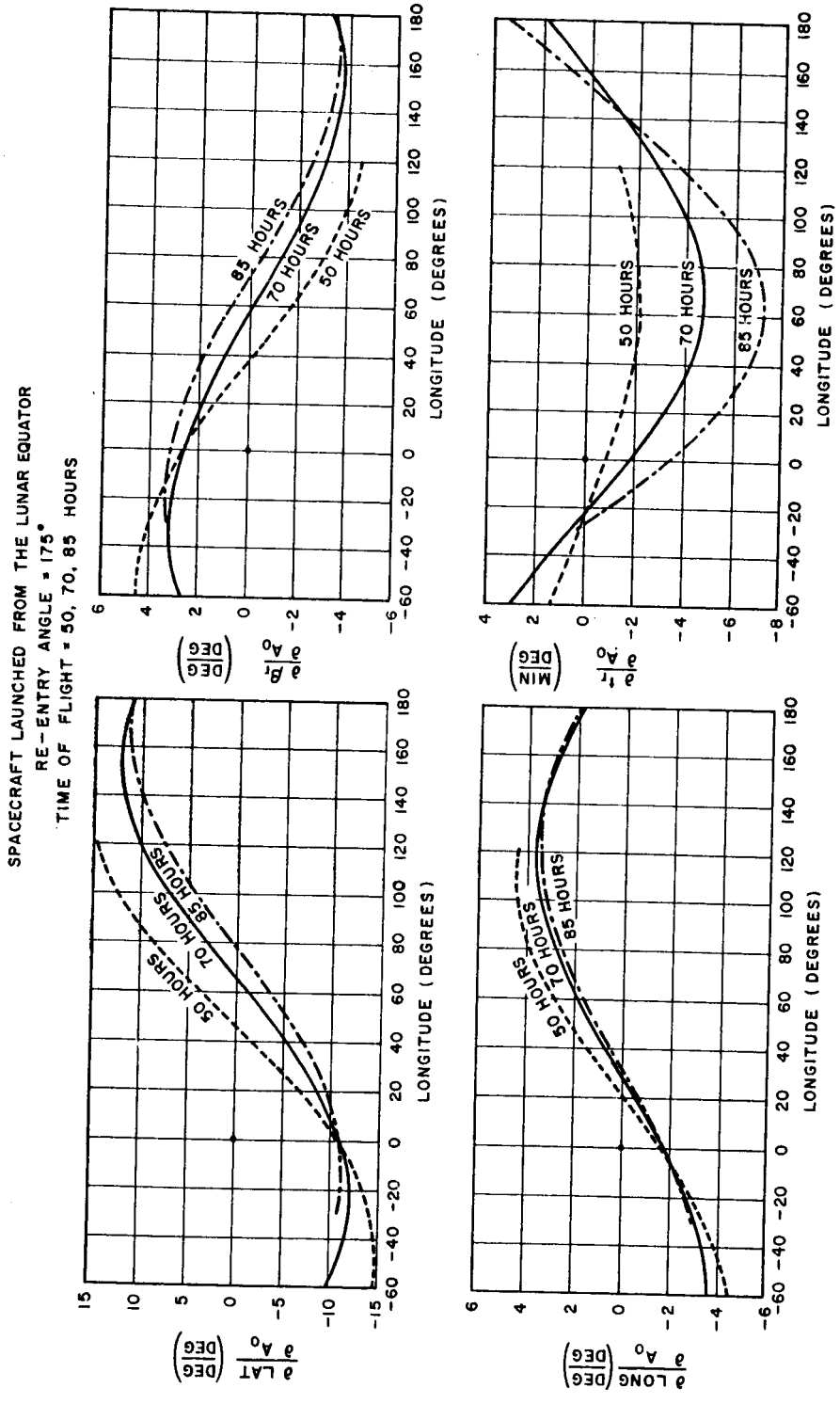

Figure 37. Sensitivity Coefficients at Re-entry to Burnout Azimuth versus Selenographic Burnout Longitude for Indicated Variables.

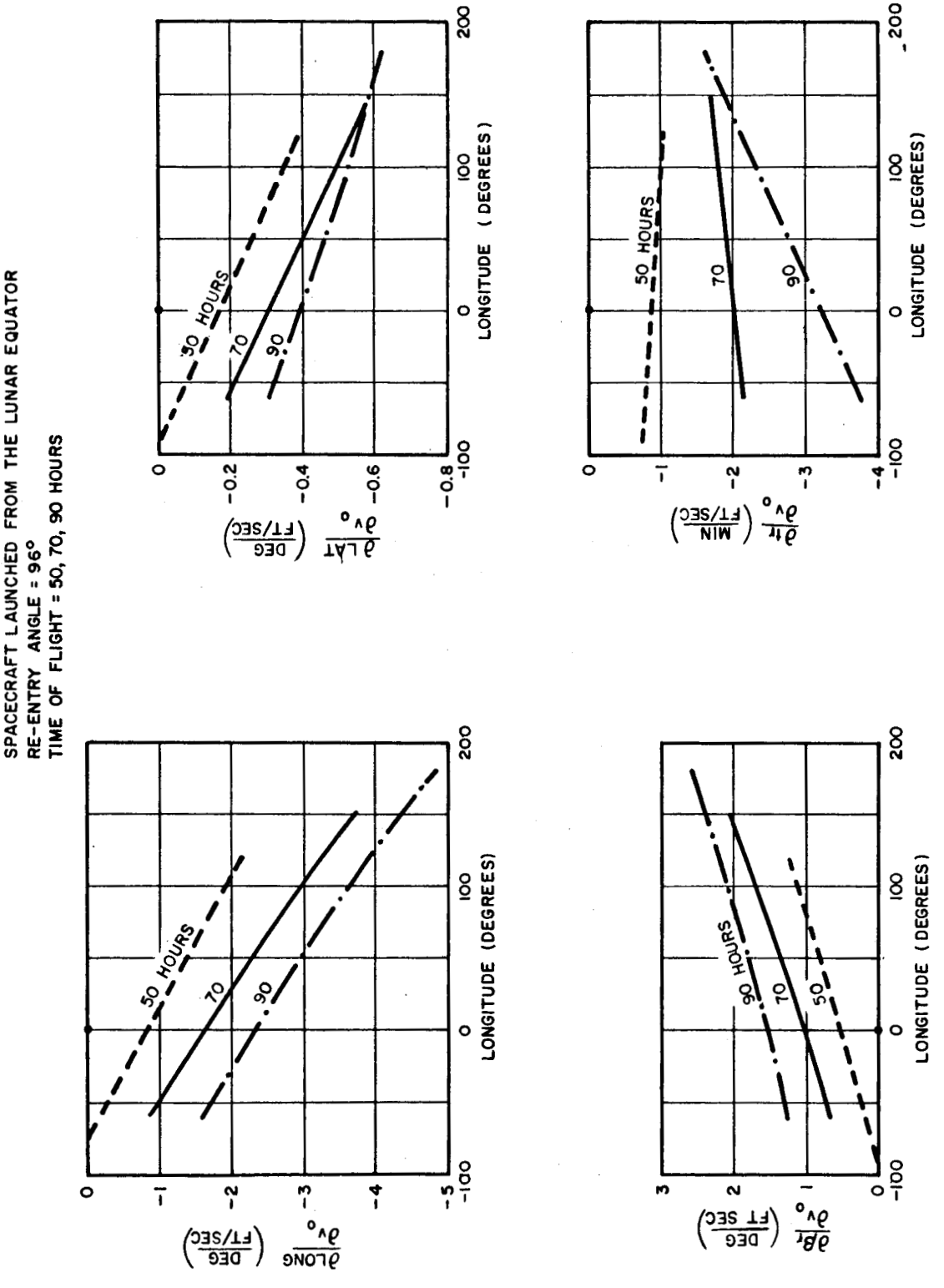

Figure 38. Sensitivity Coefficients at Re-entry to Burnout Velocity versus Selenographic Burnout Longitude.

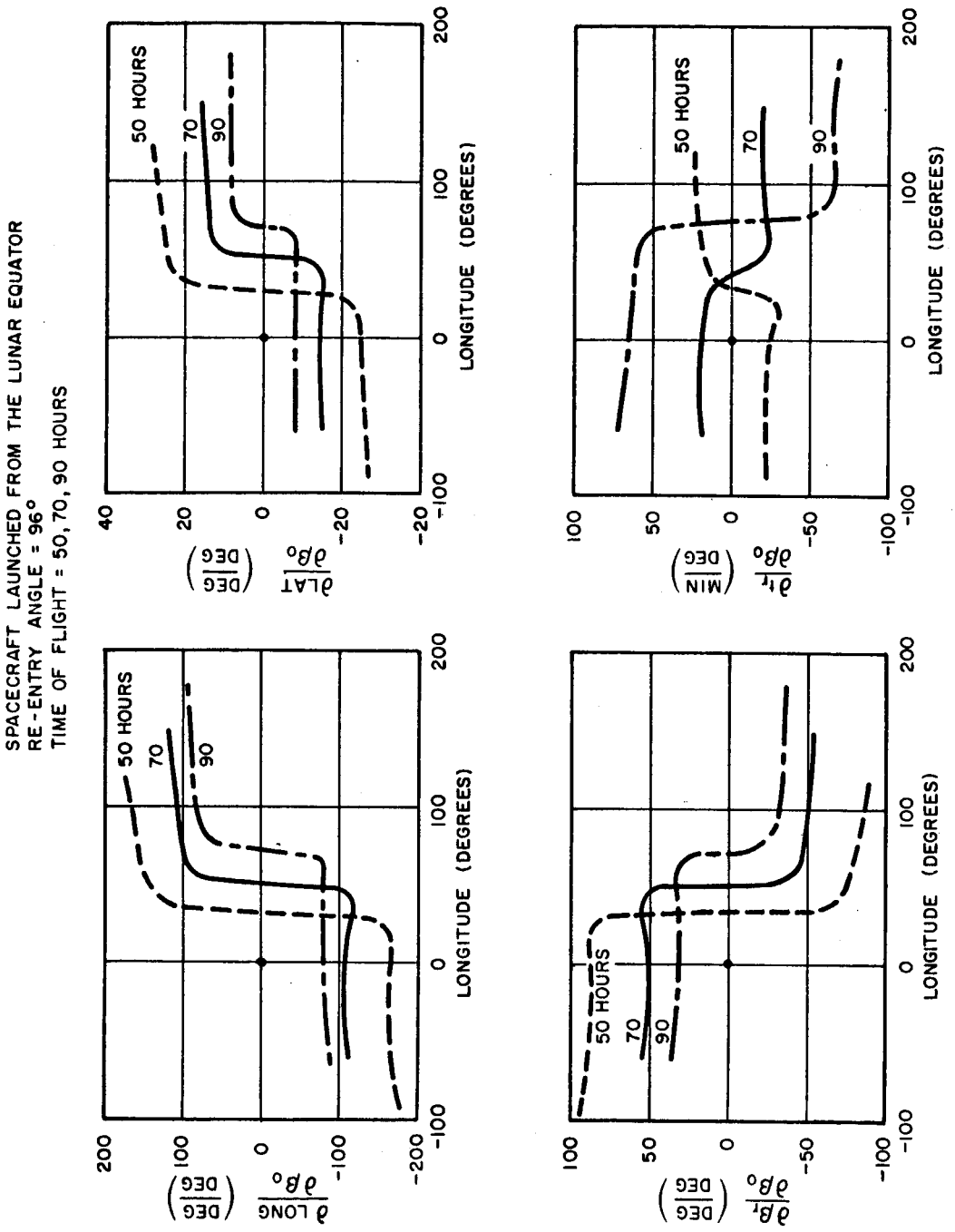

Figure 39. Sensitivity Coefficients of Re-entry to Flight Path Angle versus Selenographic Burnout Longitude.

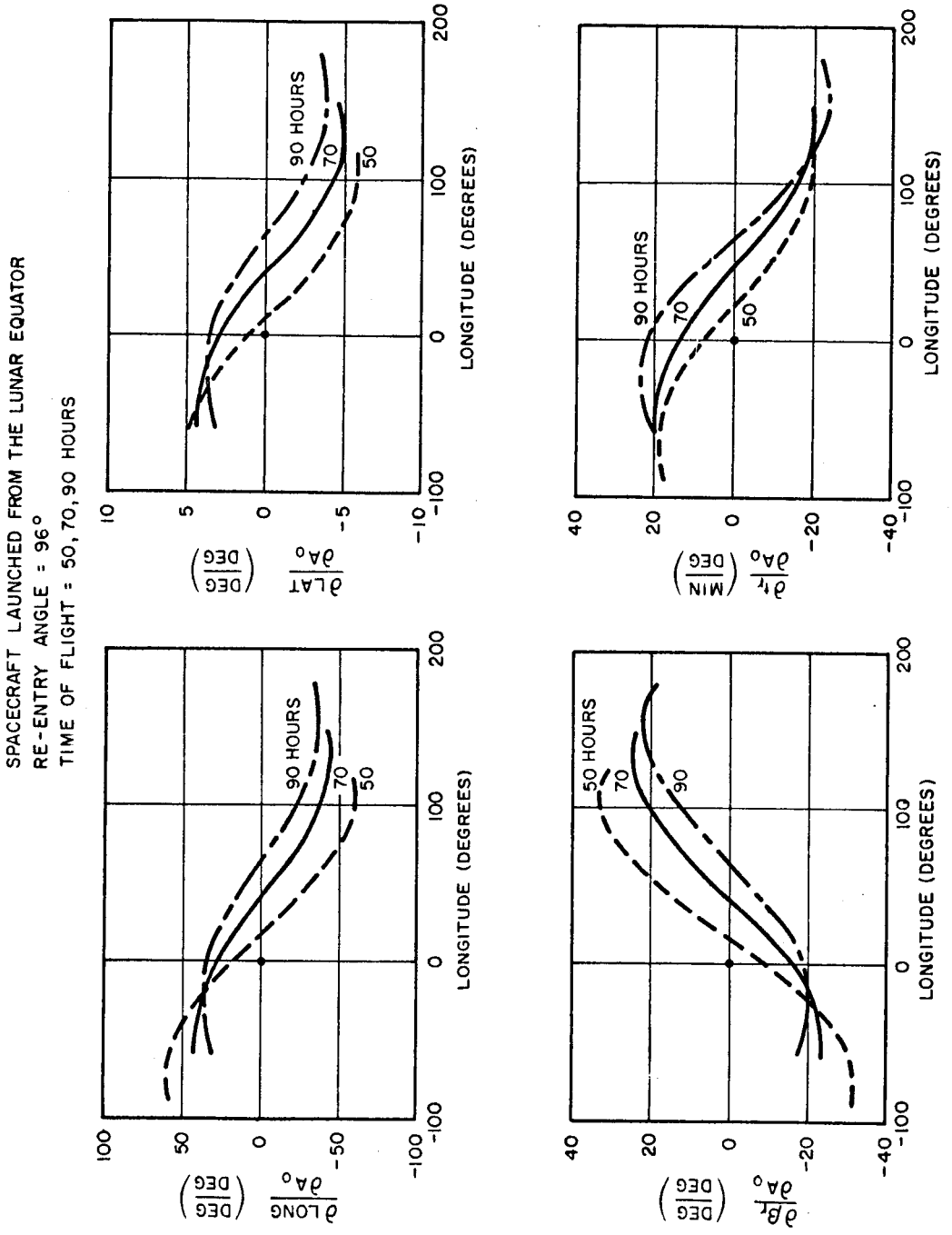

Figure 40. Sensitivity Coefficients of Re-entry to Burnout Azimuth versus Selenographic Burnout Longitude.

Figures 41 and 42 plot the same information as the previous graphs except that here they are plotted for a single flight time and re-entry angle (70 hours and 96 degrees respectively) and include the sensitivity coefficients with respect to the position radial vector r_o, the launch site latitude μ_o, and the launch site longitude λ_o. One trend that may be noted on these graphs is that, as expected, the sensitivity with respect to the radius vector varies linearly (as is the case with the burnout velocity) and in the same direction as the velocity coefficient.

The remaining four Figures, 43 through 46 present the sensitivity coefficients of the terminal parameters with respect to cartesian midcourse velocities versus the time from lunar burnout. As expected, the sensitivities decrease as the time from burnout increases. Two other observations may be made:

(1) In the vicinity of the moon the variations of the coefficients are very great. This is most likely due to the great variation of the velocity magnitude and direction in this region. After a few hours, all of the coefficients settle down and vary in a uniform manner.

(2) Some midcourse directions exist along which there will be no (or little) variation in the sensitivities of certain terminal parameters. This is particularly obvious in Figure 46 in which the variations in the re-entry longitude, latitude and flight path angle are much smaller for perturbations in the $\dot{x}$ and $\dot{z}$ directions than for perturbations in the $\dot{y}$ direction. Similar behavior, i.e., the presence of "critical midcourse directions", is well known for earth-to-moon trajectories [5], [6].

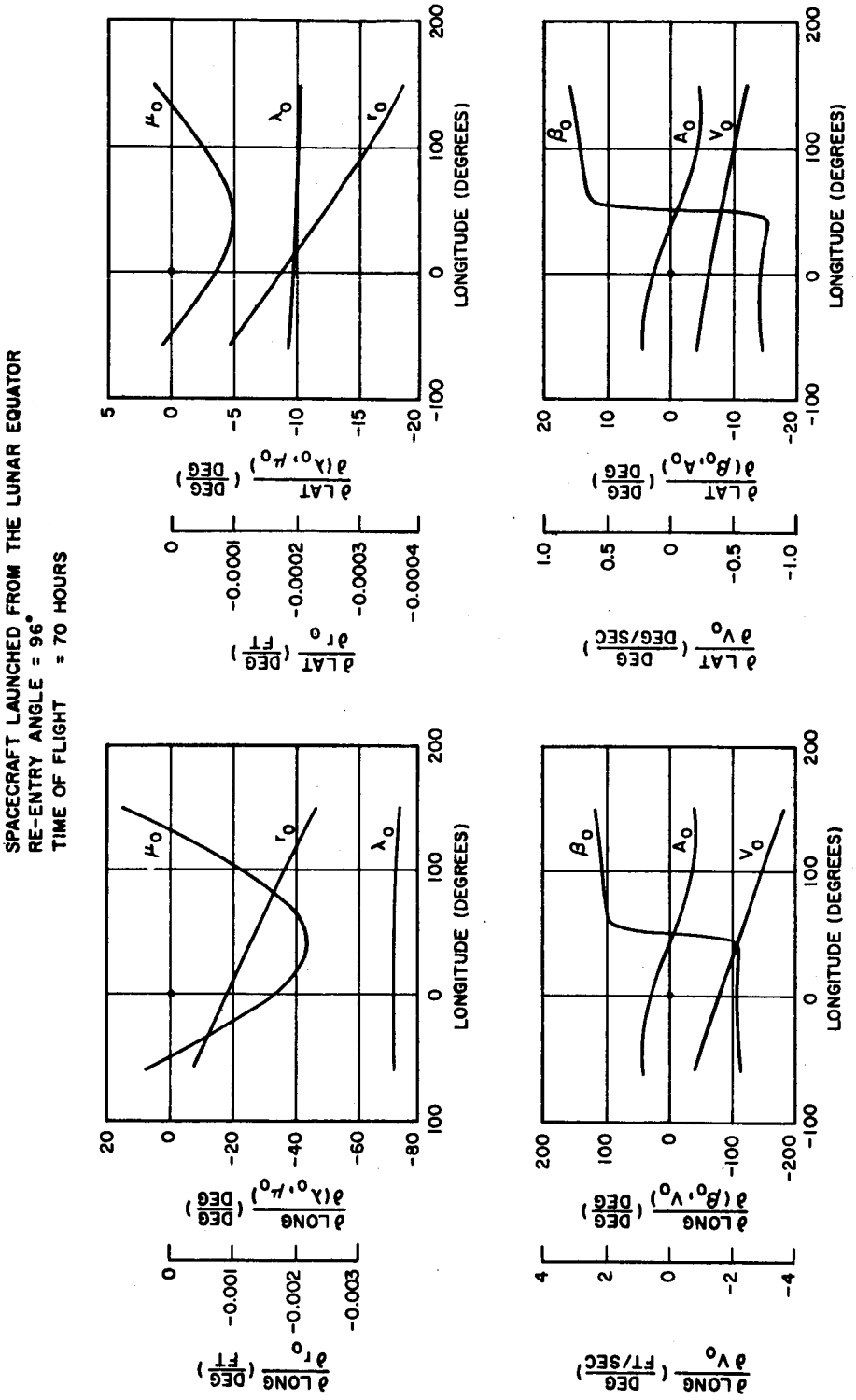

Figure 41. Sensitivity Coefficients of Re-entry versus Selenographic Burnout Longitude for Variations in Selenographic Polar Coordinates.

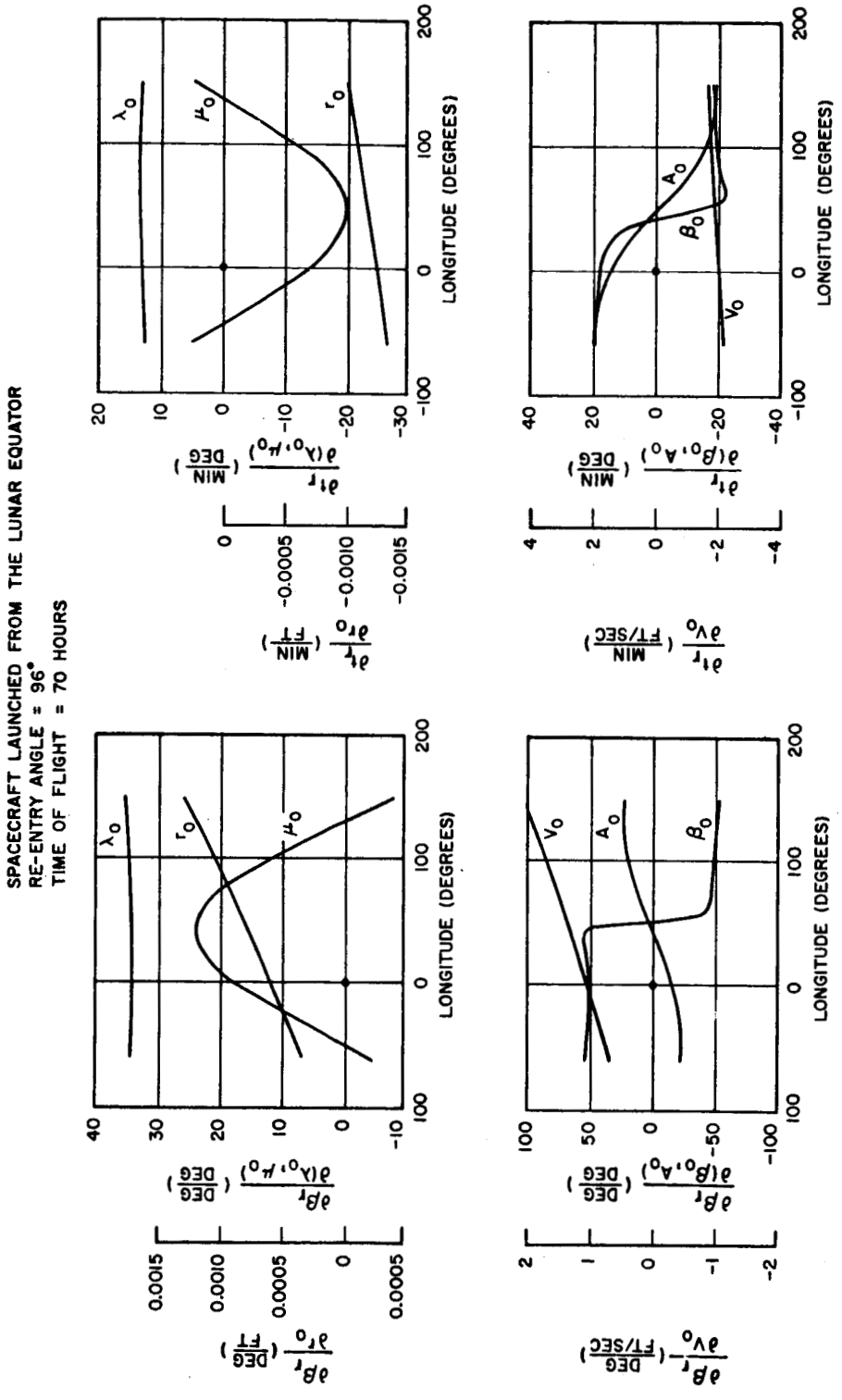

Figure 42. Sensitivity Coefficients at Re-entry versus Selenographic Burnout Longitude for Variations in Selenographic Polar Coordinates.

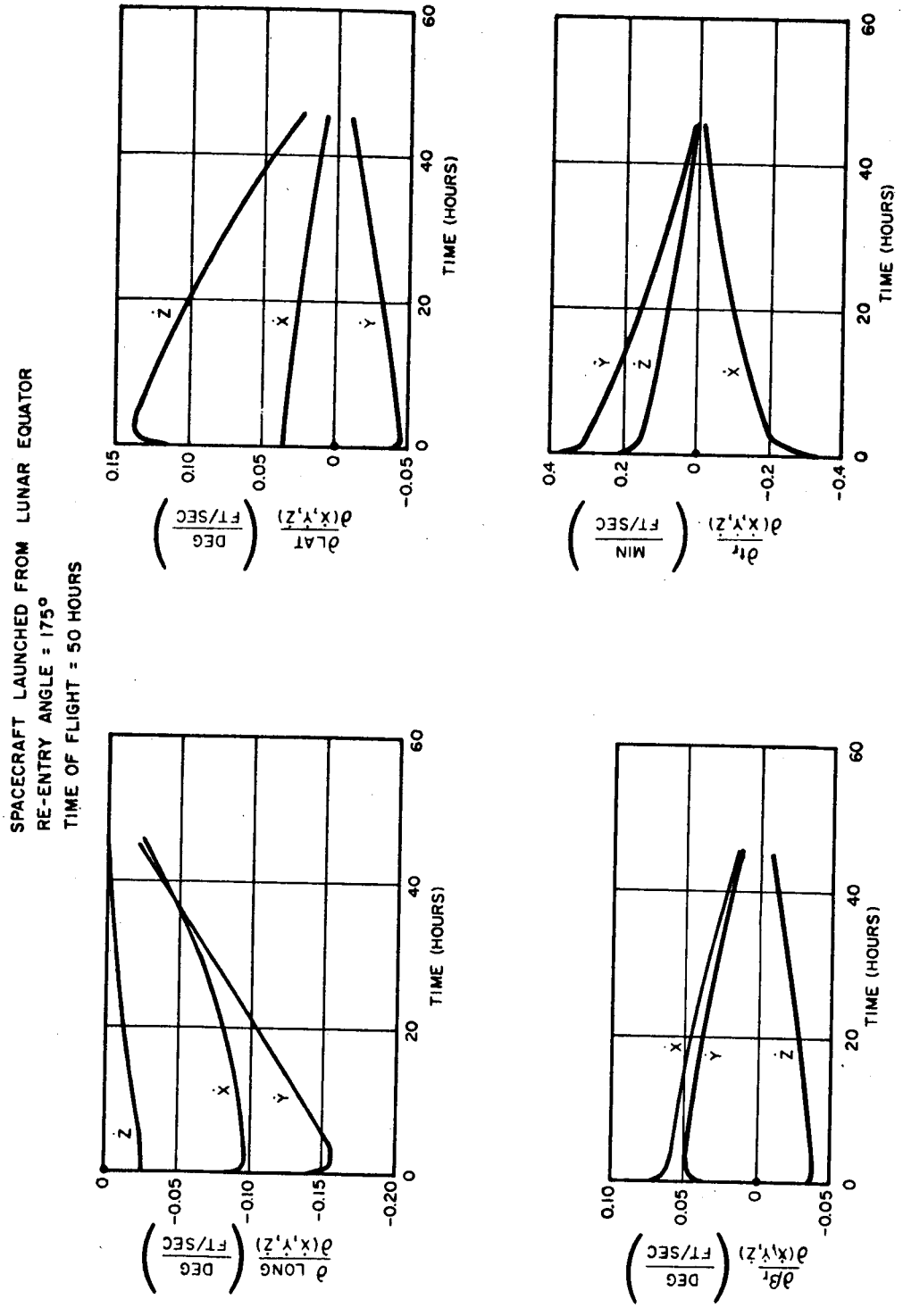

Figure 43. Midcourse Sensitivity Coefficients at Re-entry versus Time from Burnout for Variations in Equatorial Cartesian Velocity Components.

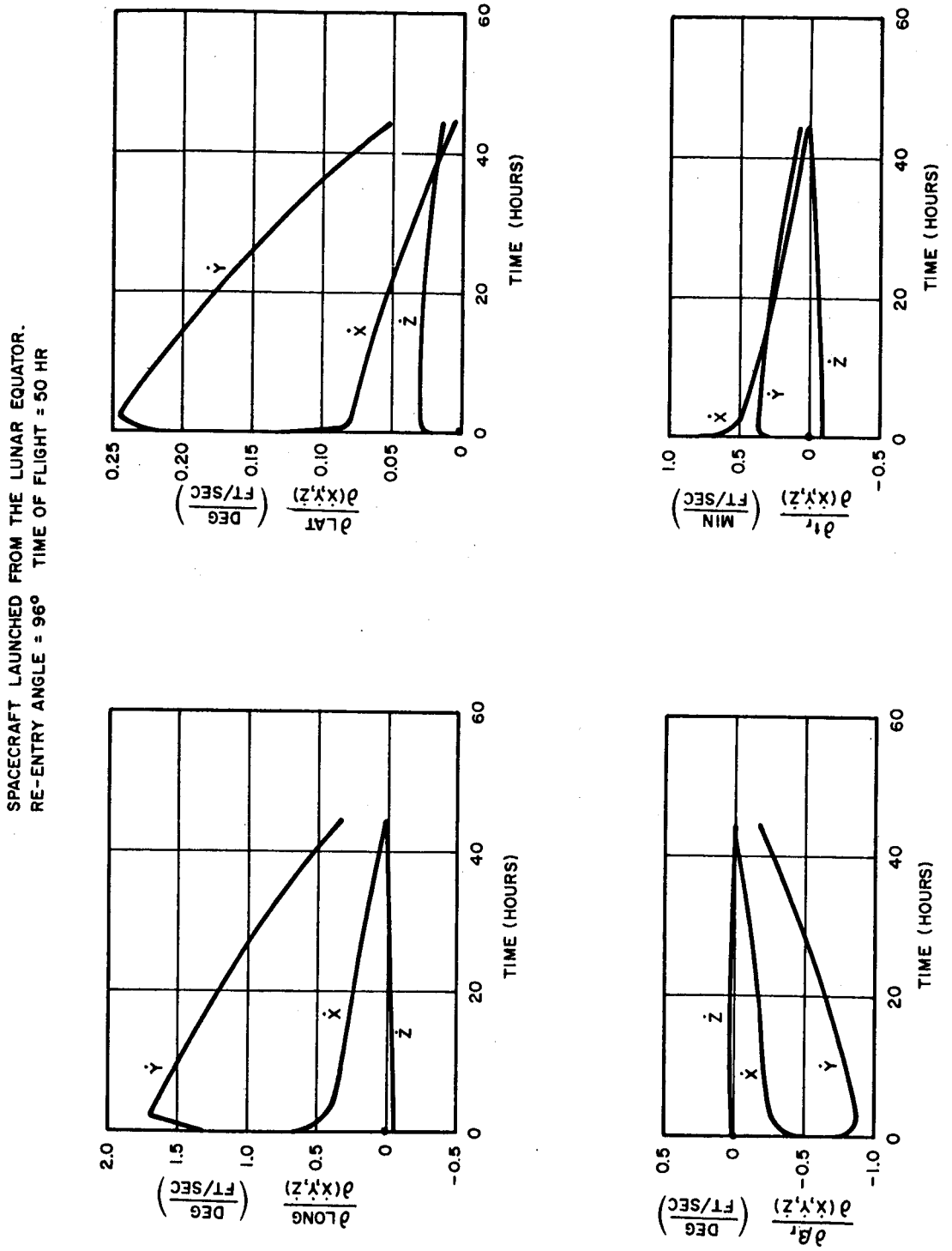

Figure 44. Midcourse Sensitivity Coefficients at Re-entry versus Time from Burnout for Variations in Equatorial Cartesian Velocity Components.

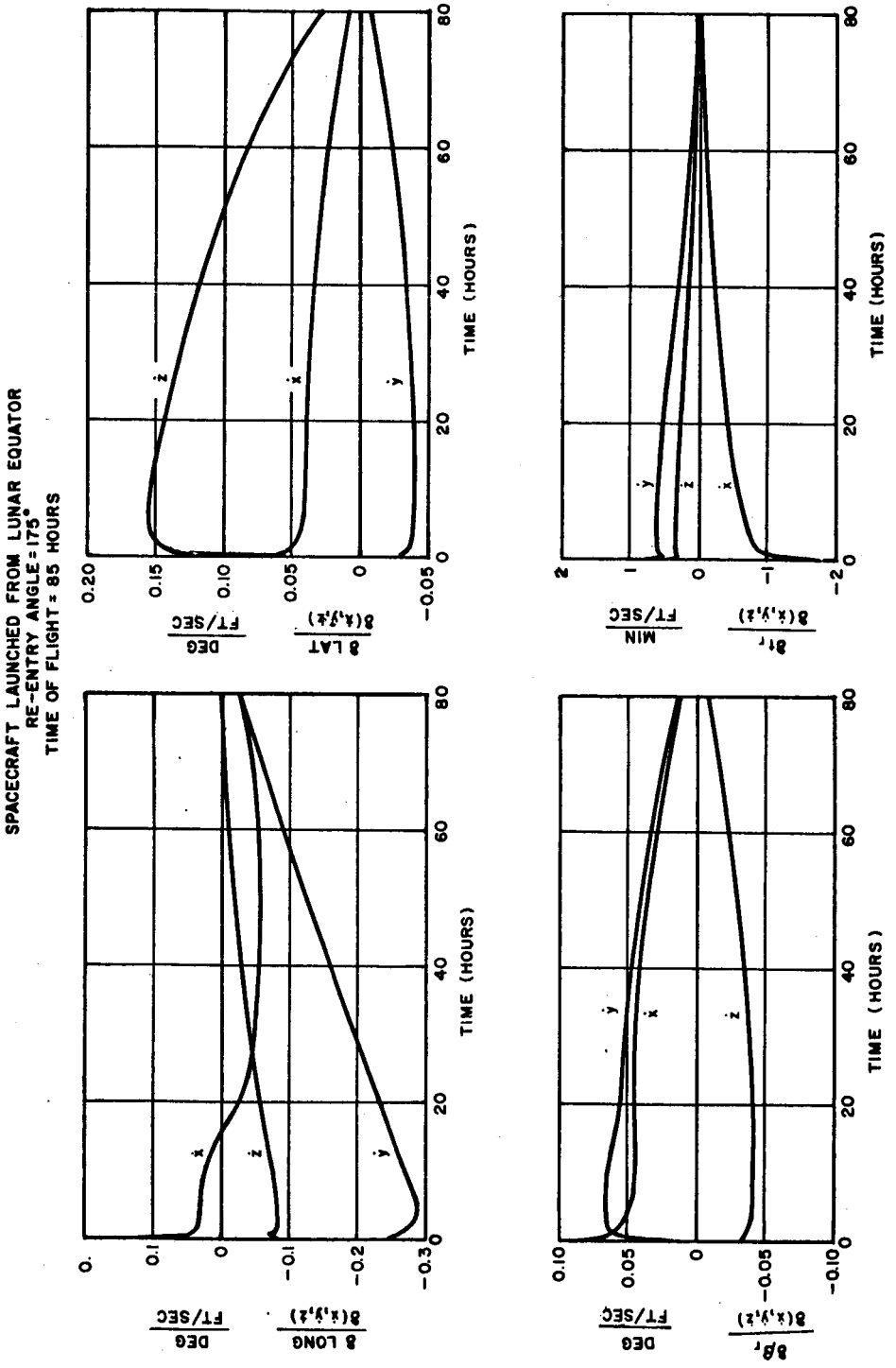

Figure 45. Midcourse Sensitivity Coefficients at Re-entry versus Time from Burnout for Variations in Equatorial Cartesian Velocity Components.

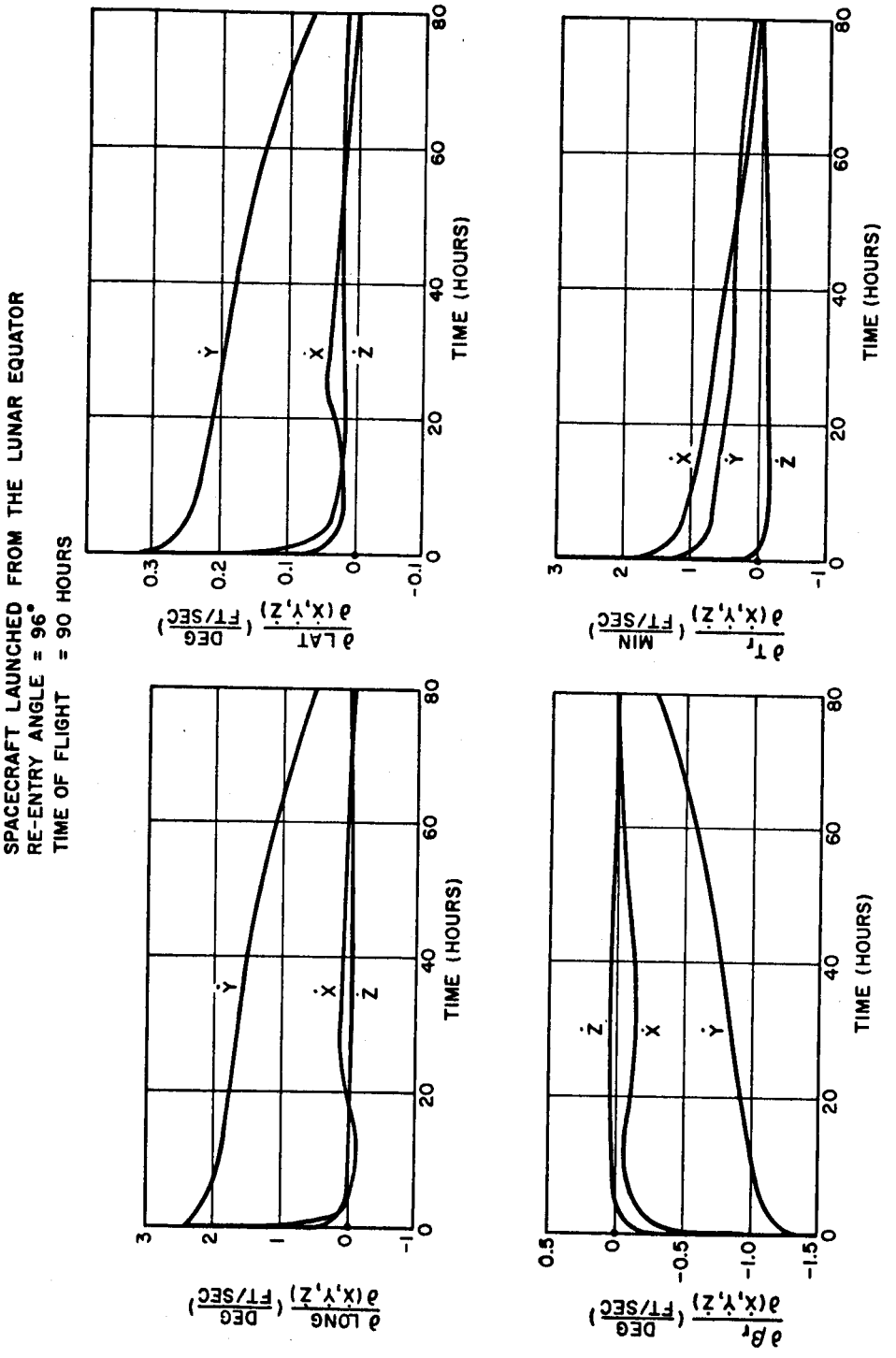

Figure 46. Midcourse Sensitivity Coefficients at Re-entry versus Time from Burnout for Variations in Equatorial Cartesian Velocity Components.

REFERENCES

1. Egorov, V. A., "Certain Problems of Moon Flight Dynamics," Russian Literature of Satellites, Part I, International Physical Index, Inc., 1958.

2. Skidmore, L. J. and P. A. Penzo, "Monte Carlo Simulation of the Midcourse Guidance for Lunar Flights," (to be presented at the January meeting of the IAS in New York City, 1962).

3. Penzo, P. A., I. Kliger and C. C. Tonies, "Computer Program Guide: Analytic Lunar Return Program," Space Technology Laboratories, Inc., Report 8976-0005-MU-000, August 1961.

4. Magness, T. A., P. A. Penzo, P. Steiner and W. H. Pace, "Trajectory and Guidance Considerations for Two Lunar Return Missions Employing Radio Command Midcourse Guidance," Space Technology Laboratories, Inc., Report No. 8976-0007-RU-000, September 1961.

5. Noton, A. R. M., E. Cutting and F. L. Barnes, "Analysis of Radio-Command Midcourse Guidance," Jet Propulsion Laboratory, Technical Report No. 32-28, September 1960.

6. Westman, J. J., "Linear Miss Distance Theory for Space Navigation," Space Technology Laboratories, Inc., Report 7340. 3-96, May 1960.